AN ABSTRACT OF THE THESIS OF

Mitchell Thomas Rasmussen for the degree of Master of Science in Environmental Engineering presented on September 14, 2018.

Title: Co-Encapsulation of Slow Release Substrates and Microbial Cultures in Alginate and Gellan Gum Beads to Promote the Co-metabolic Transformation of 1,4-Dioxane and Chlorinate Aliphatic Hydrocarbons

Abstract approved: _____

Lewis Semprini

Methods were developed for the co-encapsulation of slow release compounds (SRC) with viable microbial cells in alginate and gellan gum hydrogel beads, for the in-situ aerobic cometabolic treatment of groundwater contaminated with mixtures of 1,4-dioxane and chlorinated aliphatic hydrocarbons, which will be referred to as contaminants of concern (CoC). The bacteria used was *Rhodococcus Rhodochrous* ATCC 21198 (ATCC 21198) that is capable of cometabolically transforming mixtures of CoCs when grown on isobutane as the primary substrate. In addition to isobutane inducing cometabolic transformation, research conducted concurrently to this project has shown that the growth of ATCC 21198 on non-gaseous substrates, like the branched alcohol 2-butanol, may also stimulate the short chain alkane monooxygenase (SCAM) enzyme of ATCC 21198 that is responsible for the cometabolic transformation of CoCs. Due to this, investigation was conducted into two model slow release compounds, tetrabutylorthosilicate (TBOS) and tetra-s-butylorthosilicate (T_2BOS), which hydrolyze slowly at ester bonds to produce 1- and 2- butanol, respectively, and exist in pure phase as light non-aqueous phase liquids (LNAPL).

LNAPL SRCs (TBOS and T_2BOS) were successfully encapsulated in both alginate and gellan gum matrices at high mass loadings, >10% (w/w), and co-encapsulated ATCC 21198 was shown to be able to consume SRC products (1- and 2-butanol) prior to diffusion from the beads. The energy gained from the utilization of 1- and 2-butanol by encapsulated cultures was observed to have increased the survivability, overall activity, and contaminant transformation rate and capacity of initially augmented biomass. For example, in batch systems it was observed that cells co-encapsulated with SRSs were able to maintain cometabolic transformation potential for over 70 days, whereas, similar cellular biomass suspended in media lost the majority of CoC transformation potential after the first 12 days. Also, co-encapsulated cultures were able to transform 2-4 times more contaminants than suspended cultures over the 70 day period, and transformation within co-encapsulated systems is continuing to be observed. The results of this study provide strong evidence that the developed co-encapsulation technology may provide a useable solution to many issues encountered during current in-situ bioremediation treatment schemes.

Co-Encapsulation of Slow Release Substrates and Microbial Cultures in Alginate and Gellan Gum Beads to Promote the Co-metabolic Transformation of 1,4-Dioxane and Chlorinate Aliphatic Hydrocarbons.

by
Mitchell Thomas Rasmussen

A THESIS

submitted to

Oregon State University

in partial fulfillment of
the requirements for the
degree of

Master of Science

Presented September 14, 2018
Commencement June 2019

Master of Science thesis of Mitchell Thomas Rasmussen presented on September 14, 2018

APPROVED:

Major Professor, representing Environmental Engineering

Head of the School of Chemical, Biological, and Environmental Engineering

Dean of the Graduate School

I understand that my thesis will become part of the permanent collection of Oregon State University libraries. My signature below authorizes release of my thesis to any reader upon request.

Mitchell Thomas Rasmussen, Author

ACKNOWLEDGEMENTS

I'd like to start by thanking and recognizing the Strategic Environmental Research and Development Program (SERDP) within the Department of Defense for funding and making this research possible (Grant ER-2176). I also want to thank Oregon State Univeristy (OSU) for the initial funding and opportunity that allowed me to enter Dr. Semprini's Lab and also all of the faculty that I had the opportunity to learn from and work with as part of my degree. The success of my Master's Thesis is due to a broad group of people contributing ideas, lending hands and hours of time, and for continued support throughout the project.

This project was an engineering students dream, I was given a novel idea, a lot of direction, a brand new lab space, and a lot of trust from Dr. Semprini and asked simply to work things out. Throughout all of the failures that were apart of this process Dr. Semprini saw something good in every bit of work I brought to his desk; even when I was sure I had done something completely wrong (which was often). Dr. Semprini has a way of reading his students immediately and providing the perfect amount of guidance, motivation, and freedom to all types of students such that everyone remains interested and driven. I want to thank you Dr. Semprini for your consistent interest, enthusiasm, and the amount of time you put into me and this project which kept me motivated and has instilled in me a passion for the work I did. Also, for trusting in me to work with your idea and allowing me the freedom to make things work.

Dr. Mohammad Azizian was also very influential throughout my time at OSU. Without Mohammad the analytics in this thesis would not have been possible. Mohammad and Lew are some of the most positive people I have ever worked with. To Mohammad there is always a solution to every problem and typically as Mohammad would put it, it is "easy". Mohammad put in so much time helping me solve any issue I brought to him. I want to thank you Mohammad for everything you taught me in the lab and for always being willing to explain things 100 different times in 100 different ways when I was confused about something in the lab.

To both Lew and Mohammad I want to thank you for the freedom, support, guidance, availablity, and consistent interest and time you provided throughout this work. I have been very fortuante to work within this lab group.

I want to also thank the entire Semprini Lab group and everyone that I had the opportunity to work with; Emma Ehret, Hannah Rolston, Riley Murnane, Krysta Krippaehne, Alyssa Saito, Jon Laurance, Gillian Williams, and Grant Kresge. You guys were all so easy to work with and made the time spent in the lab go by so quickly. Thanks for all of the help collecting data and brainstorming ideas. Thanks especially to Emma and Hannah for the mentorship and patience, to Riley for the pots and pots of coffee and constant friendship, and to Alyssa and Gillian for the help in the lab while I was writing.

I want to conclude by thanking my friends and family, without which I would not have had the successes that I have. Thank you to my parents, grandparents, siblings, and partner; Wendy, Chris, Carol, Barbara, Carl, Coleen, Matison, Abbey, and Danielle for always supporting me. For all of the guidance, love, and encouragement over the years.

TABLE OF CONTENTS

TABLE OF CONTENTS (Continued)

LIST OF FIGURES

LIST OF FIGURES (Continued)

LIST OF FIGURES (Continued)

LIST OF FIGURES (Continued)

LIST OF TABLES

Table Page

LIST OF TABLES (Continued)

LIST OF ABBREVIATIONS

Abbreviation	Expansion
1,1,1-TCA	1,1,1 Trichloroethane
1,1-DCA	1,1 Dichloroethane
1,4-D	1,4 Dioxane
AC	Aerobic Cometabolism
ATCC 21198	*Rhodococcus Rhodochrous* ATCC 21198
Ba^{2+}	Barium ion
Ca^{2+}	Calcium ion
CAA	Clean Air Act
$CaCl_2$	Calcium Chloride salt
CAH	Chlorinated Aliphatic Hydrocarbon
CERCLA	Comprehensive Environmental Response, Compensation, and Liability Act
CF	Chloroform
CO_2	Carbon Dioxide
CoC	Contaminant of Concern
CT	Carbon Tetrachloride
CVOC	Chlorinated Volatile Organic Carbon
CWA	Clean Water Act
DAO	Direct Aerobic Oxidation
DCM	Dichloromethane
DNAPL	Dense Non-aqueous Phase Liquid
DoD	Department of Defense
ECD	Electrical Conductivity Detector
FID	Flame Ionized Detector
g	Gram
GC	Gas Chromatograph
GG	Gellan Gum
GS	Growth Substrate
HCL	Hydrochloric Acid
IB	Isobutane
IGS	Inducing Growth Substrate
K_{ow}	Octanol-Water Partitioning Coefficient
L	Liter

LIST OF ABBREVIATIONS (Continued)

LNAPL	Light Non-aqueous Phase Liquid
MCL	Maximum Contaminant Level
MCLG	Maximum Contaminant Level Goal
mg	Milligram
mL	Milliliter
mM	mmol/L
MSM	Minimal Salts Medium
NAWQA	National Water Quality Assessment
NCSU	North Carolina State University
NPDWR	National Primary Drinking Water Regulations
O_2	Oxygen
PaT	Pump and Treat
PCE	Tetra-chloroethene
RCRA	Resource Conservation and Recovery Act
RD	Reductive Dehalogenation
RT	Retention Time
SRCs	Slow Release Compounds
SRS	Slow Release Substrates
SVE	Surface Vapor Extraction
T_2BOS	Tetra-sec-butyl Orthosilicate
TBOS	Tetrabutyl Orthosilicate
TCD	Thermal Conductivity Detector
TCE	Trichloroethene
*t*DCE	*trans*-Dichloroethene
TPOS	Tetra-propoxy Orthosilicate
TSS	Total Suspended Solids
µM	µmol/L
USEPA	United States Environmental Protection Agency
VOC	Volatile Organic Carbon
WHO	World Health Organization

CHAPTER 1 – INTRODUCTION

Groundwater contamination is a widespread issue throughout the United States. A report published by the United States National Water Quality Assessment (NAWQA) program in 2006 reported that nearly 70 percent of over 3500 groundwater samples collected from 98 major drinking water supply aquifers from 1985-2001 contained at least one anthropogenic contaminant [1]. This study also found that volatile organic compounds (VOCs) were the most frequently detected contaminants; found in 20-50% of the samples taken, dependent on the assessment level [2]. Among the top 15 VOCs listed in this survey eight were chlorinated aliphatic hydrocarbons (CAH); chloroform (CF), perchloroethylene (PCE), trichloroethylene (TCE), 1,1,1-trichloroethane (1,1,1-TCA), *cis*-dichloroethylene (*c*DCE), *trans*-dichloroethylene (*t*DCE), dichloromethane (DCM), and 1,1-dichloroethane (1,1-DCA). All of which are listed by the Center for Disease Control (CDC) as being potential or likely human carcinogens as well as having other harmful environmental and human health concerns [3]. Also of increasing concern is that these data along with other groundwater sampling data suggest that it is highly likely for CAH contaminant plumes to contain multiple CAHs as well as the common co-contaminant 1,4 dioxane (1,4-D), which is also listed as a likely human carcinogen [4,5]. Mixtures are of increasing concern because research have begun to suggest that mixtures of contaminants can lower the acceptable exposure levels of all contaminants present, increase toxicity, and strengthen resistance to degradation [1,6].

The unique properties of CAHs which exist in pure phase as dense non-aqueous phase liquids (DNAPL) with high volatility and low solubility combined with the ubiquitous and long-term contamination of groundwater has allowed for CAHs to diffuse into saturated low permeability zones, such as clay layers, within aquifers. Many common remediation techniques like pump-and-treat and soil vapor extraction are less effective at treating compounds within low permeable zones

due to diffusion limitations and inability to remove or target the contaminant directly. Excavation can be used to remove DNAPL but this increases the already high capital investment and operation costs for these techniques. Also, the ex-situ treatment of mixtures of compounds with varying properties, such as CAHs and their common co-contaminant 1,4-D, can lead to economically burdensome and design intensive treatment systems. Issues with these and other common remediation strategies emphasize the need for exploration into more viable options. The aim of this study has been to explore advancements in in-situ bioremediation of mixtures of CoCs, which is continuing to gain interest largely due to the economics, potential for extended in-situ treatment, and mitigation of secondary contamination caused by long-term site occupation [7,8].

In the context of this study, bioremediation is referred to as the targeted use of microbial metabolism to transform or mineralize groundwater contaminants. This can be done ex-situ in bioreactors or in-situ by stimulating growth of desired microbial communities within an aquifer. Specifically, this thesis will focus on microbes capable of aerobic cometabolic degradation of CAHs and 1,4-D. Aerobic cometabolism requires a primary growth substrate (GS) to induce and sustain cellular activity and drive contaminant transformation. Through this process microbes utilize the primary GS for cellular growth and energy, and fortuitous degradation of contaminants occurs due to the stimulation of certain enzyme systems within growing microbes [7,8].

Two common methods to generate microbial biomass capable of cometabolically degrading target contaminants within the subsurface are to stimulate native microbes through the addition of substrates or nutrients (biostimulation) or by injecting pre-grown cells to a localized position around contaminants (bioaugmentation).

Biostimulation through the addition of specific substrates to contaminated groundwater has proven successful at stimulating native microbes capable of transformation of CAHs [7–10]. Though biostimulation has proven successful at certain contaminated sites, issues with non-selectivity of

substrates and toxicity of CAHs has led to unsuccessful attempts to stimulate native microbes with the capacity to cometabolically degrade target contaminants [8]. Consequently, bioaugmentation has emerged as an alternative bioremediation technique. Bioaugmentation involves the injection of laboratory grown microbes, with desired metabolisms capable of degrading target contaminants, into the subsurface at specific locations to drive the removal of contaminants for a period of time even in the presence of toxic or inhibitory compounds [7,8].

Bioaugmentation is typically successful in the short-term, but often, augmented microbes have short lifespans due to contaminant toxicity, inability to deal with fluctuations in environmental conditions, predation from protozoa, or competition for substrates and nutrients by highly adapted native microbes. This creates a need for recurring injections of microbes, which increases the cost of this strategy and can lead to issues like well clogging [7,8,11].

One solution that has been used in the past to mitigate similar issues with microbial cultures is encapsulation in hydrogel beads. Natural hydrogel matrices such as alginate, agar, and agarose have been used to physically buffer microbes from environmental conditions by providing a diffusion layer that decreases toxic levels of ambient compounds, slows changes in chemical and temperature conditions, and protects from predation by protozoa [12–14]. Recently encapsulation has been investigated for its ability to inhibit the production of biofilms which may reduce well clogging and increase transport distance of cells through aquifer material [13,15]. Also, by utilizing control over bead size, encapsulation may provide a control for bead affixation to aquifer material around low permeability zones [15].

Encapsulation of microbial cells may provide many benefits over suspended counterparts; however, the diffusion layer provided by the encapsulation matrix may exacerbate the issue of substrate limitations or out-competition by native microbes. Previous research has suggested that the inclusion of substrates or nutrients within the encapsulation matrix may provide an exclusive

substrate or nutrient source to encapsulated microbes [16–18]. Also of interest, are the continuing advancements in the medical field that have provided methods for the inclusion of slow release compounds (SRCs) within hydrogel beads for the controlled delivery of drugs [19,20]. Merging these concepts might allow for the inclusion of SRCs that produce potential microbial substrates, slow release substrates (SRS), within the encapsulation matrix to provide encapsulated cells with a prolonged substrate source, eliminating the competitive disadvantage of augmented cultures.

The overarching goals of this research were to develop and assess co-encapsulation techniques for SRS with microbial cultures to resolve issues encountered when attempting to bioaugment contaminated-aquifers with microbes to drive the remediation of mixtures of contaminants of concern (CoC).

The objectives set to meet this goal were to:

1. Adapt, develop, and optimize encapsulation techniques for the model cometabolizing-microorganism, *Rhodococcus Rhodochrous* ATCC 21198.

2. Assess the short and long-term effect on ATCC 21198s ability to utilize substrates and transform mixtures of CoCs after encapsulation using optimized techniques.

3. Adapt, develop, and optimize encapsulation techniques for the encapsulation of various SRSs and assess the effect of encapsulation on the production of SRS products.

4. Develop co-encapsulation techniques for SRSs with model microorganisms and determine the ability of non-inducing and inducing SRSs to increase and extend the successful bioremediation capacity of encapsulated microbes.

CHAPTER 2 – LITERATURE REVIEW

2.1. US Groundwater Use and Current Contamination

Data published in 2010 by the United States (US) National Water Quality Assessment (NAWQA) program showed that about 45 percent of the US population relies on groundwater as a drinking water source and just over twenty percent of all water used in the US is withdrawn from groundwater sources [21]. The same program published data collected from 1985-2002 in which around 3,500 wells distributed across 98 major drinking water source aquifers were sampled and analyzed for various known groundwater contaminants. The majority of samples were analyzed for as many as 80 pesticides, 60 volatile organic compounds, and inorganic contaminants like nitrate. In a detailed analysis of data from around 1,500 of these wells, conducted by researchers at the USGS, it was found that 70 percent of samples contained at least one anthropogenic contaminant [1]. This study also noted that VOCs were the most frequently detected groundwater contaminant, found in about 44 percent of samples.

Further research with the focused analysis of 55 VOCs within all 3,500 well water samples show that about 20 percent of the samples contained at least one VOC at the detection limit of 0.2 µg/L and just over 50 percent at a detection limit of 0.02 µg/L [2]. Twelve of the top fifteen most frequently detected VOCs were chlorinated volatile organic compounds (CVOCs) and eight of those twelve were chlorinated aliphatic hydrocarbons (CAHs). All of the detected CAHs are regulated by the US Environmental Protection Agency (USEPA) with set maximum contaminant levels (MCL) in the µg/L range and many with MCL goals (MCLG) of zero (Table 1) [22]. Regulations and health concerns are addressed in further detail below.

2.2. Chlorinated Aliphatic Hydrocarbons

2.2.1. Use and Release

Chlorinated hydrocarbons have been produced, imported and used at a large scale in the US starting in the early 1900s. The major use of CAHs were as cleaning and degreasing solvents for many industries. Of importance to this project is the use of CAHs as degreasing solvents in aerospace and other military industries, which led to widespread contamination of government sites [23]. In addition to this, many CAHs were also used in a wide variety of industries (pharmaceutical, food processing, electronics, dry cleaning, textile, etc.) and as ingredients in many commercial products including paints, inks, paint thinners, lubricants, glues, pesticides, tooth pastes, and refrigerants [23].

Four of the most widely manufactured and used CAHs in the US were carbon tetrachloride (CT), tetrachloroethylene (PCE), trichloroethylene (TCE), and 1,1,1 trichloroethane (1,1,1-TCA) [23]. The primary uses of each being vapor degreasing and to a lesser degree dry-cleaning. At one time or another, many chemical production facilities alternated between production of several CAHs depending on cost-demand cycles and regulations. This trend was also followed by CAH end users [24]. Major production peaked in the 70s and 80s at upwards of hundreds of millions of pounds, of each compound, produced per year [23].

This widespread production and use combined with a lack of knowledge of the effect these emerging compounds might have on human health and the environment led to improper use and disposal by manufactures, industries, and consumers alike. These improper management and disposal techniques combined with production and use cycles led to widespread human contact and the ubiquitous groundwater contamination with many mixtures of CoCs observed and presented in section 2.1.

2.2.2. Health Concerns and Regulations

The eight most prevalent CAH groundwater contaminants observed by the USGS are all regulated under the US Clean Water Act (CWA) and are located on the toxic and priority pollutant lists published by the USEPA. Also, all but one of the most prevalent CAH contaminants are regulated by the national primary drinking water regulations (NPDWR) set by the US EPA (Table 1).

Table 1. Summary of the US EPA NPDWR for the most prevalent CAHs groundwater contaminants..

Compound	Abbreviation	MCL (µg/L)	MCLG (µg/L)	Known Health Effects
Chloroform	CF	THM*	THM*	Cancer risk, liver, kidney, and nervous system complications
Perchloroethene	PCE	5	0	Cancer risk, liver complications
Trichloroethene	TCE	5	0	Cancer risk, liver complications
1,1,1-Trichloroethane	TCA	200	200	Liver, nervous system, and circulatory complications
Chloromethane	CM	N/A**	N/A**	Liver, nervous system, and circulatory complications
trans-1,2-Dichloroethene	*t*DCE	100	100	Liver complications
Methylene chloride	DCM	5	0	Cancer risk, liver complications
1,1-Dichloroethane	1,1-DCE	7	7	Liver complications
Total Trihalomethanes	THM	80	N/A	Cancer risk, liver, kidney, and nervous system complications

*Trihalomethanes (THM) such as CF are not regulated directly but through the total THM regulation in the last row of this table. **Chloromethane is not regulated by the NPDWR because it exists as a gaseous compound that is likely to volatilize prior to drinking water concerns

These regulations have been a work in progress since the mid-1960s and have progressively become more stringent. Toxicity data for many CAHs was being collected and published as early

as the 1940s [24]. However, the first regulations weren't implemented until 1965 at which time regions in California began to limit emissions of TCE from manufacturing plants due to the role it played in smog formation, though all other CAHs were permitted [23]. Regulations of CAHs began to steadily increase in the US with the passing of the 1970 Clean Air Act (CAA) to mitigate the formation of smog and limit ozone depleting chemicals. This was followed by the 1972 revision to the Clean Water Act, which gave the EPA more strength to regulate the release of and enforce monitoring of toxic pollutants [25]. After this bill passed it was found that tracking parties responsible for the release of contaminants was difficult which led to the Resource Conservation and Recovery Act (RCRA) in the late 1970s, which provided legislation that allowed the US EPA to regulate hazardous substances from "cradle to grave". The next major step made by the federal government was an attempt to control and remediate CAHs that were already released to the environment by passing the Comprehensive Environmental Response, Compensation, and Liability Act (CERCLA). This bill set aside large amounts of federal dollars, called superfunds, to assure the clean-up of abandoned contaminated sites, many of which are contaminated primarily with CAHs [26].

2.2.3. Mixtures and Co-Contaminants

In a study conducted at the USGS using data from the NAWQA sampled wells and other sources, presented in Section 1.1, it was found that 881 samples out of 5,000 contained at least one of four examined CAHs (DCM, PCE, TCE, and TCA). Also, thirty percent of the 881 samples found to contain VOCs consisted of a mixture of at least 2 VOCs [1]. The frequency of mixtures is thought to be due to the interchangeability of CAHs in various industrial processes as well as the common stepwise degradation pathway for one CAH to degrade into another (See Section 2.3.1) [1].

Along with CAHs existing in contaminant mixtures with one another it has more recently become a concern that 1,4 dioxane (1,4-D), a likely human carcinogen, is being found in many

CAH contaminant plumes [4,27]. This correlation is expected because 1,4-D was added to 1,1,1-TCA and likely other CAHs as a stabilizer to decrease reactivity [5]. Co-contaminants, such as 1,4-D, often increase the challenge of remediating contaminant plumes due to different physical and chemical properties. This leads to requirements for a different set of remediation techniques or the adaptation of new equipment [27]. Also, mixtures of contaminants are of increasing concern because the toxicological effects of CAHs has been found to be altered when chemicals exist in mixtures with one another [1,28]. Though little is known about the effect of mixtures of CAHs it is known that one chemical can affect the metabolism of another and increase the risk of exposure to low levels of certain mixtures [1,28].

Due to mixtures being frequently observed in sites of concern to the Department of Defense (DoD) this thesis has focused on the bioremediation potential of one chlorinated ethane, one chlorinated ethene, and one common co-contaminant; 1,1,1-TCA, *c*DCE, and 1,4-D respectively. All of which have been listed by the DoD as contaminants of concern (CoC).

2.2.4. Groundwater Remediation of Mixtures of Contaminants

i. Mixtures of Contaminants of Concern

Chlorinated solvents or CAHs are highly recalcitrant synthetic organic pollutants that exist in pure phase as dense non-aqueous phase liquids (DNAPL) with low water solubility and high volatility [29,30]. Most relevant CAHs to groundwater contamination have octanol-water partitioning coefficients (K_{ow}) greater than 1 and therefore are likely to sorb to subsurface organics [29,30]. Most CAHs have similar physical and chemical properties but mixtures with co-contaminants that have highly variable properties exist. For example, 1,4-D is a highly-stable miscible cyclic-ether with a low K_{ow} and relatively low vapor pressure. These differences in physical and chemical properties increase the complexity of remediating groundwater containing mixtures [27,31]. Physical and chemical properties of the 1,1,1-TCA, *c*DCE, and 1,4-D can be seen in Table 2.

Table 2. Compiled chemical properties on contaminants used throughout this thesis.

Compound	Molecular Weight (g/mol)[a]	Density (g/mL)[a]	Henrys Constant[b]	Water Solubility (mg/L)[c]	Vapor Pressure at 20°C (kPa)[a]	Octanol-Water Partitioning Coefficient (Kow)[a]
1,1,1-TCA	133.4	1.34	0.656	1290	13.3	2.49
*c*DCE	96.94	1.28	0.164	6410	24	2
1,4-D	88.1	1.03	N/A	Miscible	3.9	-0.27

Citations: [a] – International Chemical Safety Cards produced by the World Health Organization (WHO). [b] – Dimensionless Henry's Law Constants calculated from [32]. [c] - [33]

The characteristically low solubility and sorptive potential of CAHs inhibit the lateral mobility of these contaminants with flowing groundwater. Due to the slow advective mobility of these contaminants and of interest to this project is the likelihood for these compounds to have diffused into low permeable layers over extended periods of time. The process starts when CAH DNAPL is released to the subsurface and slowly sinks through an aquifer until it becomes perched on a low permeable layer, such as an aquitard. This perched DNAPL slowly diffuses from its stationary position, and travels with groundwater at solubility concentrations which over long periods of time has caused contaminant plumes to spread and become large [34]. The dissolved contaminants that have migrated down flow of the DNAPL have also managed to diffuse into low permeable aquitard layers [30].

Even when the DNAPL is depleted or removed, through excavation, the large contaminant plumes remain and observations have been made that concentrations are not diluted over time but contamination can continue to increase and spread [30,35]. This observation has been shown to be related to back-diffusion of "stored" CAHs that had initially diffused into the low permeable layers [30]. Therefore, despite the fact that one may be able to remove DNAPL source zones and treat currently contaminated groundwater through the methods presented below. The inability to access the waters in these low permeable layers creates a need to explore in-situ treatment techniques that

can be in place for extended durations. In addition to back diffusion issues, differing chemical properties, such as solubility, of the common co-contaminant 1,4-D can cause other issues such as differences in plume sizes and locations which all contributes to increasing the complexity of remediating groundwaters contaminated with mixtures of CoCs [4].

ii. Treatment of Mixtures of Contaminants of Concern

Current groundwater remediation strategies targeting CAH contaminants include costly ex-situ techniques such as excavation, pump-and-treat (PaT), and surface vapor extraction (SVE). Excavation can be used to target DNAPL; though as illustrated above, this does not affect currently contaminated waters and back-diffusion can continue to increase contaminant levels. Also, co-contaminants may not be associated with DNAPL and may not be removed via excavation.

PaT requires pumping liquids to the surface usually followed by sorption of CAHs to activated carbon, treatment of sorbed contaminants through incineration or other means, and reinjection of liquids [31,35,36]. PaT has been successfully used to treat CAH contaminated groundwater for decades; though, issues with long-term site occupation causing secondary contamination, inability to access groundwater in low permeable zones, and the low sorption potential of co-contaminants such as 1,4-D may require additional investments in other treatment techniques [27,31,35,36]. Surface vapor extraction (SVE) can be used to remove CAHs due to the high volatility of these compounds, but 1,4-D is not volatile and is not likely to be removed through this technique. SVE requires long-term pumping of gasses through the vadose zone followed by collection and treatment of large volumes of gases prior to exhausting them to atmosphere [7,31]. This technique also requires large operational costs and does not directly target DNAPL that may have seeped deep within the saturated zone.

Though these techniques can and have been used successfully to treat aquifers contaminated with CAHs, they require large capital investments, long-term site occupation, long-term operation

and maintenance costs, and often are not as effective at treatment of co-contaminants like 1,4-D [7,27,34]. Due to this, there is great interest in exploring more economically and environmentally favorable in-situ treatment techniques, such as bioremediation, that can also target common co-contaminants like 1,4-D.

Mixtures of CAHs and co-contaminants like 1,4-D are known to be highly recalcitrant to biodegradation, however there have been many microbes discovered with the capability of metabolizing a variety of CAHs, 1,4-D, and many other common groundwater contaminants [6–8,37–46].

2.3. In-situ Bioremediation

2.3.1. Microbial Metabolic Pathways

Many bacteria with metabolic pathways capable of transforming a wide range of CAHs have been isolated from contaminated waters and soils. However, only three key metabolic pathways for the biotic transformation or degradation of CAHs have been discovered. One anaerobic and two aerobic processes know as reductive dehalogenation (RD), direct aerobic oxidation (DAO), and aerobic cometabolism (AC) respectively.

Under anoxic conditions reductive dehalogenating cultures use CAHs as electron acceptors causing the successive cleavage of chloride ions and effectively transforming highly chlorinated compounds to less or non-chlorinated compounds [7,34,47]. The successive nature of this process can lead to issues, such as limited electron donor concentrations causing the process to be slowed or halted at an intermediate step. This has been shown in the case of TCE dehalogenation to lead to the buildup of more toxic intermediate products such as vinyl chloride, a known human carcinogen of more concern than TCE [48]. Recently, CAH contamination has been found to be positively correlated with elevated dissolved oxygen concentrations which limits the current scope of reductive dehalogenation [1]. However, this correlation is thought to be due to the increased

degradation rate of most CAHs under anaerobic conditions, meaning the persistence of most CAHs is greater in the presence of oxygen [2]. Though current applications of RD may be limited due to this phenomenon, it does illustrate the historical importance and potential usefulness of RD for the remediation of CAHs.

Direct aerobic oxidation is the term used for the direct use of contaminants by microbial cultures to sustain cell growth and other metabolic activity. By utilizing various CAHs and co-contaminants as a sole carbon and energy source it has been found that, relative to other bioremediation processes, less toxic byproducts are formed and mineralization of contaminants is possible [7]. DAO has great potential as a viable remediation option, however, very few cultures capable of DAO of CAHs have been isolated and the range of degradable contaminants is relatively small. These issues combined with knowledge about the prevalence of mixtures of contaminants has led to questions regarding the efficacy of this bioremediation technique [1,7]. Further issues with DAO have also arose due to environmentally relevant concentrations of contaminants being unable to support healthy populations of direct metabolizers [7,49].

In contrast to DAO, aerobic cometabolism requires the presence of a primary growth substrate (GS) to sustain cellular activity and drive contaminant transformation. Microbes utilize the primary substrate for cellular growth and energy and fortuitous degradation of contaminants occurs due to the presences of certain enzyme systems within growing microbes [8,39]. Transformation of cometabolic substrates, e.g. CAHs and 1,4-D, does not benefit cells via AC and often the parent cometabolic substrates and their transformation byproducts can be inhibitory and/or toxic to the cometabolizing cultures [6,50]. Contaminant transformation can be toxic to cells but these effects can be mitigated and it is possible to support healthy microbial populations with controlled additions of GSs [8,9,38,42]. Other advantages of AC are the increasing range of microbial species capable of AC, the possible range of primary substrates that will support differing AC

culture growth, and the large range of contaminants and mixtures of contaminants that can be transformed [8,39,46,47]. Known issues with AC include oxygen demand and supply, limited methods for the supply of growth substrates, non-selectivity and phase of many common growth substrates, and excessive growth of microbes in the subsurface leading to well and aquifer clogging [7,8,12]. These issues are addressed in detail in subsequent sections of this literature review.

2.4. Aerobic Cometabolism

2.4.1. Aerobic Cometabolic Induction

It is widely accepted that aerobic cometabolic transformation of CAHs, 1,4-D, and other contaminants is made possible in large part by cellular generation of non-specific oxygenase enzyme systems [8,39]. These oxygenase enzymes are thought to be generated by cells for the utilization of particular GSs, referred to here as inducing growth substrates (IGS). However, the term "inducing substrate" will be defined as any substrate that requires the generation of desired oxygenase enzymes within cells for its own consumption. This distinction is made because many cultures capable of AC are able to grow on, but may not be induced by, a large variety of substrates; including but not limited to, alkanes (C1 to C8), alkenes (C2 to C3), 1° and 2° alcohols (C2 to C8), aromatic hydrocarbons and alcohols, organic acids (C1 to C5), and various sugars [6–8,37–46]. Also, this distinction is made because it has been found that some microbial cultures may even be induced by cometabolic substrates such as TCE and 1,4-D [51,52].

2.4.2. Field Applications

There are two common approaches to achieve induced microbial biomass levels capable of aerobic cometabolic transformation of CoCs in subsurface environments. These approaches include the growth and induction of native AC microbes through the addition of inducing growth substrates

or nutrients (biostimulation) or the injection of cells pre-grown on IGSs to a localized position around contaminants (bioaugmentation).

Biostimulation through the addition of specific substrates to contaminated groundwater has proven successful, in both lab scale reactors and full scale aquifers, at stimulating native microbes capable of transformation of CAHs [9,10]. However, some biostimulation attempts have run into problems with the toxicity of some CAHs inhibiting the stimulation of native microbes [8,53]. Also, the non-selectivity of many commonly used growth substrates could lead to growth of microbial communities not capable of AC [8]. Consequently, bioaugmentation has emerged as an alternative bioremediation technique. Bioaugmentation involves the injection of microbes grown on IGSs in a laboratory to contaminated zones within aquifers. This technique allows for the control and selection of particular microbial cultures and targeted injection of healthy populations of pre-grown cells that can degrade contaminants for a period of time even in the presence of toxic or inhibitory compounds [6,50,54].

Bioaugmentation is typically successful in the short-term, but often injected microbes have short lifespans due to contaminant toxicity, inability to deal with fluctuations in environmental conditions, predation from protozoa, or competition for substrates and nutrients by highly adapted native microbes [7,15,43,55,56]. This can create a need for recurring injections of microbes which increases the cost of this strategy and can lead to issues like well clogging [8].

2.4.3. Growth Substrate Limitations

Some of the most commonly researched, referenced, and efficient microbes capable of AC of CAHs and co-contaminants are known to be highly induced by aliphatic and aromatic hydrocarbons such as methane, propane, butane, and toluene [8,39]. Over the past several decades many microbial cultures have been discovered with the capability of growing on various gaseous hydrocarbons (methane, propane, isobutane, etc.) and degrading many contaminants including

CAHs, 1,4-D, other common contaminants, and various mixtures of contaminants. Toluene and phenol are other IGSs that have been discovered and frequently used to drive the cometabolic degradation of CAHs and other contaminants [8,9,39,53,57]. Table 3 shows some of the more well studied AC microbes along with *Rhodococcus Rhodochrous* ATCC 21198 (ATCC 21198) and a list of contaminants they have been found to degrade, citations included. Though ATCC 21198 has less published work, it is the primary culture studied in this work.

Table 3. Summary of well-studied cometabolizing microorganisms observed transformation potential for common CAH contaminants and the common co-contaminant 1,4-Dioxane. Transformation indicated by (x), however, blank areas only indicate that a well cited publication was not found suggesting that the culture transforms the corresponding contaminant. Blank areas do not indicate that the culture does not transform the given contaminant.

Microbial Species	*Mycobacterium Vaccae* JOB5	*Methylosinus Trichosporium* OB3b	*Pseudomonas Mendocina* KR1	*Rhodococcus Rhodochrous* ATCC 21198
Primary Growth Substrate	Propane	Methane	Toluene	Isobutane
1,4-D	x	x*	x*	x
TCE	x	x	x	
*c*DCE	x	x	x	x
*t*DCE	x	x	x	x
1,1-DCE	x	x		x
VC	x	x		x
1,1,1-TCA	x	x		x
1,1,2-TCA				x
1,1-DCA		x		x
1,2-DCA		x		x
CF	x	x	x	
DCM		x		
Citations	38,39,46,58–63	38,39,63–66	38,39,63,67,68	69–72

*A single paper published suggested that these cultures could degrade 1,4-D [38], though other work refutes the claim that these cultures can transform environmentally relevant concentrations of 1,4-D.

Though these commonly used substrates work well in lab settings, they have their limitations in field applications. As mentioned above biostimulation requires the addition of substrates to the subsurface and many of the commonly used IGSs are gaseous hydrocarbons with explosive potentials and low solubility in water. Even with these limitations, successful attempts have been

made to stimulate native microbial populations capable of AC by supplying gaseous hydrocarbons[10,73,74]. Connon et al. (2005) and Kim et al. (2008) showed that through repeated sparging of the saturated zone with a propane or methane and air mixture they were able to alter the native microbial populations and stimulate propane-utilizing cultures. Kim et al. also demonstrated the ability of these cultures to degrade TCE and *c*DCE in-situ. However, other issues with this technique have become apparent due to increased volatilization of contaminants from forced gas flow through the vadose zone similar to SVE. Due to this, it has been suggested that attempts to biostimulate with gaseous substrates must be paired with SVE techniques of capturing and treating large volumes of air [7].

Liquid substrates such as toluene and phenol have also been used successfully at the field/pilot scale to stimulate native microbes capable of oxidizing mixtures of TCE, DCE, and the oxygenase indicator substrate isobutene [9,53]. The addition of soluble liquid substrates is preferable due to the ability to add greater concentrations to the saturated zone and mitigate volatilization of CAHs and GSs which would decrease the overall cost of this treatment technique [7]. Though liquid substrates such as toluene and phenol are preferable, the toxic nature of these two compounds is a hazard and a health concern when making additions to major groundwater sources [75,76]. In addition to health concerns of application, toluene has a regulated drinking water MCL of 1 ppm [22].

Issues with gaseous and common toxic liquid IGSs has recently driven laboratories, including ours, to explore alternative non-toxic water soluble and lipophilic liquid substrates capable of inducing microbial cultures typically grown on aliphatic hydrocarbons or toluene. It has been found that some known AC microbes are capable of growth on various alcohols, sugars, and some non-toxic lipid soluble organic aromatics like limonene and cumene [46,77]. However, induction of desired monooxygenase enzyme systems has proven to have variable degrees based upon the microbial culture, GS, and target contaminant or mixture of contaminants [7,8,39,46,77].

Selective non-toxic liquid substrates may mitigate many issues that have arisen with biostimulation, however, there are still necessary steps needed to solve other problems with the application of bioremediation treatment schemes such as aquifer clogging due to excessive biomass growth, cell washout and die off, low selectivity of substrates, and toxicity of target CoCs. These issues and proposed solutions are presented below.

2.4.4. *Rhodococcus Rhodochrous* ATCC 21198

The work within this thesis focuses on the aerobic cometabolic degradation of CAHs and co-contaminants carried out by pure culture *Rhodococcus Rhodochrous* ATCC 21198. ATCC 21198 was obtained from Dr. Michael Hyman at North Carolina State University (NCSU). The work conducted throughout this thesis is focused on pure culture ATCC 21198; however, the methods developed are designed to be modular and therefore, replacement of ATCC 21198 by another cometabolizing culture will be possible.

ATCC 21198 is an isobutane utilizing culture that has been shown to be capable of degradation of a wide range of CAHs and other common groundwater contaminants (Table 3). A 1,4-D transformation model for pure culture ATCC 21198 has been developed as part of [69] and is currently being adapted to transformation of mixtures of CoCs.

Induction of ATCC 21198 by non-toxic liquid substrates is currently under investigation in parallel projects. As part of that work, it has been discovered that ATCC 21198 can grow well on various substrates, though induction of mono-oxygenase enzymes by these substrates is still under investigation (Table 4) [51,70,78]. Growth is not indicative of induction but data suggest that ATCC 21198 may experience some level of immediate induction on some substrates other than gaseous alkanes such as branched alcohols (isopropanol and 2-butanol), organic acids (acetate), and other ethers (tetrahydrofuran) (Table 4).

Table 4. List of known growth substrates for ATCC 21198 [70,78].

Alkanes	Alcohols	Organic Acids	Other
ethane*	ethanol	acetate*	dextrose
propane*	1-propanol	lactate	tetrahydrofuran*
butane*	isopropanol*	butyrate	1,4-dioxane
isobutane*	1-butanol	--	--
--	2-butanol*	--	--
--	isobutanol	--	--

* Appreciable induction of cometabolic enzymes within ATCC 21198 was observed when grown on this substrate.

2.5. Slow Release Compounds

Slow release compounds (SRCs) have been developed and used to slowly produce nutrients such as phosphorus and nitrogen to the subsurface to help create environments more favorable to cellular activity and potentially increase the bioremediation potential of contaminated aquifers [16]. These SRCs were designed to sorb to aquifer materials to reduce washout and provide a localized nutrient source. Similar to this, SRCs have been proposed as a means to supply low but constant concentrations of IGSs through a single injection of a larger molecule that will slowly degrade to produce an effective IGS over time [18,79]. The idea is that injection of less bioavailable SRCs could potentially mitigate problems caused by excessive cellular growth caused by injections of non-specific substrates and lower operation costs by reducing pumping and supply durations.

Silicon-based organic compounds known as tetra-alkoxysilanes, such as tetrabutyl-orthosilicate (TBOS), exist in some CAH contaminant plumes and due to this have been investigated for their bioremediation potential and as possible slow release compounds that could drive reductive dechlorination of CAHs [80,81]. These large molecular weight compounds consist of a silicon center bound via ester linkages to four alcohols that can vary in carbon chain length and structure. These compounds are insoluble in water and exist in pure phase as lipophilic light non-aqueous phase liquids (LNAPL) [82]. The ester linkages have been found to hydrolyze abiotically at

varying rates based largely upon the pH of solution and the size of the leaving group [80,82,83]. The hydrolysis of these compounds is acid and based catalyzed and slowest at a pH of 7 [80].

Experimental data has shown that the larger the attached groups are to the silicon center of orthosilicate compounds the slower the initial hydrolysis [82]. This is thought to be due to increased steric hindrance preventing hydrolysis at the centralized ester bonds. Of particular interest to this project is that these compounds can be made containing a wide variety of alcohols such as methanol, 1-butanol, 2-butanol, and phenol; all of which have been shown to be consumed by various cometabolizing cultures [39,46]. Also, previous research has shown that as alcohols hydrolyze from these SRCs, surrounding microbial cultures can utilize them immediately at low concentrations [81].

This thesis utilized TBOS and tetra-sec-butylorthosilicate (T_2BOS) as model slow releasing compounds that are designed to hydrolyze to produce 1- and 2-butanol as usable substrates for microbial cultures (Figure 1). These compounds were chosen due to known growth of the target model cometabolizing organism ATCC 21198, their low solubility in water, low human health concerns, historical work with hydrolysis rates, and their availability and low cost.

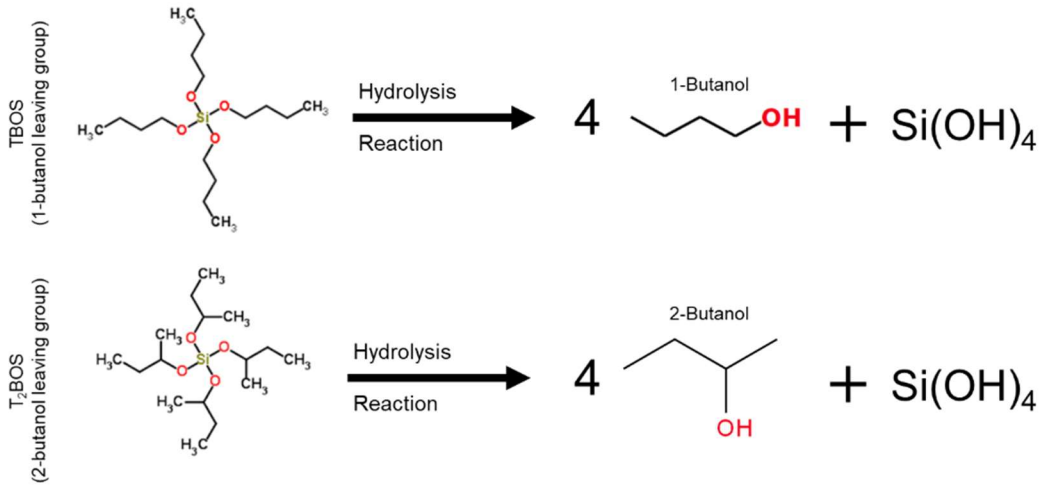

Figure 1. Chemical structure and complete hydrolysis reactions for TBOS (above) and T_2BOS (below). Chemical structure graphics obtained from [84].

2.6. Encapsulation

2.6.1. Microbial Encapsulation Background

Encapsulation of microbial cells in this thesis will be defined as the entrapment of microbial cells in an insoluble polymeric hydrogel such as agar, agarose, alginate, and gellan gum. Encapsulation has been used in the past to provided advantages to cells such as increased metabolic activity, protection from toxic substances, protection from ambient stressors like temperature and pH, protection from predation by protozoa, and ability to obtain and maintain high cell densities [12–14,85–87]. Also, it has been suggested that encapsulation of microbes inside micron scale hydrogel beads may increase transport distance of cells in aquifer material due to decreased biofilm production and cell affixation to aquifer material [13,15,88]. Encapsulation may also provide a mechanism to enhance augmented cell survival, mitigate cell washout, and for the targeted affixation of cells around low permeability zones via control over bead sizing, influent well location, and bead straining [13,15,79,88].

Though encapsulation affords microbes many advantages over suspended counterparts, some studies have shown that the diffusion of electron donors and acceptors through immobilization matrices may be a large disadvantage of immobilization [89–91]. In many of these diffusion studies beads are on the millimeter scale, referred to here as macro-beads, to provide sufficient lengths to study diffusion. Though this is important at these scales, as diffusion lengths decrease, e.g. smaller beads, these limitations can be mitigated [91]. Therefore, the final applications of this project will be influenced to a much lesser degree by diffusion limitations due to the target size of micro-beads (10-40 um). Another impediment to encapsulation is the loss of cell viability after encapsulation [92]. However, this can also be avoided by optimizing methods and encapsulation matrix selection [79]. Often the encapsulation process of natural gelling polysaccharides like alginate, agarose, and more recently discovered gellan gum is more simple than synthetic polymers and requires no toxic

compounds which mitigates the loss of cell viability [79]. An objective within this thesis has been to investigate and optimize encapsulation procedures for ATCC 21198 such that cell viability loss is minimized.

2.6.2. Alginate Encapsulation

Encapsulation of cells in alginate spheres ranging in size from below 100µm to 5mm has been one of the most common microbial immobilization techniques for several decades [87,93]. Alginate is a naturally occurring polysaccharide produced by various microbial and plant species consisting of chains of mannuronic and guluronic acids that vary in combination and length [87]. Beads are made via ionic crosslinking of connected acid structures with divalent cations such as calcium (Ca^{2+}) and barium (Ba^{2+}) [94] (Figure 2).

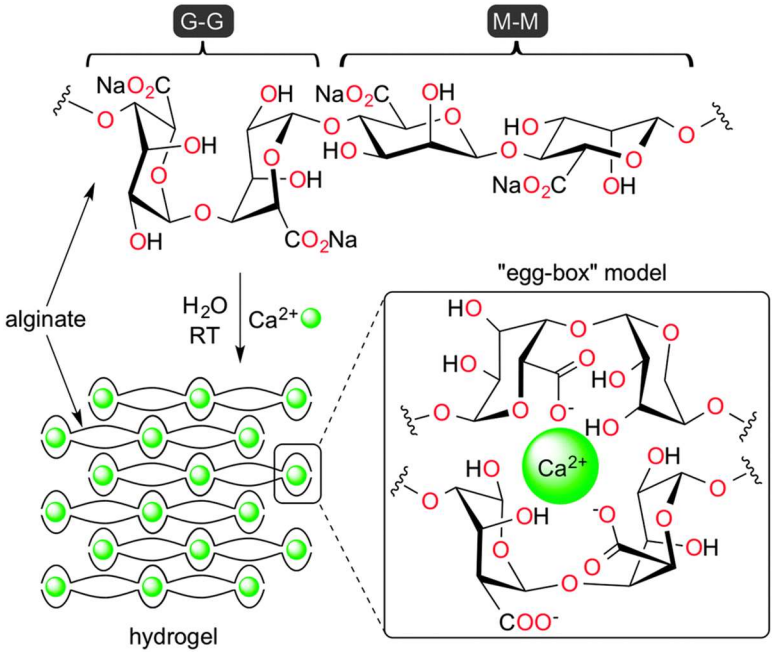

Figure 2. (Top) Hydrated alginate pre-gel chemical structure. (Bottom) Graphical depiction of ionically cross-linked stable alginate structure [95].

There are two common methods for alginate gelation that achieve stable crosslinked beads; dropwise extrusion of alginate pre-gel solution through a needle or nozzle into divalent cation

solutions, and emulsification in hydrophobic liquids followed by internal or external gelation with divalent cations. Both gelation methods are relatively simple and are conducted under very mild conditions relative to other encapsulation techniques [93,96,97]. External gelation can be conducted via a simple one step method and has been show to produce more structurally sound beads with greater diffusivities than internal gelation [92]. Techniques have been developed for both gelation methods to produce beads smaller than 100 um [96,98].

The mild process for encapsulation of microbial cells in alginate beads makes it a viable method for encapsulation of most microbial species [93]. Though many microbial species have been successfully encapsulated in alginate, including cultures capable of AC of CAHs, issues have arisen with the chemical stability of alginate beads [94,99,100]. The ionic bonds formed during gelation of alginate gels are unstable and reversible in the presence of chelating agents such as phosphate buffer and sodium citrate that attract and bind Ca^{2+} ions [101]. These issues can be mitigated by use of different crosslinking ions such as barium or by coating alginate beads in hydrogels that are not effected by chelating agents such as chitosan [94,102]. For experimental testing with alginate encapsulated cells it is best to avoid the use of phosphate buffers in general, though addition of calcium chloride salts to media solutions can increase stability of beads [103]. Control over chelating agents is possible in lab scenarios but groundwater is much less predictable and there are many naturally occurring chelating agents [104]. Stability issues of alginate beads in the presence of chelating compounds could lead to application issues when attempting to use alginate-encapsulated cells to bioaugment particular groundwaters.

2.6.3. Gellan Gum Encapsulation

Gellan gum is a relatively newly discovered natural gelling polysaccharide produced primarily by Sphingomonas elodea, consisting of chains of glucose, glucuronic acid, and rhamnose molecules (Figure 3) [105–107]. Similar to alginate the gelation of gellan gum (GG) occurs via ionic

crosslinking; however, in contrast to alginate crosslinking can occur with a variety of mono and divalent cations. Though GG gelation is ionically activated, the gelation process is more similar to the thermal hysteresis type gelation of agar and agarose [108,109]. GG gelation temperatures are dependent on the type and concentration of crosslinking cations, concentration of GG, and concentration of chelating agents [106,109,110]. Over the past decade GG has become a widely used hydrogel matrix replacing matrices like agar and alginate because it has been found to have superior rheological properties, chemical stability, temperature resistance, enzyme resistance, and clarity at lower concentrations of hydrogel and ionic crosslinkers [97,106,108,110]. In summary, GG has a similar structure but is more durable and similarly biocompatible at lower concentrations than other natural polysaccharides, which may decrease operational costs of producing large quantities of bioactive beads.

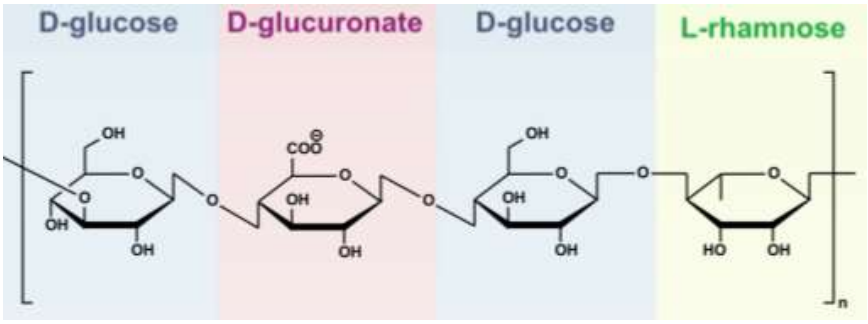

Figure 3. Low-Acyl Gellan Gum repeating structure [107].

Microbial encapsulation with GG is more involved than the alginate encapsulation methods presented in section 3.4.1 because gelation is a function of temperature as well as crosslinking concentration [109,110]. The gelation process requires heating of pre-gel solution to at least 60°C followed by a direct addition of crosslinking cation salts or solutions and cooling typically to about 35°C to initiate gelation. Although the basic method is more complicated than alginate the temperature dependent crosslinking of GG has allowed for development of more simple emulsification internal gelation procedures [79,85]. These methods have been optimized and can be

used to create highly stable spherical micro-beads ranging in size from below 20 um to above 150um [79].

GG micro-beads produced via this method have been found to be stable at elevated microbial biomass loadings of up to 8 grams of cells measured as total suspended solids per liter (L) of pre-gel solution [79]. No published work was found for methods used to generate GG macro-beads, but previous work has been done on macro-encapsulation of microbes in agar and agarose that have been adapted in this thesis, see methods section 3.4.2 below [86,103].

2.6.4. Encapsulated Cell Bioremediation

The benefits of encapsulating cells for the remediation or transformation of compounds has been a topic of interest for decades, though using encapsulated cells for the bio-augmentation of aquifers is a relatively new research topic that has yet to be implemented in a full scale project. However, the possible benefits of encapsulating cells prior to bioaugmentation are promising. Bettmann et al. (1984) showed that degradation rates of the model toxic compound, phenol, by alginate encapsulated cells were greater than suspended cells and that encapsulated cells were able to tolerate higher concentrations of the toxic substrate [111]. These researchers suggested that high cell densities concentrated at the outer edges of the beads may have protected the cells by lowering local concentrations through high cell degradation and slower diffusion of compounds into the beads. Dwyer et al. (1986) also investigated phenol biodegradation but with agar encapsulated cultures. These data supported the idea that encapsulated cultures are afforded some relief from the inhibitory effects of high toxic substrate concentrations [86]. However, in contrast to the Bettmann study, degradation rates were found to have been reduced. This could be due to a difference in encapsulation method and material between the two studies. Dwyer et al. also developed one of the first successful models for encapsulated cell bioremediation of contaminants using an adapted Monod kinetics model that included inhibition of toxic substrates.

Work has also been done to investigate the effects encapsulation has on aerobic cometabolizing cultures transforming CAHs. Uchiyama et al. (1995) encapsulated a methane utilizing culture in calcium alginate beads and investigated TCE degradation rates. Encapsulated cells were found to degrade TCE in a simulated groundwater media and were more viable than free cells at low pHs and higher temperatures. As mentioned previously, oxygen diffusion into the beads was found to be the rate-limiting step likely due to high cell densities. This study also investigated the storability of alginate encapsulated cells and found that cells stored at 4°C with an air or nitrogen headspace retained over 50 percent of their original activity over a 6 day period. These data suggest that encapsulated microorganisms could be stored for some duration of time and transported prior to application in a field setting. Long-term storage of beads will be investigated as part of this thesis.

Most bioremediation research done with encapsulated cultures has been conducted with macro-scale beads, though as methods continue to be developed for the micro-scale encapsulation of microbial cultures more research related to bioaugmentation with encapsulated microbes is being published. Moslemy et al. (2002b) developed an emulsification internal gelation technique for the micro-encapsulation of a gasoline degrading consortium in GG beads in the range of 10-135um in diameter [79]. The developed method showed promise for precise control over the average bead diameter and ability to reduce the range of observed diameters. The concentrations of cells encapsulated in micro-beads was found to have little effect on bead formation and encapsulated cell gasoline degradation activity was greater than that of suspended cells. The encapsulated cells were also able to degraded higher concentrations of gasoline without any lag period [12]. The transport of these micro-beads in aquifer material was also investigated and it was found that micro-beads could be transported over the entire length, 110cm, of three different columns packed with aquifer materials with varying porosity [15]. Bead straining was an issue in more fine aquifer media

and total breakthrough of micro-beads was not observed in all columns. It was suggested that lowering bead injection concentrations and fluctuating the pumping rate might have mitigated some straining observed in this study.

Other research has shown that encapsulating cells in alginate beads prior to bioaugmenting soil microcosms increased the travel distance and survivability of cells when compared to additions of free suspended cells [18,88]. Though these projects were investigating the survivability of cells in soils that were released from beads, it does provide supporting evidence that encapsulated pure cultures are more likely to successfully adapt to soil environments than their suspended counterparts.

CHAPTER 3 – MATERIALS AND METHODS

3.1. Chemicals

Chemicals of note to this thesis are listed in Table 5. All chemicals used but not listed in Table 5 were of reagent grade.

Table 5. List of analytical grade chemicals used throughout this thesis.

Compound	Abbreviation	Manufacturer	Purity
Sodium Alginate	Alginate	Spectrum Chemical	--
Gellan Gum	GG	C.P. Kelco	--
Canola Oil	Canola Oil	Kroger	--
Iso-butane	IB	Gas Innovations	99.99%
1-Butanol	1-butanol	Sigma-Aldrich	99.80%
2-Butanol	2-butanol	Sigma-Aldrich	99.00%
Tetra-butylorthosilicate	TBOS	Gelest Inc.	97.00%
Tetra-s-butylorthosilicate	T_2BOS	Gelest Inc.	95.00%
1,1,1 Trichloroethane	1,1,1-TCA	Tokyo Chemical Industry	98.00%
cis-Dichloroethene	*c*DCE	Tokyo Chemical Industry	99.00%
1,4 Dioxane	1,4-D	J.T. Baker	99.00%

3.2. Analytical Methods

3.2.1. Direct Gas Injection Gas Chromatography

All gaseous and volatile compounds (oxygen, carbon dioxide, isobutane, and chlorinated CoCs) were measured in reactors by sampling of gas headspace through septa with a 100uL gas tight Hamilton syringe followed by injection on a Hewlett Packard 5890 or 6890 series gas chromatograph (GC). A summary of the information presented below can be seen in Table 6.

Isobutane was separated within an Agilent GS-Q capillary column (30m x 0.53mm) and a response was detected using a flame ionization detector (FID). The developed method used helium as the carrier gas flowing at 15 mL/min and ran isothermally with an oven temperature of 150°C. The retention time (RT) of isobutane in the column was 0.8 minutes. Chlorinated CoCs were

separated with an Agilent DB-624 UI capillary column (30m x 0.53mm) and the signal was detected using a micro-electron capture detector (ECD). The ECD operating method ran helium as the carrier gas flowing at 15 mL/min with an isothermal oven temperature of 50°C. Using this method *c*DCE and 1,1,1-TCA were resolved and eluted at 2.0 and 2.4 minutes, respectively. Oxygen (O_2) and carbon dioxide (CO_2) signals were separated using a Supelco 60/80 Carboxen-1000 packed stainless steel column (15ft x 1/8in.) and detected using thermal conductivity detectors (TCD). The operating method developed for detecting O_2 used helium as the carrier gas flowing at 30 mL/min and an oven temperature of 40 °C, whereas, CO_2 detection required argon as the carrier gas and an oven temperature of 220 °C.

Table 6. Summary of gas chromatograph methods.

Compound	GC Column	Detector	Carrier Gas/ Flow Rate (mL/min)	Oven Temperature (°C)
Oxygen	Supelco 60/80 Carboxen 1000 Stainless Steel Packed Column	TCD	Helium / 30	40
Carbon Dioxide	Supelco 60/80 Carboxen 1000 Stainless Steel Packed Column	TCD	Argon / 30	220
Isobutane	Agilent GS-Q Capillary Column (30m x 0.53mm)	FID	Helium / 15	150
*c*DCE	Agilent DB-624 UI Capillary Column (30m x 0.53mm)	ECD	Helium / 15	50
1,1,1 - TCA	Agilent DB-624 UI Capillary Column	ECD	Helium / 15	50

Measured gas concentrations were used to calculate the total mass in reactors via Henry's Law as seen in equation 1.

$$Total\ Mass = C_g * V_g + \frac{C_g}{H_{cc}} * V_L\ , where, \qquad \text{Eqn 1}$$

$C_g =$ *Headspace Gas Concentration,* $H_{cc} =$ *Henry's Law Constant*

$V_g =$ *Volume of Headspace,* $V_L =$ *Volume of Liquid*

An important note is that, oxygen measurements below a total mass of ~180µmol are considered to be near zero due to a vacuum created in reactors from successive GC sampling and cellular respiration. The vacuum in the bottles causes the GC sampling needle to be under negative pressure and as it is removed from the reactor, some atmospheric oxygen contaminates the sample. This causes the lowest measureable O_2 concentration to be ~180µmol.

3.2.2. Direct Liquid Injection Gas Chromatography

Alcohols produced by LNAPL slow release substrates, 1- and 2-butanol, were measured by sampling 1-5uL of liquid media through reactor septa followed by direct liquid injections onto a Supelco 80/100 Carbopack-C packed column (6ft x 1/8 in.). The developed method used nitrogen as the carrier gas at a constant column pressure of 40 psi and an oven temperature of 105°C. The injection and detector port temperatures were set at 150°C and 175°C, respectively.

LNAPL slow release substrates (TPOS, TBOS, and T_2BOS) were quantified by liquid-liquid (dichloromethane-aqueous) extractions, similar to [80]. In summary, reactors were vigorously shaken for 30-60 seconds to ensure adequate homogenization of LNAPL and surrounding media. Mixed liquid samples were taken through reactor septa using 1mL liquid syringes. The sampled liquid was directly added to 1mL dichloromethane (DCM) containing ~3000 mg/L tetra-n-propoxysilane (TPOS) as an internal standard. These samples were then vortexed for 15 minutes in 4mL gas tight glass vials.

Immediately after vortexing, liquid DCM was separated from the aqueous sample and transferred into 2 mL gas tight glass auto-sampler vials with rubber septa. Vials were loaded onto a 100-sample Hewlett Packard HP 6890 Series auto-sampler that automatically injected 5uL DCM liquid samples onto a HP 6890 series GC. The GC was equipped with a Restek RTX-20 capillary column (15m x 0.53um) and an FID detector. The developed method used helium as the carrier gas flowing at 12 mL/min with an initial oven temperature of 100°C. The initial temperature was held

for one minute followed by a 35°C/minute temperature ramp to 220°C, which was held to a final run time of five minutes. DCM, TPOS, T_2BOS, and TBOS peaks were all resolved using this method at RTs of 0.8, 3.2, 3.9, and 4.3 minutes, respectively. Aqueous concentration measurements were converted to total mass in reactors and reported as total mass throughout this thesis for consistency.

3.2.3. Heated Purge and Trap Gas Chromatography Mass Spectrophotometry

Due to the relatively low vapor pressure of 1,4-D a Tekmar Dohrmann 3100 heated purge and trap was used to volatilize and concentrate liquid samples. Purging of aqueous phase 1,4-D from 5mL liquid samples was done by heating samples to 80°C for 20 minutes while bubbling nitrogen through samples at 20 mL/min. The vapor phase 1,4-D that is purged from the liquid is swept through a three-sorbent-bed trap where it is trapped. The trap is then headed and flushed with helium to desorb the 1,4-D. The concentrated gas was then injected into a HP 6890 series GC and 1,4-D was separated using a Restek Rtx-VMS column (30m x 0.2mm) and a signal was detected using a 5973 Mass Selective Detector. Deuterated 1,4-D was used as an internal standard at a concentration of 5 ppb and peaks were detected and resolved by the MS analyzing for mass to charge ratios, both peaks eluted at 7.1 minutes. Culture Growth, Storage, and Quantification

ATCC 21198 was maintained on minimal salts media (MSM) agar plates. ATCC 21198 culture plates were stored at 30°C in 3.5L gas tight jars, autoclaved prior to use. The headspace of the jars were kept at a slight positive pressure by adding 45mL pure isobutane (IB), as the carbon source. IB was refreshed each time the containers were opened to the atmosphere maintaining headspace IB levels of 1.25% (v/v). For experimentation, biomass was grown by inoculating sterile 300mL pH-7 phosphate buffered MSM in 710mL glass Wheaton bottles with a group of colonies from the agar storage plates. Ingredients of phosphate and carbonate MSM are provided in Table

7. The Wheaton bottles were sealed with a reusable screw on cap fitted with gray butyl rubber septa. New storage plates were created after about 70 percent of the colonies were used.

Table 7. ATCC 21198 mineral salts media growth-solution ingredient list.

Compound	Phosphate MSM Concentrations	Carbonate MSM Concentrations	Unit
NH4Cl	2.000	2.000	g/L
MgCl2*6H20	0.075	0.075	g/L
(NH4)2SO4	0.100	0.100	g/L
EDTA	0.010	0.010	g/L
ZnSO4*7H2O	4.40E-03	4.40E-03	g/L
CaCl2	0.001	6.01E-01	g/L
MnCl2*4H2O	1.01E-03	1.01E-03	g/L
FeSO4*7H2O	1.00E-03	1.00E-03	g/L
(NH4)6Mo7$O_2$4*4H2O	2.20E-04	2.20E-04	g/L
CuSO4*5H2O	3.01E-04	3.01E-04	g/L
CoCl2*6H2O	3.42E-04	3.42E-04	g/L
NaHCO3	--	1.34	g/L
K2HPO4	1.55	--	g/L
NaH2PO4	0.85	--	g/L
pH	7	7	--
Estimated Ionic Strength	0.040	0.043	mol/L

Additions of IB as a primary growth substrate were made to growth bottles through the septa. Electron-donor equivalent masses of IB were added such that the oxygen in the 410 mL air headspace could oxidize two thirds of the added substrate; this was done to ensure a constant substrate rich growth environment. An initial addition of IB was made at growth reactor setup followed by 4 days of shaking at 200 rpm on a rotary shaker table in a 30°C temperature controlled room. After initial growth, the reactors received a headspace air, oxygen, refresh by removing the cap and allowing to set in a laminar flow hood for 10 min. Caps were replaced and a second spike of IB was added. After another 24 hours on the shaker table, the cultures were at peak exponential growth phase and ready to be harvested and used for experimentation. Cells were harvested by

centrifugation at 15,000G for 10 minutes followed by washing and re-suspension in 50mM pH-7 phosphate buffer. All cells were streaked on a non-specific tryptic-soy growth agar to ensure purity prior to experimental use. Cells were typically used in experiments the day of harvesting; however, occasionally cells were used 4 days after harvesting. In these cases, cells were stored in phosphate buffer at 4 °C. All cell mass values reported in this thesis are based on total suspended solids (TSS) analysis of harvested cultures. The TSS of concentrated cells was quantified via vacuum filtration of a known volume of cells through an Advantec 0.45um mixed cellulose-ester membrane filter and drying at 105°C for 30 minutes.

3.3. Microbial Encapsulation

3.3.1. Alginate Encapsulation

External crosslinking methods for the successful encapsulation of *Rhodococcus Rhodochrous* ATCC 21198 in stable alginate macro spheres, 2mm in diameter, were adapted from the literature [87,93,94]. A 2% stock of alginate pre-gel solution was created by hydrating alginate powder in heated 200mL Nanopure water. Nanopure water was heated to 85°C on a hot plate while being constantly mixed with a magnetic stir bar. When the liquid reached 85°C, an addition of sodium alginate powder was made to achieve a final concentration of 2% (w/w) alginate. The pre-gel solution was mixed for 30 minutes to ensure complete hydration, followed by autoclaving at 121°C for 15 minutes to degas and ensure the final pre-gel solution was sterile. The pre-gel solution was allowed to cool to room temperature prior to use for encapsulation. Typically, alginate pre-gel solution was used for experimentation the day of creation, but on occasion was used up to four days later. Pre-gel solution was stored at room temperature in a gas tight jar.

For microbial encapsulation, a known volume of room temperature pre-gel solution was transferred to a 50mL Falcon tube and the pH was adjusted to seven. Adjustment of pH was done by making additions of dilute hydrochloric acid (HCl) or by a single addition of concentrated pH-

7 phosphate buffer to achieve a final concentration of 4mM total phosphate. In either case, the volume of liquid added to correct for pH changed the final volume less than 1%. After the pH was adjusted, a known volume of concentrated cell slurry suspended in 50mM phosphate buffer was added to the alginate pre-gel solution and vortexed for 30 seconds. Cell masses were added to obtain a desired final cell concentration in beads, reported throughout this thesis as mg cells as TSS per gram of bead (mg_{TSS}/g_{bead}).

Following the addition of cells, the pre-gel solution was transferred to 5-20mL Luer lock liquid syringes fitted with a 25 gauge x 1 inch needle. The pre-gel solution was then extruded into 900mL of 0.25-1% calcium chloride ($CaCl_2$) solution from a distance of 2-5cm above liquid surface (Figure 4). $CaCl_2$ solution was continuously mixed with a magnetic stir plate at 150-250rpm. The beads were allowed to crosslink for a total of 60 minutes, measured from the time that the last bead was formed.

Figure 4. Calcium-alginate macro-bead formation by extrusion into crosslinking solution.

Microbially active macro-beads were separated from the crosslinking solution via filtration using a vacuum pump fitted with a 70mm plastic filter funnel. The filtered beads were washed three times with pH-7 carbonate buffered MSM and dried a final time using the vacuum pump. The final mass of beads was measured with minimal exogenous liquid and an assumption was made that all cells added to pre-gel solution were encapsulated. Using the known mass of cells added and the measured final mass of beads created a cell mass loading was calculated as mg_{TSS}/g_{bead}. Typically, microbially active beads were used for experimentation the day they were made; however, on occasion beads were stored overnight in pH-7 carbonate buffered MSM at 4°C.

Figure 5. Gelated alginate macro-beads with a VWR ruler for scale.

3.3.2. Gellan Gum Encapsulation

i. Micro-encapsulation

The method used for the micro-encapsulation of ATCC 21198 in gellan gum was developed in the early 2000s by researchers at McGill and Queen's Universities [79]. An attempt was made to replicate the optimized method in full; though, due to lab equipment limitations some parts were altered. A summary of the method used is presented below and graphically in Figure 7.

Gellan gum pre-gel stock solution was made in a 200mL volume of autoclaved 2mM pH-7 phosphate buffered Nanopure water in a 250mL Pyrex glass bottle. Gellan gum powder was added

immediately after removing the solution from the autoclave to achieve a concentration of 0.75% (w/v). The pre-gel solution was shaken vigorously for 30 seconds and placed on a heated magnetic stir plate keeping the solution at ~85°C while mixing at 200rpm for 30 minutes. After complete hydration of gellan gum powder, a known volume of pre-gel solution was transferred to a 50mL Falcon tube. To initiate gelation an appropriate volume of 10% $CaCl_2$ stock solution was added to make a final concentration of 0.06% (w/v). The Falcon tube lid was replaced and the solution was vortexed for 30 seconds. The pre-gel solution was then left at room temperature to cool to ~60°C at which time the pH was adjusted to seven with dilute NaOH, if necessary. The pre-gel solution was again left at room temperature to cool to ~45°C before adding a known volume of concentrated cell slurry that was suspended in 50mM phosphate buffer. At this point, the pre-gel solution was finalized and ready for complete gelation.

To form gellan gum microspheres the pre-gel solution was added directly to an appropriate amount of heated canola oil, at ~45°C, to achieve a disperse phase volume fraction of 0.15. To increase emulsion stability Span-80 was added at 0.1% (v/v) and the entire solution was transferred to a 125mL wide-mouth glass beaker (Figure 7, Stage 1). The canola oil and pre-gel solution were then mixed with an IKA RW-20 digital overhead impeller mixer at 2500rpm for 10 minutes (Figure 7, Stage 2). The impeller blade was ~5cm in diameter and was positioned 1/3 the way up from the bottom of the vial to the top of the liquid mixture (Figure 6).

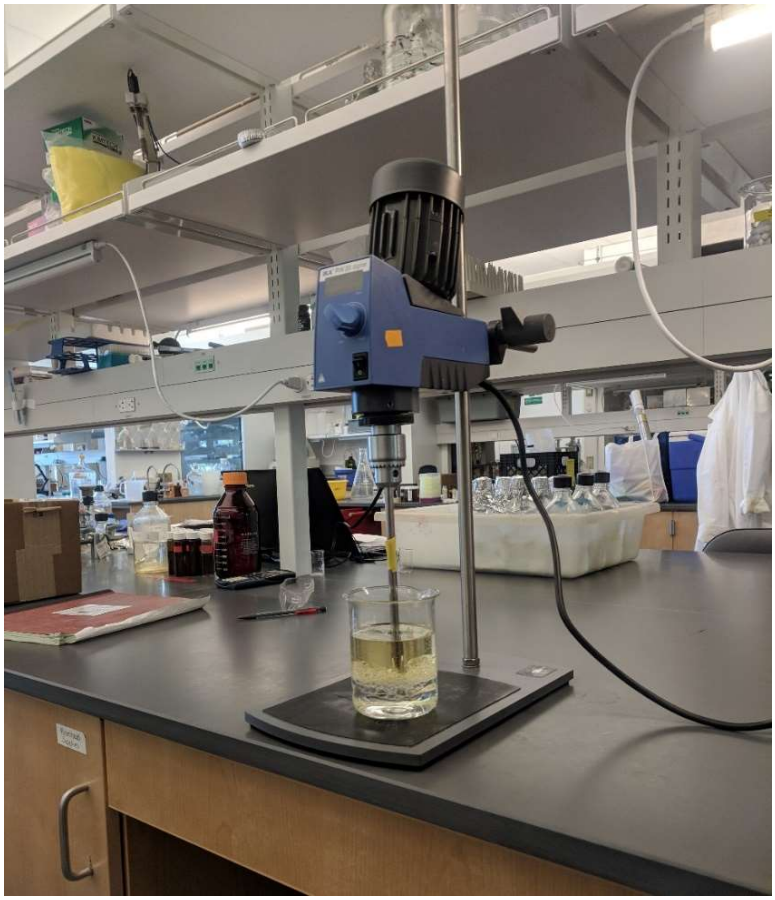

Figure 6. IKA RW 20 digital overhead impeller mixer set up for gellan gum emulsification within canola oil.

To force gelation of emulsified gellan gum droplets, the emulsified solution was transferred to an ice bath and cooled until the solution reached a temperature of 15°C (Figure 7, Stage 3). The canola oil and micro-bead mixture was stirred slowly at room temperature for 90 minutes to begin separation of micro-beads from canola oil. The mixture was then transferred to a 1L beaker containing 500mL of 0.25% (w/v) $CaCl_2$ solution to allow beads to partition into the aqueous phase and increase bead stability (Figure 7, Stage 4). A large portion of canola oil was removed by aspiration. However, a separatory funnel was necessary to achieve complete separation (Figure 7, Stage 5). Micro-beads were removed from the $CaCl_2$ solution using a vacuum pump fitted with a 1.2um glass fiber filter and washed repeatedly with pH-7 carbonate buffered MSM. To calculate

the final mass loading of cells in beads as mg_{TSS}/g_{bead}, assumptions were made that 1mL of pre-gel solution would form 1g of beads and that all cells added were encapsulated. Typically, microbially active beads were used for experimentation the day they were made; however, on occasion beads were stored overnight in a pH-7 carbonate buffered MSM at 4°C.

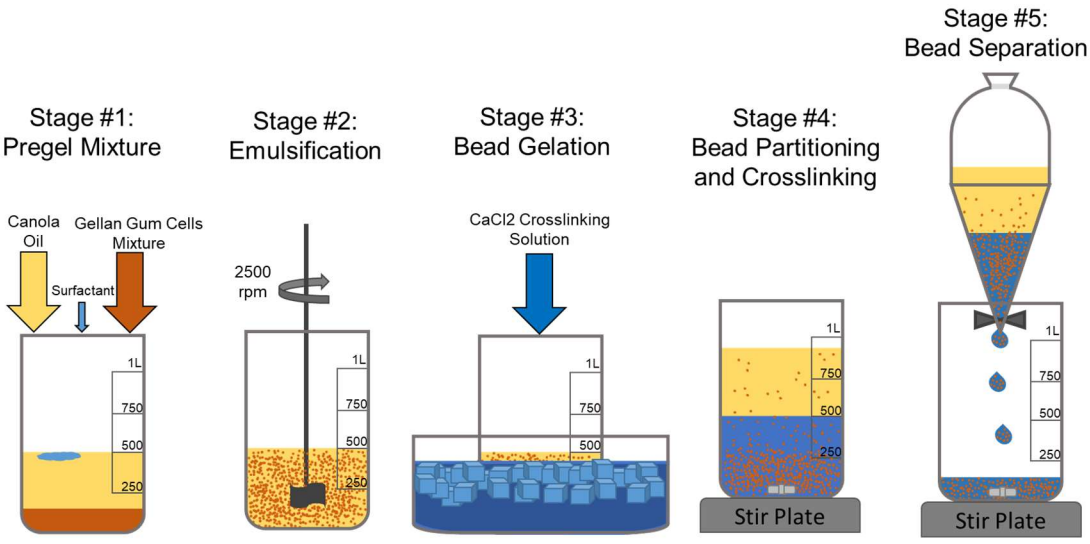

Figure 7. Graphical representation of the method developed for the generation of gellan gum microspheres though a gellan gum emulsification internal gelation method.

Micro-beads made using the above method ranged in size from ~10-100µm in diameter, as determined through repeated bright field images taken with a Leica DM 2500 benchtop microscope.

ii. Macro-encapsulation

Methods beyond what is contained in the literature for gellan gum were developed as part of this thesis in order to encapsulate ATCC 21198 in gellan gum macro-beads. The method developed follows a similar procedure presented by [112,113] in which cylindrical macro-beads were created. It became necessary to develop this method to meet key project objectives, including proof of overarching concept. The detailed method presented below is a summary of the optimized gellan gum macro-encapsulation method.

The preparation of gellan gum pre-gel solution followed the same procedure as the above section 3.4.2.i to the point just before gellan gum emulsification in canola oil. In summary a 0.75% (w/v) gellan gum pre-gel solution was prepared in autoclaved ~2mM pH-7 phosphate buffered nanopure water at ~85°C. A $CaCl_2$ solution was added to the pre-gel solution to a final concentration of 0.06% (w/v) $CaCl_2$. The solution was allowed to cool to ~60°C and the pH was adjusted to seven. The solution was then cooled to ~45°C and cells were added. At this point the pre-gel solution was finalized and ready for gelation.

To create macro-beads from the warm pre-gel solution a 60mL plastic syringe was used to draw the solution into an attached 1.5m section of flexible rubber tubing with an inner diameter of ~2mm (Figure 8). Once the tubing was filled with pre-gel solution, it was coiled and set on ice to cool to ~15°C to finish gelation and completely solidify all gel within the tubing. After cooling to ~ 15°C, the gel-filled tubing was placed in a laminar flow hood for 60 minutes to provide extra time for internal crosslinking prior to extrusion of thin cylindrical sections of gel from the tubing. In the laminar flow hood, the hardened gellan gum was pushed from the tubing onto long sections of Parafilm using the attached 60mL syringe filled with air or a buffer solution (Figure 9). The extruded sections of hardened gellan gum were ~2mm in diameter by ~15-30cm in length. A razor blade was used to cut the long sections into ~2mm sections such that the height of each cylinder was approximately the same as the diameter (Figure 10).

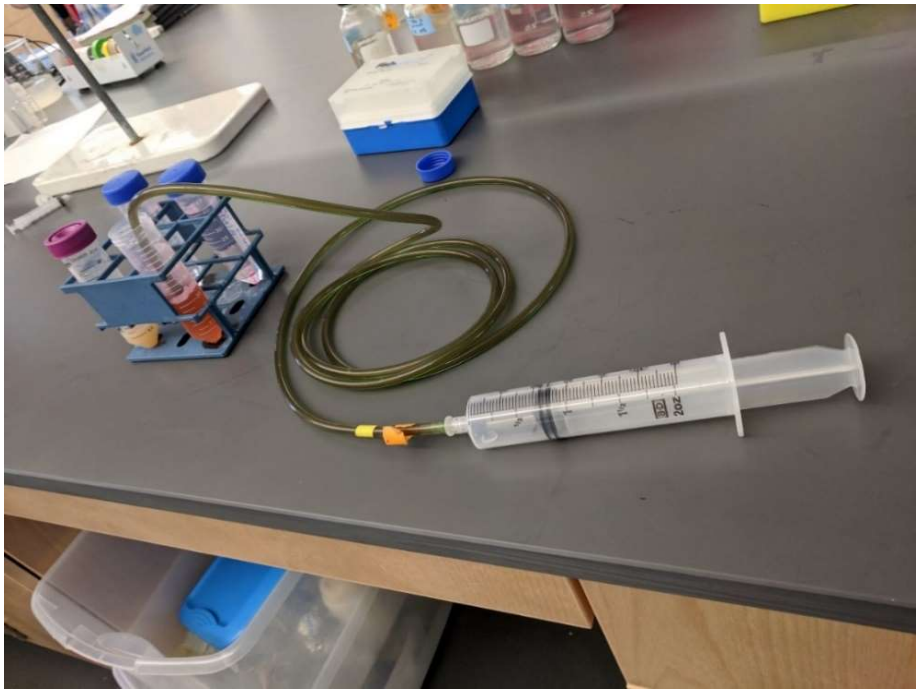

Figure 8. Gellan gum macro-bead generation step 1. Warm gellan gum pre-gel solution is drawn into the green tubing with a 60mL syringe. Orange dye was added such that GG pre-gel solution could be better visualized.

Figure 9. Extrusion of solidified gellan gum cylindrical sections from rubber tubing onto Parafilm. Orange dye was added such that GG pre-gel solution could be better visualized.

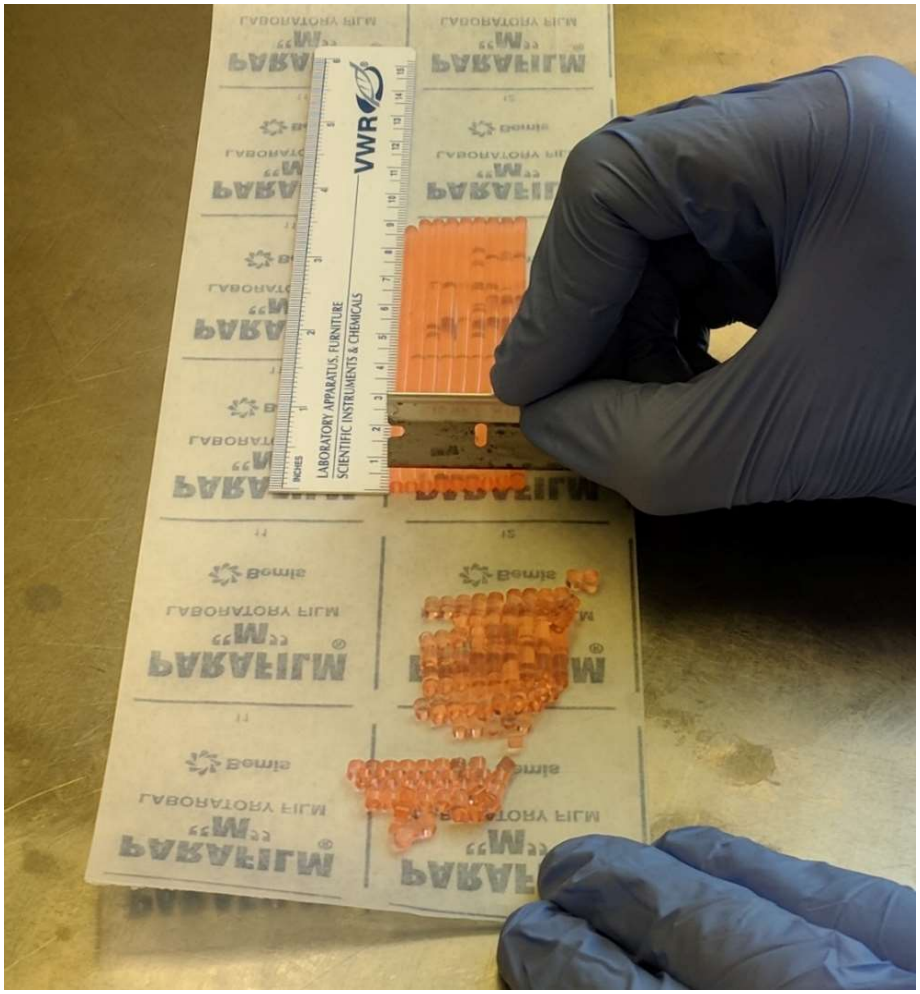

Figure 10. Manual cutting of gellan gum strands into 2mm right cylinders for experimental use. Orange dye was added such that GG pre-gel solution could be better visualized.

At this point, the cylinders were allowed to cure for 10 minutes in the laminar flow hood before being transferred to a 1L beaker containing 500mL of 0.25% (w/v) $CaCl_2$ solution for 60 minutes. Microbially active macro-beads were separated from the external crosslinking solution using a vacuum pump fitted with a 70mm plastic filter funnel. The filtered beads were washed three times with pH-7 carbonate buffered MSM and dried a final time using the vacuum pump. The final mass of beads was measured with minimal exogenous liquid and an assumption was made that all cells added to pre-gel solution were encapsulated. To calculate the final mass loading of cells in beads as mg_{TSS}/g_{bead}, assumptions were made that 1 mL of pre-gel solution would form 1g of beads

and that all cells added were encapsulated. Typically, microbially active beads were used for experimentation the day they were made; however, on occasion beads were stored overnight in pH-7 carbonate buffered MSM at 4°C.

3.4. Slow Release Compound Encapsulation

3.4.1. Alginate SRC Encapsulation

The methods used to encapsulate LNAPL SRCs in alginate were adapted from Soliman et al. (2013). who developed an emulsification based method to encapsulate essential oils at mass loadings as high as 30% (w/w) in alginate microspheres, ~500um in diameter [114]. The final method followed the same approach to make 2% (w/v) alginate pre-gel solution as section 3.4.1 above. Alginate was added to warm Nanopure water and mixed for 30 minutes to complete hydration, and was then autoclaved. After removing the alginate pre-gel solution from the autoclave a known amount, typically around 40-50mL, was transferred to a 125mL wide mouth glass vial and allowed to cool to ~70°C.

After the solution cooled, Span-80 emulsifier was added to achieve a concentration of 0.1% (v/v). A known volume of LNAPL SRC was added to the pre-gel solution and the mixture was emulsified using an IKA RW 20 digital overhead impeller mixer at 2500rpm for 10 minutes. Following emulsification, the pre-gel solution was transferred to a 50mL Falcon tube and allowed to cool to ~45°C. The pH was then adjusted to seven by addition of pH-7 phosphate buffer to achieve a final concentration of 4mM total phosphate. If co-encapsulation of cells was desired a known volume of concentrated cell slurry suspended in 50mM phosphate buffer was added at this point to the SRC containing alginate pre-gel solution and vortexed for 30 seconds. Following the addition of cells or just after pH adjustment, the emulsified pre-gel solution was transferred to 5-20mL liquid syringes fitted with a 25 gauge x 1 inch needle. The pre-gel solution was then extruded into 900mL of 0.25% (w/v) $CaCl_2$ solution from a distance of 2-5cm above liquid surface (Figure

4). $CaCl_2$ solution was continuously mixed with a magnetic stir plate at 150-250rpm. The beads were allowed to crosslink for a total of 60 minutes measured from the time that the last bead was formed.

Macro-beads containing SRCs were separated from the crosslinking solution using a vacuum pump fitted with a 70mm plastic filter funnel. The beads were washed three times with a 0.1% (v/v) Tween-80 sterile microbe safe soap wash to rinse any exogenous SRCs from their surface. This was followed by rinsing three times with pH-7 carbonate buffered MSM and dried a final time using the vacuum pump. The final mass of beads was measured with minimal exogenous liquid and an assumption was made that all cells added to pre-gel solution were encapsulated. Using the known mass of cells added, and the measured final mass of beads created, a cell mass loading was calculated as mg_{TSS}/g_{bead}. Typically, microbially active beads were used for experimentation the day they were made; however, on occasion beads were stored overnight in pH-7 carbonate buffered MSM at 4°C.

To determine the SRC mass loading in beads as g_{SRC}/g_{bead} and encapsulation efficiency of this process, two ~0.25g samples of beads were taken and transferred into 27 mL vials containing 10mL of 2mM sodium citrate solution. These vials were placed on a shaker table shaking at 250rpm for 90 minutes. Sodium citrate solution was used to chelate calcium and help break apart the alginate spheres such that any encapsulated SRC was released into solution. The amount of released SRC was quantified using the DCM extraction method presented in section 3.2.2. Using the measured mass of SRC released and the known initial mass of beads broken down a mass loading could be determined (g_{SRC}/g_{bead}). The process encapsulation efficiency, the percent of added SRC that was successfully encapsulated, was then determined from the measured mass loading (g_{SRC}/g_{bead}), the measured final mass of beads (g_{bead}), and the known mass of SRC added

3.4.2. Gellan Gum SRC Co-encapsulation

i. Micro-encapsulation

Methods for the microencapsulation of SRCs were explored during this thesis but little success or progress was achieved. Future work on this project will focus on development of methods to encapsulate SRCs in micro-beads ranging in size from 10-40μm.

ii. Macro-encapsulation

The encapsulation of LNAPL SRCs in gellan gum macro-beads required a single additional step to the microbial encapsulation method presented in section 3.4.2.ii above. That step was emulsification of SRCs within autoclaved gellan gum pre-gel solution prior to adding $CaCl_2$ crosslinking solution. For clarity, the entire process is presented below.

Gellan gum pre-gel stock solution was made in a 200 mL volume of autoclaved 2mM pH-7 phosphate buffered nanopure in a 250mL Pyrex glass bottle. Gellan gum powder was added immediately after removing the solution from the autoclave to achieve a concentration of 0.75% (w/v). The pre-gel solution was shaken vigorously for 30 seconds and placed on a heated magnetic stir plate keeping the solution at ~85°C while mixing at 200rpm for 30 minutes. After complete hydration of gellan gum powder, a known volume of warm pre-gel solution, typically 40-50mL, was transferred to a 125mL wide mouth glass vial. Span-80 emulsifier was added to achieve a concentration of 0.1% (v/v). A known volume of LNAPL SRC was then added to the pre-gel solution and the mixture was emulsified using an IKA RW 20 digital overhead impeller mixer at 2500rpm for 10 minutes. Following emulsification, the pre-gel solution was heated back to ~80°C and transferred to a 50mL Falcon tube. To initiate gelation an appropriate volume of 10% $CaCl_2$ stock solution was added to make a final concentration of 0.06% w/v. The Falcon tube lid was replaced and the solution was vortexed for 30 seconds. The pre-gel solution was then left at room temperature to cool to ~60°C before the pH was adjusted to seven with dilute NaOH, if necessary.

If co-encapsulation of cells was desired, the pre-gel solution was again left at room temperature to cool to ~45°C before adding a known volume of concentrated cell slurry that was suspended in 50mM phosphate buffer. At this point, the pre-gel solution was finalized and ready for complete gelation.

To create macro-beads from the warm pre-gel solution a 60mL plastic syringe was used to draw the emulsified SRC containing pre-gel solution from the Falcon tube into an attached 1.5m section of flexible rubber tubing with an inner diameter of ~2mm (Figure 8). Once the tubing was filled with pre-gel solution, it was coiled and set on ice to cool to ~15°C to finish gelation and completely solidify all gel within the tubing. After cooling to ~15°C the gel filled tubing was placed in a laminar flow hood for 60 minutes to provide extra time for internal crosslinking prior to extrusion of thin cylindrical sections of gel from the tubing (Figure 9). In the laminar flow hood, the hardened gellan gum was pushed from the tubing onto long sections of Parafilm using the attached 60mL syringe filled with air or a buffer solution. The extruded sections of hardened gellan gum were ~2mm in diameter by ~15-30cm in length. A razor blade was used to cut the long sections into ~2mm sections such that the height of each cylinder was approximately the same as the diameter (Figure 10).

The cylinders were allowed to cure for 10 minutes in the laminar flow hood before being transferred to 1L beaker containing 500 mL of 0.25% (w/v) $CaCl_2$ solution for 60 minutes. Microbially active macro-beads were separated from the external crosslinking solution using a vacuum pump fitted with a 70mm plastic filter funnel. To rinse any exogenous SRCs from the surface of beads they were washed three times with a 0.1% (v/v) Tween-80 sterile microbe safe soap wash. Followed by rinsing three times with pH-7 carbonate buffered MSM and dried a final time using the vacuum pump. The final mass of beads was measured with minimal exogenous liquid and an assumption was made that all cells added to pre-gel solution were encapsulated. To

calculate the final mass loading of cells in beads as mg_{TSS}/g_{bead}, assumptions were made that 1mL of pre-gel solution would form 1g of beads and that all cells added were encapsulated. Typically, microbially active beads were used for experimentation the day they were made; however, on occasion beads were stored overnight in pH-7 carbonate buffered MSM at 4°C.

To determine the SRC mass loading in beads as g_{SRC}/g_{bead} and encapsulation efficiency of this process, two ~0.25g samples of beads were taken and transferred into 27mL vials containing 10mL of 2mM sodium citrate solution. These vials were heated to ~°80C then placed on a shaker table shaking at 250rpm for 120 minutes. Sodium citrate was used to chelate calcium and help break apart the gellan gum cylinders such that any encapsulated SRC was released into solution. Due to the increased stability of gellan gum cylinders over alginate macrospheres, heating and excess physical agitation of gellan gum cylinders was required to ensure all encapsulated SRC was released.

The amount of released SRC was quantified using the DCM extraction method presented in section 3.2.2. Using the measured mass of SRC released and the known initial mass of beads broken down a mass loading could be determined. The process encapsulation efficiency, the percent of added SRC that was successfully encapsulated, was then determined from the measured mass loading (g_{SRC}/g_{bead}), the measured final mass of beads (g_{bead}), and the known mass of SRC added.

3.5. Batch Kinetic Studies

3.5.1. Encapsulation Assessment Studies

Short-term primary substrate utilization tests, that often lasted less than 24 hours, were used to determine the immediate effect encapsulation had on cell viability. These batch reactor tests were conducted at a constant 20 °C in glass 27mL crimp top vials sealed with gray butyl rubber septa (Figure 11). Ten mL of pH-7 carbonate buffered MSM was added to each sterile vial followed by an addition of a known mass of suspended, encapsulated, or co-encapsulated ATCC 21198, ranging

from 0.5-5mg cells as TSS. The determined encapsulated cell mass loadings as g_{TSS}/g_{bead} were used to calculate the necessary mass of beads to add to each reactor. For ease of comparison, attempts were made to keep the total suspended and encapsulated cell masses added to each reactor the same between each experiment.

Following addition of cells, septa were added and crimped in place to seal vials. Pure isobutane gas was provided as the primary substrate through the septa using a plastic 1mL Luer Lock syringe. Typically, ~8µmol of IB was added to each vial. Vials were shaken rapidly on a rotary shaker table at 200rpm throughout the experiment to ensure constant equilibration of added IB. The assumption was made that cellular utilization rates of IB were slower than the diffusion rate of IB into solution such that equilibrium between the liquid and gas phase of IB was constantly maintained and measured gas concentrations could be used to predict liquid concentrations and total mass of IB in reactors, through Henry's law (Equation 1).

Figure 11. Short-term batch substrate (IB) utilization kinetic tests.
(Left two bottles) Abiotic (Middle two bottles) Suspended cells. (Right two bottles) Encapsulated cells.

IB gas concentrations were monitored using GC methods presented in section 3.2.1 and the total mass of IB remaining in each reactor was calculated using equation 1. Dependent on the mass of cells added and the rate at which IB was being consumed, IB concentrations were monitored every 20-60 minutes to develop a defined cellular IB utilization curve. Substrate utilization rates

were calculated through linear regression of the collected IB mass data and normalized to the cell mass added to each reactor. Substrate utilization rates were presented as, μmol_{IB}/day-mg_{TSS}. Suspended cell IB utilization rates were used as a benchmark to assess the effect encapsulation had on cellular viability.

In each test, abiotic reactors were used to ensure disappearance of IB was related to cellular utilization. Also, kinetic testing was conducted with duplicate or triplicate reactors to ensure reliable and repeatable data sets.

3.5.2. Long-Term Batch Cometabolic transformation Studies

i. CoC Mixtures Transformation

Batch kinetic reactors were used to evaluate the long-term, weeks to months, remediation performance of suspended, encapsulated, and co-encapsulated cells. These batch kinetic tests were conducted at a constant 20°C in 155-310mL glass Wheaton bottles sealed with reusable screw on caps fitted with gray butyl rubber septa (Figure 12). Reactors were filled with 100-200mL of pH-7 carbonate buffered MSM followed by an addition of suspended, encapsulated, or co-encapsulated cells to achieve an initial cell mass concentration of 10 mg/L as TSS. Encapsulated bead cell mass loadings as g_{TSS}/g_{bead} were used to calculate the necessary mass of beads to add to each reactor. For ease of comparison, and attempt was made to keep all encapsulated cell mass loadings at 0.5 mg_{TSS}/g_{bead} and the total suspended and encapsulated cell mass added to each reactor between each experiment was kept constant at ~10 mg/L.

Due to mixtures being frequently observed at sites of concern to the DoD this thesis has focused on the bioremediation potential of ATCC 21198 to transform a mixture of 1,1,1-TCA, *c*DCE, and 1,4-D. All reactors in all of the transformation experiments presented below received initial and/or successive spikes of environmentally relevant concentrations of each contaminant ~250-1000 ppb. CAHs were added via additions of saturated Nanopure liquid solutions through

reactor septa and 1,4-D was added by dilution of a 1000 ppm stock solution. The solubility of CAHs can be seen in Table 2.

Reactors were monitored over a period of ~30-200 days for respiration data (O_2/CO_2), substrate data (SRC/alcohols), and contaminant data (1,1,1-TCA, *c*DCE, and 1,4-D) according to methods presented in section 3.2.1.

Abiotic controls were used to ensure transformation of CoC mixtures was biotic. Also, to monitor the potential mass of substrate being released from encapsulated SRCs, long-term reactors that mimicked active co-encapsulated cell reactors were created, then poisoned with 2% (w/v) sodium azide to ensure cells would not consume the hydrolysis byproducts, 1- or 2-butanol, of added SRCs. These bottles were not spiked with contaminants but were monitored for respiration and substrate data to determine an experimental hydrolysis rate of substrates.

Figure 12. Long-term CoC transformation reactors. Abiotic, Suspended ATCC 21198, and Gellan Gum Encapsulated ATCC 21198 in duplicate reactors, left to right, respectively.

3.5.3. Abiotic Hydrolysis Experiments

Batch reactors similar to the CoC transformation reactors presented in section 3.6.2 were used to determine the rate of hydrolysis of TBOS and T_2BOS free suspended in solution and encapsulated at different mass loadings in both alginate and gellan gum. These batch kinetic tests

were conducted at a constant 20°C in 155mL glass Wheaton bottles sealed with reusable screw on caps fitted with gray butyl rubber septa (Figure 12). Reactors were filled with 100mL of pH-7 carbonate buffered MSM followed by an addition of free suspended or encapsulated SRCs. The total mass of SRC added to each reactor was dependent on various parameters but ranged from 1000-1500 mg/L. All hydrolysis rates observed here were abiotic hydrolysis rates, which was ensured by the addition of 0.2% (w/v) sodium azide as a microbial poison and typically measurements of respiration data (O_2/CO_2).

CHAPTER 4 – RESULTS AND DISCUSSION

4.1. Overview and Introduction

The work presented below was conducted with the overarching aim of developing experimental techniques to test the following hypothesis:

> *If ATCC 21198 is successfully co-encapsulated with SRSs, the encapsulated microbial population will consume substrates as they are produced within beads, and the energy gained by cells from the consumption of SRS products will extend the duration of cometabolic transformation and increase the total mass of CoCs an initial population of ATCC 21198 can degrade.*

The following chapter has been separated into broad sections that follow objectives outlined to test the above hypothesis:

1. Adapt, develop, and optimize encapsulation techniques for the model-cometabolizing microorganism, *Rhodococcus Rhodochrous* ATCC 21198.
2. Assess the short and long-term effect of optimized encapsulation methods on the ability of ATCC 21198 to utilize substrates and transform mixtures of CoCs.
3. Adapt, develop, and optimize encapsulation techniques for the encapsulation of LNAPL SRSs and assess the effect of encapsulation on the production of SRS products.
4. Develop co-encapsulation techniques for SRSs and model microorganisms and determine the ability of non-inducing, and inducing SRS products to increase and extend the successful cometabolism of mixtures of CAHs and 1,4-D by encapsulated microbes.

When necessary brief experimental descriptions are provided in the overview portion of each results section; however, experimental methods presented in detail in Chapter 3 are referenced when possible. This thesis focused on the encapsulation of ATCC 21198 (a model isobutane utilizing microorganism capable of cometabolic transformation of a wide range of CoCs) in two hydrogel matrices (alginate and gellan gum) with the slow release compounds TBOS and T_2BOS

(alcohol-releasing orthosilicate compounds that hydrolyze to produce 1- and 2-butanol, respectively).

Alginate was chosen as the initial encapsulation matrix due to the ease of encapsulation (Section 3.4, 3.5, 4.2). However, issues with the stability of alginate arose and literature review led to the selection and investigation of gellan gum as an alternative hydrogel matrix with greater durability (Section 2.6). Orthosilicate compounds were investigated as SRSs due to their low solubility in water, low human health concerns, historical work with hydrolysis rates, production of alcohols that have been shown to be inducing growth substrates for ATCC 21198, and their availability and low cost. In addition to this, data collected prior and in parallel to this project investigated 1- and 2-butanol as IGSs for ATCC 21198. It was determined that growth occurred on both alcohols; however, results suggested that no immediate induction of cometabolic enzymes occurred with growth on 1-butanol, but induction was observed with growth on 2-butanol. Though induction of cometabolic monooxygenase enzymes was observed in ATCC 21198 when grown on the branched alcohol, 2-butanol, the degree of induction was lesser than ATCC 21198 grown on the primary substrate isobutane (IB).

4.2. Microbial Encapsulation Method Development and Optimization

4.2.1. Experimental Overview

Short-term isobutane utilization tests, presented in section 3.6.1, were used to determine the impact of encapsulation in hydrogel beads on ATCC 21198. Reactors containing a similar mass of suspended or encapsulated biomass were created and an addition of IB was made to each reactor. The disappearance of IB was monitored over time and utilization rates were calculated via linear regression of the measured decrease in IB mass over time, presented as (μmol_{IB}/day-mg_{TSS}). Suspended cell utilization rates were measured during each experiment due to possible differences in utilization rates between different growth batches of cells. Measured suspended cell rates were

used as a benchmark to assess the effects of encapsulation on a particular batch of cells. Reactors were created in duplicate or triplicate to ensure repeatable data and abiotic controls were used to ensure the disappearance of isobutane was related to added biomass.

4.2.2. Alginate Encapsulation of ATCC 21198

The initial alginate encapsulation method tested was adapted from [93] in which a 2% (w/v) pre-gel alginate solution was made followed by an addition of a known mass of concentrated cells suspended in phosphate buffer. The pre-gel solution was then extruded into a 1% (w/v) $CaCl_2$ crosslinking solution.

It was found that encapsulation of ATCC 21198 in alginate with this initial recommended method, produced stable macro-beads, ~2.5mm in diameter, but cellular IB utilization rates were reduced by ~60% after encapsulation. (Figure 13) (Table 8).

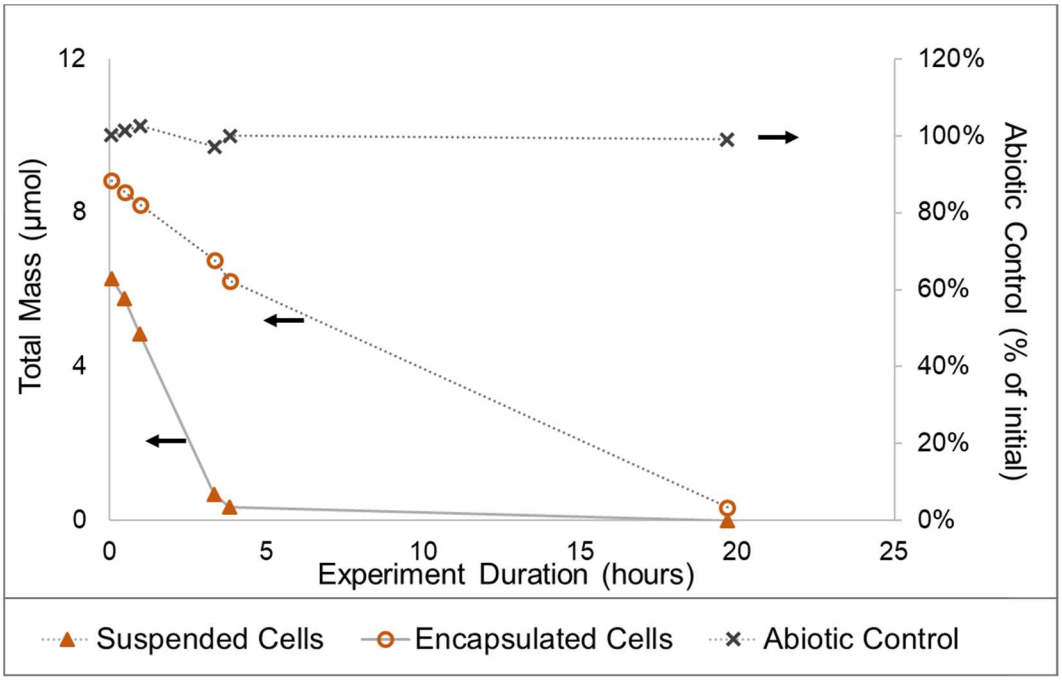

Figure 13. Isobutane utilization curve measured for ATCC 21198 suspended in media and encapsulated in alginate prior to the optimization of encapsulation techniques. Black arrows signify the axis that time-series correspond to.

Table 8. Alginate encapsulated cell viability assessment prior to encapsulation method optimization. Percent difference is calculated as the percent change from suspended cell utilization rates to encapsulated cell utilization rates.

Treatment	Calculated IB Utilization Rate (µmol/day/mg$_{TSS}$)	Percent Difference from Suspended
Suspended Cells	17	--
Alginate Encapsulated Cells	6.4	-62.60%

Despite the fact that encapsulated cells consumed IB at reduced rates, these results provided positive evidence that ATCC 21198 could be encapsulated and maintain substrate utilization activity. It was expected that encapsulation would reduce utilization rates due to possible reduction of cell access to substrates from diffusion limitations, though this significant of a decrease was not expected [13,89,90]. To investigate the observed activity loss further several encapsulation method parameters; such as the ionic strength and concentration of alginate pre-gel solution, $CaCl_2$ crosslinking concentrations, and $CaCl_2$ crosslinking durations; were altered incrementally in subsequent experiments.

From this incremental optimization it was determined that an addition of concentrated pH-7 phosphate buffer to the alginate pre-gel solution to a final concentration of ~4mM prior to addition of cells was essential to ensure a favorable environment for the added cells, likely due to assurance of correct pH and ionic strength. Also, it was found that the higher crosslinking concentration of 1% $CaCl_2$ suggested by [93] was likely causing cell lysis due to high osmotic stress. The concentration of the crosslinking solution was lowered to 0.25% (w/v) $CaCl_2$ in the final method, which was on the lower end of the range recommended by Soliman et al. (2013). Optimization of these two parameters led to a drastic improvement in alginate encapsulated cell viability (Figure 14) (Table 9).

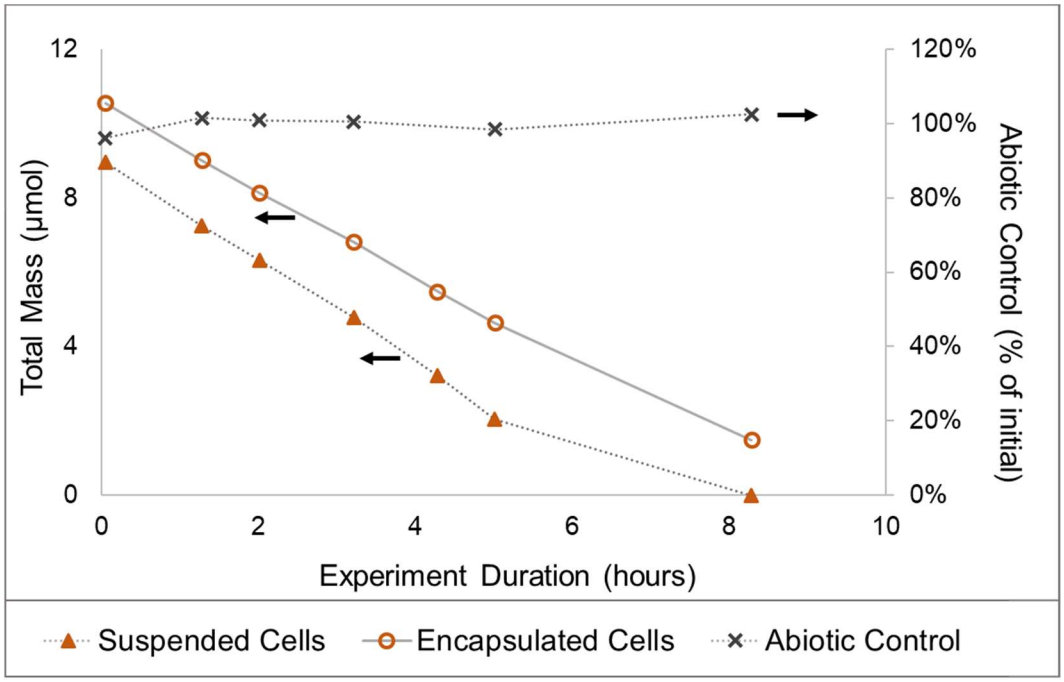

Figure 14. Isobutane utilization curve measured for ATCC 21198 suspended and encapsulated after optimization. Black arrows signify which axis time-series correspond to.

Table 9. Optimized alginate encapsulated cell viability assessment. Percent difference is calculated as the percent change from suspended cell utilization rates toencapsulated cell utilization rates.

Treatment	Calculated IB Utilization Rate (µmol/day/mg$_{TSS}$)	Percent Difference from Suspended
Suspended Cells	15.8	--
Alginate Encapsulated Cells	14.2	-10.1%

In the final method developed as part of this thesis for the encapsulation of ATCC 21198 in alginate macro-beads, it was found that cells retain around 90% of their original activity and beads were highly stable in carbonate buffered MSM for at least 24 hours. Subsequent long-term experiments provided evidence that alginate macrospheres are stable for several months, even while shaking quickly, ~100rpm, on a rotary shaker table (Section 4.3).

4.2.3. Gellan Gum Encapsulation of ATCC 21198

i. Macro-beads

Due to similarities between the hysteresis gelation mechanism of agarose and gellan gum, initial methods for the encapsulation of ATCC 21198 in gellan gum macro-beads were adapted from [103] where microbes were encapsulated in half sphere agarose macro-beads by extruding droplets of heated pre-gel solution onto a hydrophobic surface and allowing to cool at room temperature to gelate (Figure 15 A). This method produced stable gellan gum macro-beads with viable microbial cultures as determined from batch isobutane utilization tests (data not shown). However, encapsulation using this method produced beads of irregular size and shape and encapsulation of LNAPL SRSs via this method was not possible (Section 4.4.2). Due to these issues, the method presented in section 3.4.2 was developed and initial attempts to encapsulate ATCC 21198 with this method produced stable and uniform cylindrical macro-beads containing ATCC 21198 (Figure 15 B), that experienced minimal to no effect on substrate utilization (Figure 17 B).

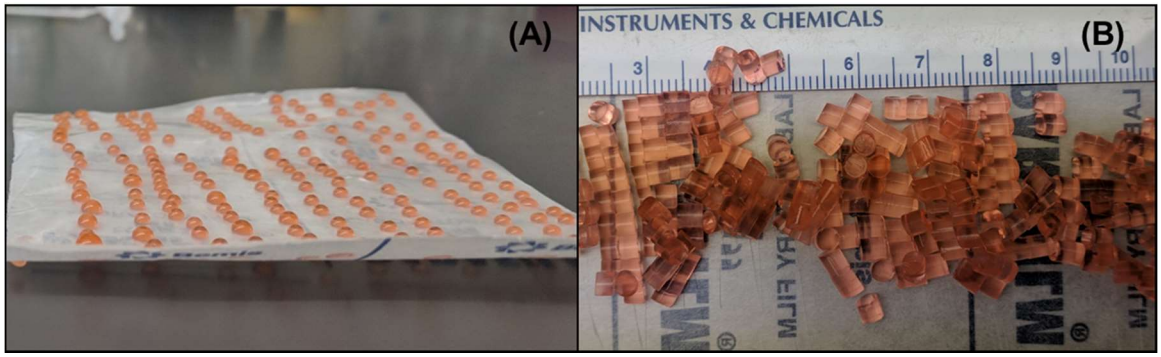

Figure 15. (A) Gellan gum macro-beads made through extrusion of pregel onto Parafilm and allownig surface tension of water to form half spheres prior to cooling. (B) Gellan gum macro-beads made after otimization of method presented in setion 3.4.2.

ii. Micro-beads

Using methods adapted from [79], ATCC 21198 was successfully encapsulated in micro-beads ranging in size from ~10-100µm, determined manually from repeated bright field microscopic

images (Figure 16). ATCC 21198 encapsulated in gellan gum micro-spheres also experienced minimal to no loss of substrate utilization rates when compared with suspended cells (Figure 17 C).

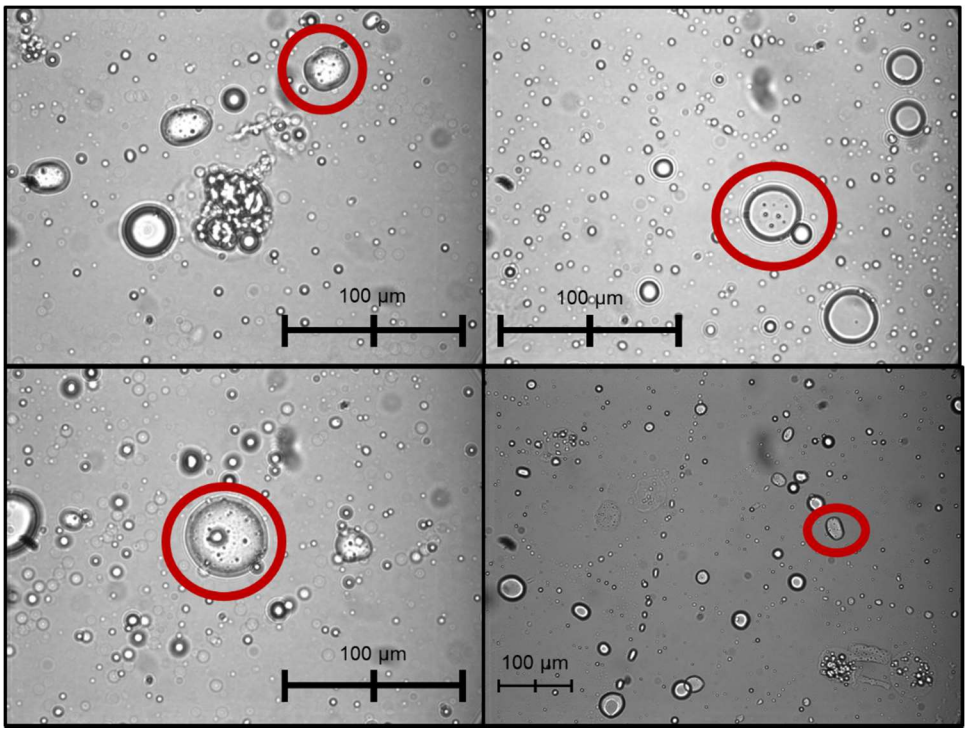

Figure 16. Bright field images of gellan gum micro-beads taken just after creation, with a benchtop Leica DM 2500 microscope. Gellan gum microspheres are circled in red and the scale was determined from images taken with a calibration microscope slide.

4.2.4. Microbial Encapsulation Data Summary and Discussion

After optimization of encapsulation methods it was determined that ATCC 21198 could be encapsulated in both alginate and gellan gum matrices with minimal to no loss of cell viability, as determined via comparison to suspended cell substrate utilization rates (Table 10) (Figure 17).

Table 10. Encapsulated cell viability assessment. Percent difference is calculated as the percent change from suspended cell utilization rates toencapsulated cell utilization rates. Alginate macrobeads were spherical and ~2mm in diameter. Gellan gum macrobeads were cylindrical and ~2mm in diamter by ~2mm tall. Gella gum micro-beads were spherical ~10-100 um in diameter.

Encapsulation Matrix/Method	Benchmark Suspended Cell Utilization Rate (µmol/day/mg)	Encapsulated Cell Utilization Rate (µmol/day/mg)	Percent Difference
Alginate Macro-bead	15.8	14.2	-10.1%
Gellan Gum Macro-bead	13.3	13.3	-0.6%
Gellan Gum Micro-bead	11.1	11.0	-0.7%

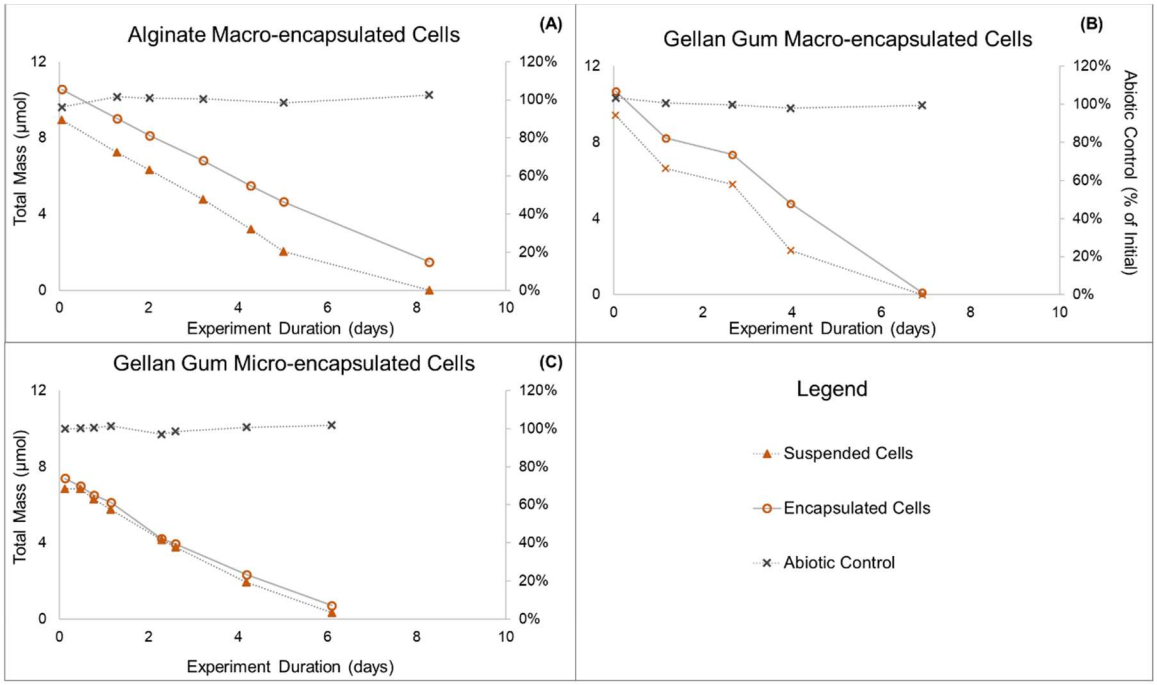

Figure 17. Isobutane utilization curves measured for ATCC 21198 suspended and encapsulated in (A) spherical alginate macro-beads ~2mm in diameter, (B) cylindrical gellan gum macro-beads ~2mm x 2mm and, (C) spherical gellan gum micro-beads ~10-100µm in diameter. All data points are averages of duplicate reactors.

The results presented in Figure 17 contradict previous research that suggests encapsulated cells experience limitations in comparison to suspended cells due to slow oxygen or substrate

diffusion into porous hydrogel bead matrices [89,90]. One explanation for the observed similarity in IB utilization rates between encapsulated and suspended cultures could be the relatively low mass loading of cells within beads in comparison to most hydrogel diffusion studies, ~0.5 mg_{TSS}/g_{bead} and >10 mg_{TSS}/g_{bead}, respectively. Hiemstra et al. investigated the influence of cell mass loadings in alginate macro-beads and found that the higher the mass loading of cells the greater diffusion inhibited oxygen utilization. It was suggested that this is due to excess cellular utilization of oxygen and substrates at the outer edges of beads, which limits oxygen or substrate access to cells located in the center of beads. Therefore, as cells are spread more sparsely throughout beads the cellular utilization rate at the outer edges of beads is reduced below the diffusion rate of O_2 and substrate into beads, which mitigates the influence of diffusion limitations.

In summary, it was determined that after optimization of encapsulation techniques, ATCC 21198 could be successfully encapsulated in both alginate and gellan gum matrices with minimal to no effect on substrate utilization rates. Inferences from these data indicate the metabolic activity of encapsulated cells was not hindered, however, these data provide no information about the long-term effects of encapsulation.

4.3. Encapsulated Cell Cometabolic Transformation Capacity and Longevity

4.3.1. Experimental Overview

To access the long-term effect of encapsulation on the cometabolic transformation potential of encapsulated ATCC 21198, reactors were set up, as presented in section 3.6.2, with the following treatments; abiotic controls (AC), suspended cell controls (SC), alginate encapsulated cells (AEC), and gellan gum encapsulated cells (GGEC) (Table 11). ATCC 21198 was encapsulated in both alginate and gellan gum beads at a mass loading of ~0.5mg_{TSS}/g_{bead} and all active reactors received an addition of cells to a concentration of ~10 mg_{TSS}/L. Reactors were created in triplicate to ensure reliable and repeatable data.

The two main parameters under investigation were the difference between suspended and encapsulated cells contaminant transformation rates and capacities. The rate at which a contaminant is transformed is important and can indicate levels of cell activity (transformation rate), though, the total mass of a contaminant that can be transformed prior to the toxic effects of contaminant transformation inhibiting cells is also important (transformation capacity).

Suspended cell transformation rates and capacities were used as a control to assess the effect of encapsulation on cells. All reactors were spiked three times over ~120 days with the chosen CoC mixture and environmentally relevant aqueous concentrations; 1,1,1-TCA (~250ppb), *c*DCE (~250ppb), and 1,4-D (~500ppb). Respiration (O_2/CO_2) and cometabolic activity data, CoC mixture, were monitored every 5-7 days on average.

Table 11. Summary of treatments within encapsulated cell cometabolism study.

Treatment Name	Abbreviation	Number of Reactors	Reactor Contents		
			Beads (2g)	Cells ($1mg_{TSS}$)	CoCs
Abiotic Control	AC	3	--	--	✓
Suspended Cell Control	SC	3	--	✓	✓
Alginate Encapsulated Cells	AEC	3	✓	✓	✓
Gellan Gum Encapsulated Cells	GGEC	3	✓	✓	✓

4.3.2. Initial Cellular Viability

Figure 18 is a clipped and magnified presentation of initial contaminant transformation and respiration data collected over the first addition of contaminants to all reactors. The initial transformation rates of all contaminants were similar between all active treatments, observed visibly (Figure 18).

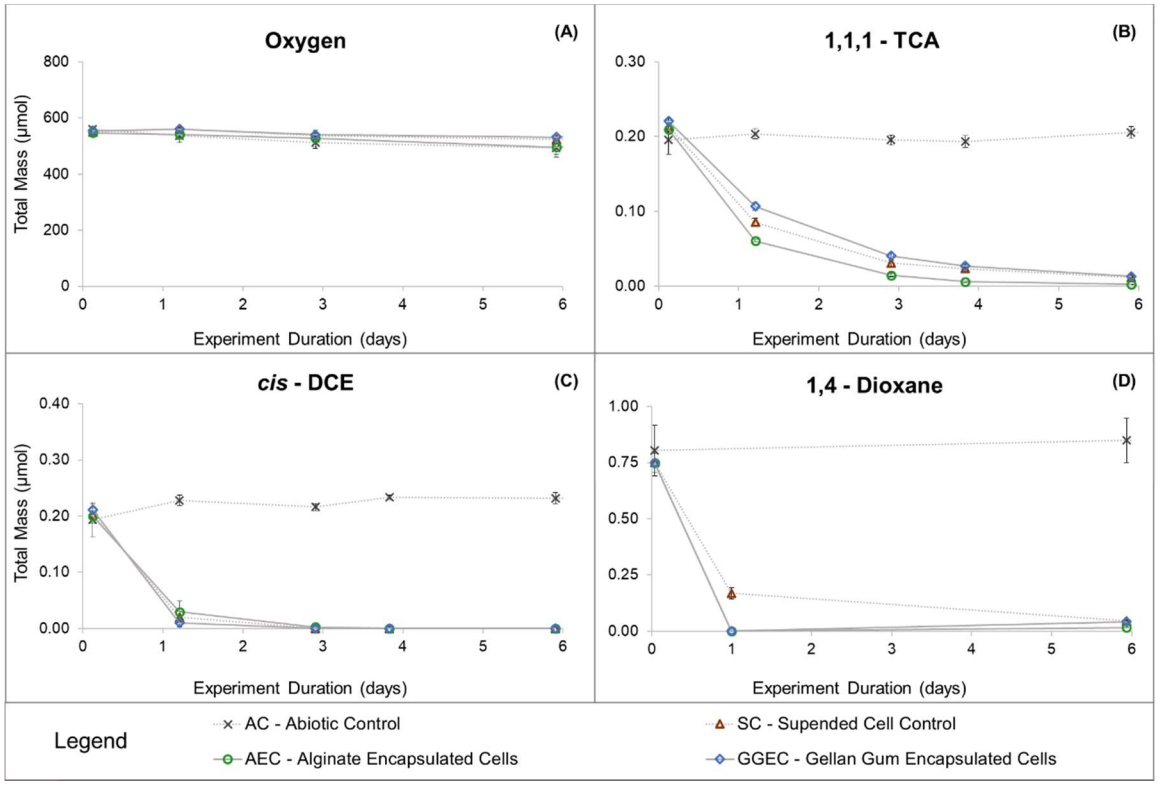

Figure 18. Contaminant transformation data for the initial spike of contaminants. These data have been clipped from the entire time-series data presented below to illustrate initial transformation rates and provide a comparison between suspended and encapsulated cell reactor treatments initial ability to transform contaminants. Data points are averages between triplicate reactors and errors bars are 95% confidence intervals.

These data confirm that ATCC 21198 has the ability to simultaneously transform a mixture of chlorinated contaminants and 1,4-D at environmentally relevant concentrations. Respiration data has changed minimally over the first 7 days of this experiment, as expected due to the absence of a primary substrate or carbon source and the low masses of contaminants transformed, <2µmol, not requiring measureable amounts of O_2 to oxidize (Figure 18 A); CO_2 data, not presented here, follow the same horizontal trend, showing minimal CO_2 production.

4.3.3. Successive Contaminant Additions

Active reactors received successive additions of contaminants when the majority of the previous addition had been transformed. Upon injection of the second and third addition of

contaminants, a decrease in cellular transformation rates were observed, visibly, for all treatments (Figure 19 C-E). The decrease was expected, due to cell population decay in the absence of a growth substrate combined with the toxic effect from transforming contaminants, i.e. the transformation capacity of added biomass was likely met at ~120 days.

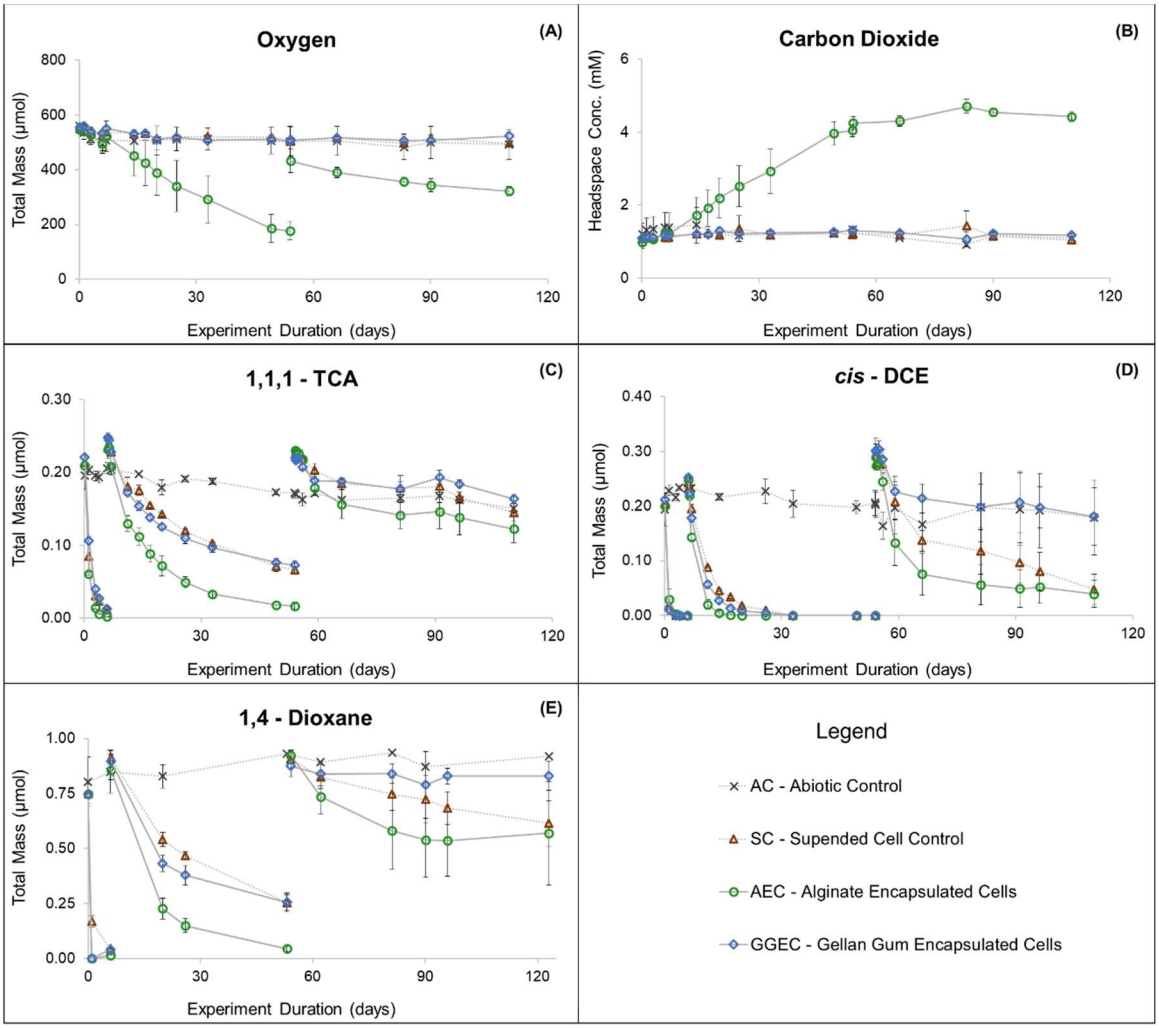

Figure 19. Long-term encapsulated cell cometabolic transformation study. (A-B) Respiration data. O_2 measurements reported as ~180µmol is assumed to be near zero due to vacuum created within reactors (see Section 3.2.1 pg 32). CO_2 data are presented in terms of measured headspace concentrations due to speciation of CO_2 in carbonate system in the aqueous phase and lack of pH measurements throughout experiment. (C-E) Contaminant transformation data. Three contaminant additions were made to each reactor and breaks in time-series connection lines signify successive additions. Data points are averages between triplicate reactors in each treatment and errors bars are 95% confidence intervals.

Figure 19 (C-E) illustrates that ATCC 21198, even in suspended cell reactors, maintained some cometabolic activity for over 120 days. This finding suggests that ATCC 21198 has the capability under certain growth conditions to store energy during growth, which can be utilized over extended durations, to produce or maintain non-specific oxygenase enzymes that are responsible for cometabolism. The production of particular proteins that are produced to collect and store diverse compounds for later use as energy or nutrients has been observed by other *Rhodococcus* species in previous studies and may explain the observed long-term activity above [115].

Also surprisingly, alginate encapsulated cells were able to transform a greater percent of successive spikes at a faster rate than suspended or gellan gum encapsulated cells (Figure 19) (Table 12). Data became variable within reactors of the same treatment in the third spike of contaminants and cometabolic activity in one gellan gum reactor ceased, as indicated by the deviation of the gellan gum time-series from the suspended in transformation of *c*DCE, and the large error bars in the replicate treatments. To examine any statistical difference in cometabolic transformation ability between treatments, average transformation capacities within each treatment were calculated based on the mass of each contaminant transformed per mass of cells over the duration of this experiment (Table 12).

Table 12. Contaminant Transformation capacities calculated from the summation of all contaminants transformed over all three spikes added to each reactor. Data are average transformation capacities between triplicate reactors bounded by calculated 95% confidence intervals.

Treatment	Abbreviation	Transformation Capacity (mg_{CoC}/mg_{TSS})		
		1,1,1-TCA	*c*DCE	1,4-Dioxane
Suspended Cell Control	SC	0.43 ± 0.04	0.66 ± 0.09	1.65 ± 0.20
Alginate Encapsulated Cells	AEC	0.51 ± 0.04	0.68 ± 0.05	1.90 ± 0.38
Gellan Gum Encapsulated Cells	GGEC	0.42 ± 0.01	0.57 ± 0.06	1.39 ± 0.13

Transformation capacity data in Table 12 suggest there is inconclusive evidence of a statistical difference between treatments due to 95% confidence intervals overlapping, however further statistical analysis of 1,1,1-TCA transformation capacities provided evidence that alginate encapsulated cell transformation capacities were statistically greater than both suspended and gellan gum encapsulated cells (Appendix B). In addition to greater transformation capacities, the rate at which alginate encapsulated cells transformed contaminants was greater (Figure 19). It was also shown that suspended and gellan encapsulated cell transformation capacities did not have a statistically significant differences (Appendix B). The calculated transformation capacities are higher than previously observed capacities for ATCC 21198, though previous studies were short-term and did not allow slow long-term transformation to proceed [72].

Respiration data for suspended and gellan gum encapsulated cells show little activity, as expected, due to no primary substrate addition and the relatively small amount of contaminants added, <5μmol total. However, measureable amounts of O_2 consumption and CO_2 production began in alginate bottles around day 10 (Figure 19 A-B). This oxygen consumption followed a negative linear trend out to day 54 when the O_2 was effectively depleted (Section 3.2.1). The

headspace in the AEC reactors was refreshed with pure O_2 on day 54 to ensure transformation of CoCs proceeded.

The depletion of O_2 in alginate encapsulated cell reactors is suspected to be due to cellular utilization of the alginate encapsulation matrix because it is the only carbon source within the reactors other than biomass. Energy gained by the consumption of alginate is one theory for the elevated cellular activity and corresponding rate and capacity of CoC transformation observed within these reactors.

Conservative stoichiometric analysis, based on equation 2, using the measured amount of O_2 consumed over the entire duration of this experiment, suggests that cells in AEC reactors have consumed ~25% of the added alginate. Conservatively assuming the biomass yield constant for ATCC 21198 grown on alginate is at least 50% of the yield constant for isobutane, then the estimated amount of alginate consumption would correspond to an increase in biomass of ~7 times compared to the biomass initially added to AEC reactors, over the ~120 day period.

$$C_6H_8O_6 + 5O_2 \xrightarrow{\text{Respiration}} 4H_2O + 6CO_2 \qquad \text{Eqn 2}$$

Transformation rates and capacities in alginate reactors were greater on average than suspended cells, though not in proportion to the estimated cell population growth. Also, the observed decrease in transformation rate in successive spikes is not indicative of cellular growth. However, it could be that alginate is a non-inducing growth substrate that provided energy for the slow growth of ATCC 21198 while not inducing the production of excess cometabolic enzymes.

Issues with this theory arose due to short-term studies conducted in a partner lab at North Carolina State University (NCSU) that suggested ATCC 21198 does not have the genes necessary to break into the alginate structure and utilize the matrix as a carbon source [51]. Nonetheless, slight differences in alginate preparation and formation might explain the difference observed within

these studies; e.g., alginate pre-gel solution within this work was autoclaved prior to bead formation, which may have facilitated breakdown of the alginate structure prior to bead formation.

Another theory for the observed O_2 consumption in alginate reactors is that over the course of this long-term experiment, while sampling through the septa with non-sterile GC syringes, the reactors became contaminated with a microbial species capable of consuming alginate and may be capable of cometabolism themselves. To investigate this further liquid from all reactors within this experiment was streak plated on non-specific tryptic-soy growth agar plates after ~120 days (Figure 20).

In all reactors, it was observed that the growth on streaked plates was in large part ATCC 21198 but plates were also contaminated with a microbe other than ATCC 21198 (Figure 20). This does not confirm the above theory only lends to the idea that the reactors contain another microbial species suggesting it is possible that another microbe is responsible for degradation of the alginate matrix.

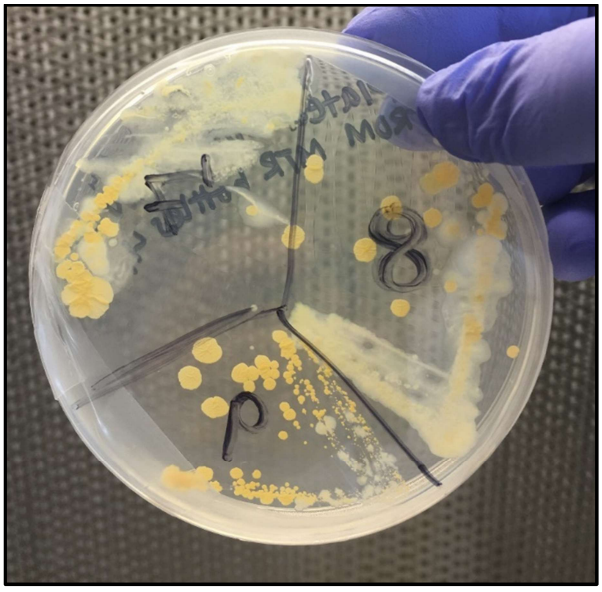

Figure 20. ATCC 21198 is easily visualized as the orange cultures. Though streaks are not pure as seen by the milky white culture overlapping portions of the streaks.

Interesting to the goals of this project was the observation that the slow consumption of alginate correlated with an increase in cellular activity and cometabolic transformation potential, indicating that the encapsulation matrix may have been acting as a SRS for encapsulated cultures. However, the observed respiration of alginate in combination with physical agitation from reactors being stored on a rotary shaker table shaking at ~100rpm led to instability and disintegration of alginate beads, visibly observed starting at ~60 days. Upon field scale application of the proposed technology being developed within this thesis, there will be no control over native microbes and therefore, higher resistance to enzymatic degradation is desired in order to maintain the integrity of augmented beads. Unfortunately, no rheological analysis were conducted pre- or post-experiment though photographs were taken in which the deterioration of alginate beads is visible (Figure 21). As expected, gellan gum macro-beads were observed, visibly, to have deteriorated much less over the ~120 day period.

Figure 21. Long-term CoC transformation reactors. Suspended (Left 2), Alginate Encapsulated (Middle 2), and Gellan Gum Encapsulated (Right 2) ATCC 21198 in duplicate reactors. Triplicate reactors exist but were excluded to increase picture quality and scale. Alginate beads have deteriorated into threads of alginate, while gellan gum beads have maintained original structure. Picture taken after 120 days of reactors stored on rotary shaker table continuously shaking at ~100rpm.

4.3.4. Long-term Encapsulated Cell Cometabolism Summary and Discussion

The data collected provide evidence that both suspended and encapsulated ATCC 21198 can maintain cometabolic transformation potential for extended periods. In addition to this, it was confirmed that alginate beads were less resistant to degradation than gellan gum [97,108].

The observed cellular utilization of alginate was not an expected observation, though it did provide evidence that a slowly accessible carbon source can potentially improve an augmented cultures cometabolic transformation potential. However, the objectives of this project require prolonged cellular and SRC encapsulation in order to prevent issues including SRC release and transport, cellular release and transport, and potential excess biological oxygen demand by a non-inducing growth substrate. Important to this point is the finding that an oxygen demand was not observed with gellan gum in comparison to suspended cells, even in the presence of a contaminant microbe, and gellan gum encapsulated cells were also found to have minimal to no loss of cometabolic activity when compared to suspended cells over the extent of this experiment (Appendix B).

The findings of this experiment shifted the major focus of work conducted as part of this thesis to investigating Gellan Gum (GG) as the primary encapsulation matrix.

4.4. SRS Encapsulation Method Development and Optimization

4.4.1. Overview

The SRSs that were analyzed for their potential to supply substrates to encapsulated microbes, TBOS and T_2BOS, exist in pure phase as light non-aqueous phase liquids (LNAPLs). Previous work conducted to entrap NAPLs, essential oils, in alginate hydrogel matrices showed that it is possible to load beads with oils as high as ~25% (w/w) [114]. Under certain encapsulation conditions, the developed methods were found to be highly efficient, successfully entrapping ~90% of the oil added. Using the optimized methods for encapsulating ATCC 21198, presented above, in

combination with oil encapsulation methods developed by Soliman et al. (2013), methods were developed for the successful encapsulation of SRSs within alginate and gellan gum matrices.

4.4.2. Alginate Encapsulation of SRSs

TBOS was used as the model LNAPL SRS for encapsulation method development due to its availability and low cost. Initial attempts were aimed at creating alginate macro-beads with TBOS mass loadings on the low and high end of what Soliman et al. (2013) achieved, 5 and 30 % (w/w), respectively. To do so, TBOS was added to alginate pre-gel solution at 5 and 30% (w/v). This mixture was emulsified with the aid of Span-80 emulsifier and beads were created as presented in section 3.5.1.

Through the initial method developed TBOS could be encapsulated successfully in beads at 5 and 30% (w_{TBOS}/w_{bead}) (Figure 22). Approximately ~75% of the added TBOS was recovered within beads in both cases (Figure 22).

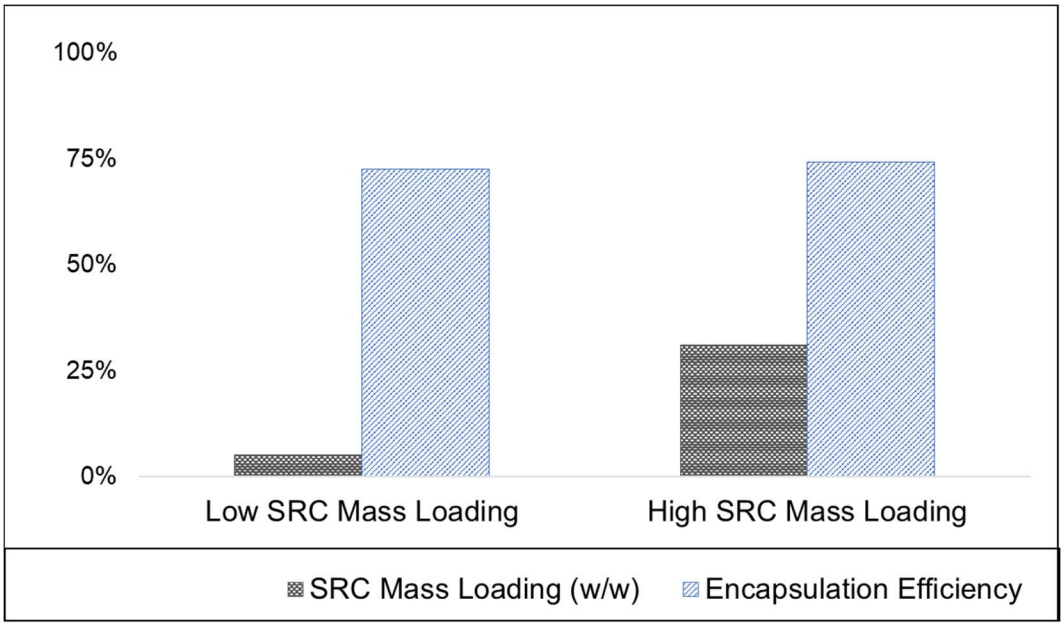

Figure 22. TBOS encapsulation in alginate parameter summary. Low SRC Mass Loading (5% w/w). High SRC Mass Loading (30% w/w).

4.4.3. Gellan Gum Encapsulation of SRSs

Due to similarities between the hysteresis gelation mechanism of agarose and gellan gum, initial attempts to encapsulate SRSs in gellan gum macro-beads followed [103] in which half sphere agarose macro-beads were made by extruding drops of heated pre-gel solution onto a hydrophobic surface and allowing to cool at room temperature to gelate (Figure 23 A).

From the successful encapsulation techniques developed for alginate, it was determined that inclusion of LNAPL SRSs within a hydrogel matrix required the creation of a stable emulsified SRS-hydrogel solution. To create a stable emulsion the addition of Span-80 as an emulsifier was necessary; however, the emulsifier reduced the surface tension of the gellan gum pre-gel solution. After extrusion of the heated pre-gel drops onto the hydrophobic surface, the lowered surface tension caused the droplets to flatten into one another or form disc shaped beads (Figure 23 B).

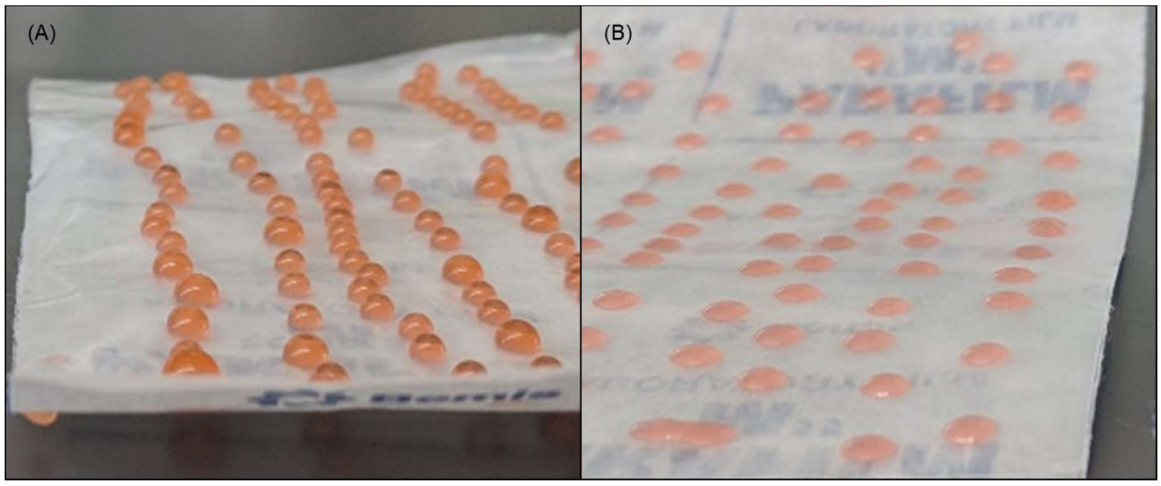

Figure 23. (A) Half-sphere gellan gum macro-beads made without an addition of emulsifier. (B) Attempt to make half-sphere gellan gum macro-beads with an addition of emulsifier and SRS. Reduced surface tension from emulsifier led to the creation of flat fragile disc shaped beads.

The thin disc shaped beads were fragile and difficult to remove from the drying surface without tearing. Measurements of SRS mass loading were not conducted with disc-shaped beads, though it was observed visibly that beads did contain SRSs within the encapsulation matrix. Issues with this method led to the development of the method presented in section 3.5.2, by which stable

cylindrical gellan gum macro-beads that contained SRSs at mass loadings up to ~8% (w/w) with encapsulation efficiencies of ~80% were created. Only a single attempt using this final method was made to encapsulate both TBOS and T_2BOS within gellan gum, though it is likely that the method could be further optimized and higher mass loadings could be achieved with a greater efficiency.

Methods for the micro-encapsulation of LNAPL SRSs were explored as part of this thesis but little success or progress was achieved. Future work on this project should focus on development of methods to encapsulate SRSs in micro-beads ranging in size from 10-40μm.

4.4.4. LNAPL SRS Encapsulation Summary and Discussion

From direct analysis of SRSs entrapped within alginate and gellan gum macro-beads it was determined that LNAPLs, such as TBOS and T_2BOS, could be successfully encapsulated in both alginate and gellan gum matrices at mass loadings as high as 30 and 8% (w/w), respectively. In addition to this success, encapsulation efficiencies were above 75% for both methods.

From these results it was conservatively estimated that it would be possible to generate ~89mg_{TSS} of biomass per gram of bead. This was based on the complete hydrolysis of 10% encapsulated TBOS to 1-butanol and the assumption that the biomass yield coefficient for ATCC 21198 grown on 1-butanol was 50% of the known yield for isobutane [69]. The calculated ~89mg_{TSS}/g_{bead} is several times more biomass per gram of bead than has been encapsulated in stable macro-beads in all of the studies referenced within this thesis [79,87,89,90,100,113,113,114]. These calculations provide positive evidence that if encapsulated SRSs produce inducing growth substrates and encapsulated cultures can utilize those substrates, it will be possible to increase and extend the cometabolic remediation potential of initially augmented biomass.

4.5. Abiotic Hydrolysis of Encapsulated Slow Release Substrates

4.5.1. Overview

TBOS and T_2BOS were encapsulated in alginate and gellan gum beads and were suspended in solution, as presented in section 3.6.3, to investigate the rate of substrate release, 1- and 2-butanol respectively, after encapsulation. It was important to determine the rate at which these compounds hydrolyze and produce substrates in order to understand the possible duration of hydrolysis, rate of substrate production and cellular growth, oxygen demand related to product consumption, and to be able to distinguish possible biotic hydrolysis when orthosilicate compounds are co-encapsulated with microbes.

Reactors with TBOS and T_2BOS in free suspension at concentrations that replicate encapsulated SRS reactors were created to determine the effect of encapsulation on SRS hydrolysis. Substrate production rates were used as a proxy for SRS hydrolysis, due to the simplicity of substrate analysis. Direct measurements of 1- and 2-butanol in solution were made in order to determine substrate production rates and measurements are presented on a total mass produced basis. Hydrolysis of orthosilicate compounds is acid and base catalyzed and therefore, observed hydrolysis rates are on the low end of what is possible, due to suspension in pH-7 media.

Previous research suggests that the concentration of TBOS and T_2BOS in solution effect the rate of hydrolysis [80]; and therefore, concentrations of SRSs in abiotic reactors were created to mimic the concentration of SRSs in biotic co-encapsulated reactors, ~1000-1500 mg/L. Biotic and abiotic reactors were created in unison and monitored alongside one another, though abiotic data have been separated and are presented below. To prevent contamination from occurring over the long duration of these experiments an addition of sodium azide, 0.2% (w/v), was made to all abiotic reactors.

4.5.2. Alginate Encapsulated SRSs

Due to the ease of encapsulation of SRSs within alginate (Section 4.4.2), initial abiotic hydrolysis work was conducted using alginate encapsulated TBOS. TBOS was encapsulated in abiotic alginate macro-beads at a mass loading of ~5 and 30% (w/w). These beads were then added to triplicate reactors, as presented in section 3.6.3, such that the final TBOS concentration in pH-7 carbonate buffered media was kept constant at ~1000 mg/L; i.e., 2 grams of 5% beads and 1/3 grams of 30% beads were added to 100mL media solution. This corresponds to total TBOS masses in reactors of ~100mg or ~312μmol and to maximum 1-butanol production masses of ~92.5 mg or ~1250μmol. To illustrate the effect of encapsulation on the hydrolysis rate of TBOS, reactors containing similar concentrations of suspended TBOS were created and monitored alongside encapsulated TBOS reactors.

All reactors were monitored for 1-butanol production over ~140-day period (Figure 24). 1-butanol production rates were modeled via linear regression over the full time period of data collection and comparisons were made between the three treatments; suspended TBOS, low mass loaded beads (5% TBOS w/w), and high mass loaded beads (30% TBOS w/w) (Table 13).

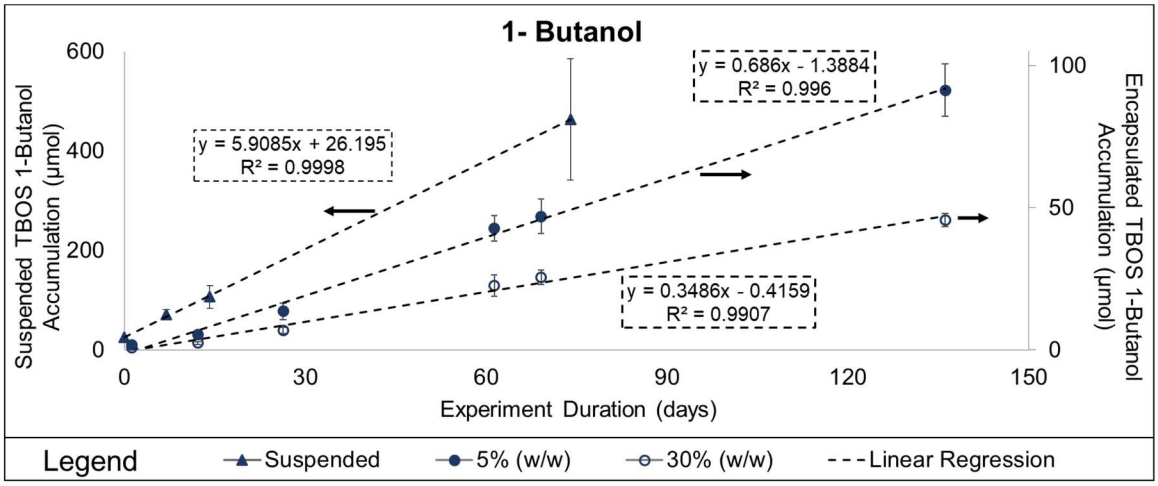

Figure 24. Measured 1-butanol masses in solution from the abiotic hydrolysis of suspended (left-axis) and alginate encapsulated TBOS (right-axis). Total TBOS solution concentrations of ~1000 mg/L and bead mass loading ~5 and 30% (w/w). Black arrows signify which axis each time-series corresponds to. Excel linear trend-line functions are fit to the time-series and black-dashed boxes represent linear regression equations calculated by excel linear trend-line tool. Boxes are placed next to corresponding time-series. Data points are averages between duplicate (suspended) or triplicate (encapsulated) reactors in each treatment and errors bars are 95% confidence intervals. Suspended TBOS reactors were created after encapsulated reactors and therefore, have a shorter total duration of measurements

1-Butanol was produced at an order of magnitude greater rate when TBOS was in free suspension than when encapsulated (Figure 24) (Table 13). One theory for this observed phenomenon is that while reactors are stored on a shaker table, at ~100rpm, the LNAPL TBOS in suspension forms a quasi-emulsion within the aqueous phase and the small droplets of LNAPL in solution provide a large surface area for hydrolysis to occur. This does not occur in encapsulated LNAPL reactors, because LNAPL droplets are held within a physical barrier and do not spread throughout solution. Due to this, it is suggested that 1-butanol diffusion away from hydrolysis sites, out of beads, and water exchange to hydrolysis sites, into beads, limits the rate of hydrolysis.

Table 13. Modeled abiotic hydrolysis rates and known mass of TBOS added to reactors used to predict the lifetime of encapsulated TBOS.

Treatment	Measured Initial TBOS Mass (µmol)	Maximum Possible Butanol Release (µmol)	Butanol Production Rate (µmol/day)	Estimated Exhaustion of TBOS (years)
Suspended TBOS	312	1247	5.9	0.6
Encapsulated TBOS (5% w/w)	326	1305	0.69	5.2
Encapsulated TBOS (30% w/w)	324	1295	0.35	10.1

TBOS encapsulated at ~30% (w/w) hydrolyzed at half the rate of TBOS encapsulated at ~5% (w/w). This observation may be due to a difference in the effective or active surface area for hydrolysis. For example, Figure 25 scenario 1 depicts a case in which LNAPL droplets in high mass loaded beads (30%) are similar in size to LNAPL droplets in low mass loaded beads (5%) though there are 6 times as many droplets. In scenario 2, the 30% LNAPL droplets are greater in size than the 5% droplets though there are a similar number of droplets. In both cases, the total LNAPL surface area is greater in 30% beads; however, the path for water exchange and access to SRSs in the center of the beads is restricted by SRSs encapsulated at the outer edges of beads. The restricted water exchange and 1-butanol diffusion out of beads is suspected to cause a slowing in hydrolysis. Therefore, the more TBOS encapsulated within a single bead, the more tortuous the path for 1-butanol diffusion out of beads and water into beads causing the effective hydrolysis surface area to be reduced (Figure 25).

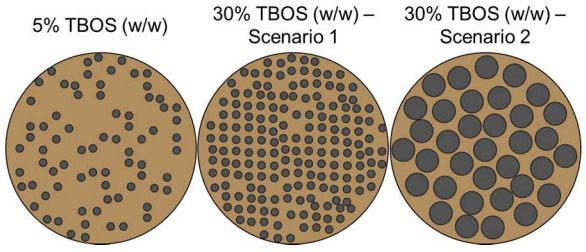

Figure 25. 2D depiction of low SRS mass loading beads (5%) versus possible scenarios for high mass loading beads (30%).

4.5.3. Gellan Gum Encapsulated SRSs

The abiotic hydrolysis rate of both TBOS and T_2BOS encapsulated in gellan gum was also investigated. Both SRSs were encapsulated in cylindrical gellan gum macro-beads at mass loadings of ~8% (w/w). For this work ATCC 21198 was also co-encapsulated within the gellan gum matrix at initial concentrations of ~0.5mg_{TSS}/g, and an addition of 0.2% (w/v) sodium azide was added as a cellular poison to ensure cells were not alive within the matrix. Biomass was encapsulated because, prior to this experiment it had been determined that encapsulated SRSs may hydrolyze more quickly with cells present within the encapsulation matrix (Appendix C). Although, the increase in hydrolysis rate was not proven to be from biotic hydrolysis of SRSs and may have been due to the presence of biomass within the matrix allowing more diffusion of water into and butanol out of beads. Therefore, poisoned biomass was included within the matrix to ensure encapsulated SRS abiotic hydrolysis rates would be directly comparable to co-encapsulated reactors containing active biomass (section 4.6).

Two grams of beads were added to each abiotic reactor such that a final concentration of ~1500 mg/L TBOS and T_2BOS was achieved, or a total mass of ~155mg or ~484µmol was added. Reactors containing suspended T_2BOS at ~1500 mg/L were created for comparison.

Analogous to alginate encapsulated and suspended TBOS data presented above, encapsulated T_2BOS hydrolyzed an order of magnitude more slowly than suspended T_2BOS (Figure 26) (Table 14).

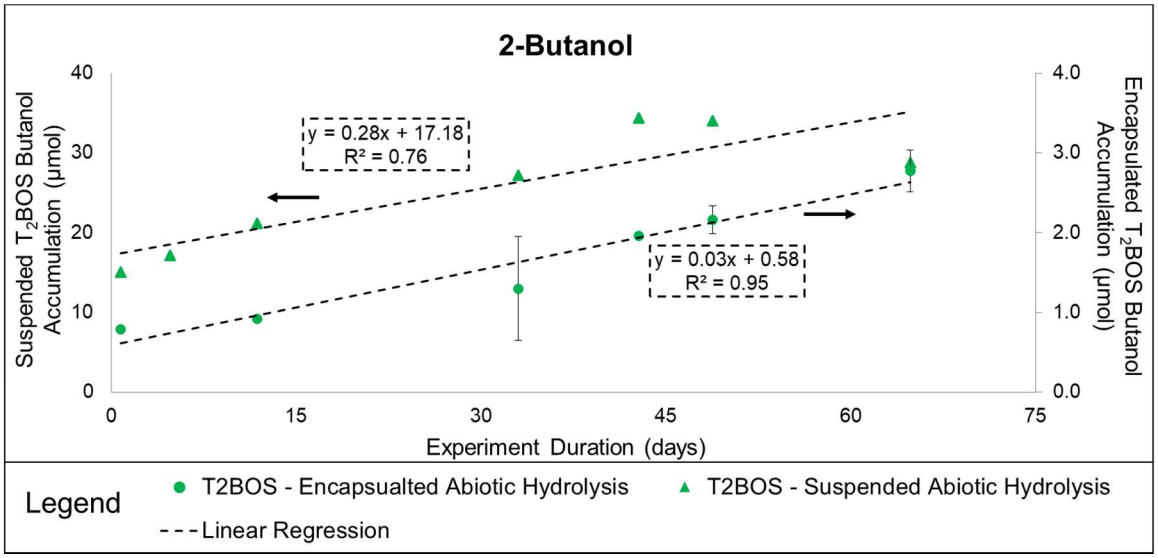

Figure 26. Measured 2-butanol masses in solution from the abiotic hydrolysis of suspended (left-axis) and gellan gum encapsulated T_2BOS (right-axis). Total T_2BOS solution concentrations of ~1500 mg/L and bead mass loading ~8% (w/w). Black arrows signify the axis that time-series correspond to. Excel linear trend-line functions fit to time-series and the black-dashed boxes represent linear regression equations calculated by excel linear trend-line tool. Boxes are placed next to corresponding time-series. Data points are averages between duplicate reactors in each treatment and errors bars are 95% confidence intervals.

The hydrolysis rate for TBOS encapsulated in gellan gum at ~8% (w/w) and at total solution concentrations of ~1500mg/L, presented in Figure 27 (1.3 µmol/day), are within the range observed for TBOS at ~1000mg/L presented in section 4.5.2 (0.34 - 5.9 µmol/day) (Figures 24 & 27). However, gellan gum encapsulated TBOS hydrolyzed ~2-4 times more quickly than alginate encapsulated TBOS (Table 15). This is likely be due to higher solution concentrations of TBOS in gellan gum reactors than in alginate reactors; however, differences in the encapsulation matrix and the inclusion of ATCC 21198 biomass within gellan gum beads and not in alginate beads may have also played a role in the observed difference.

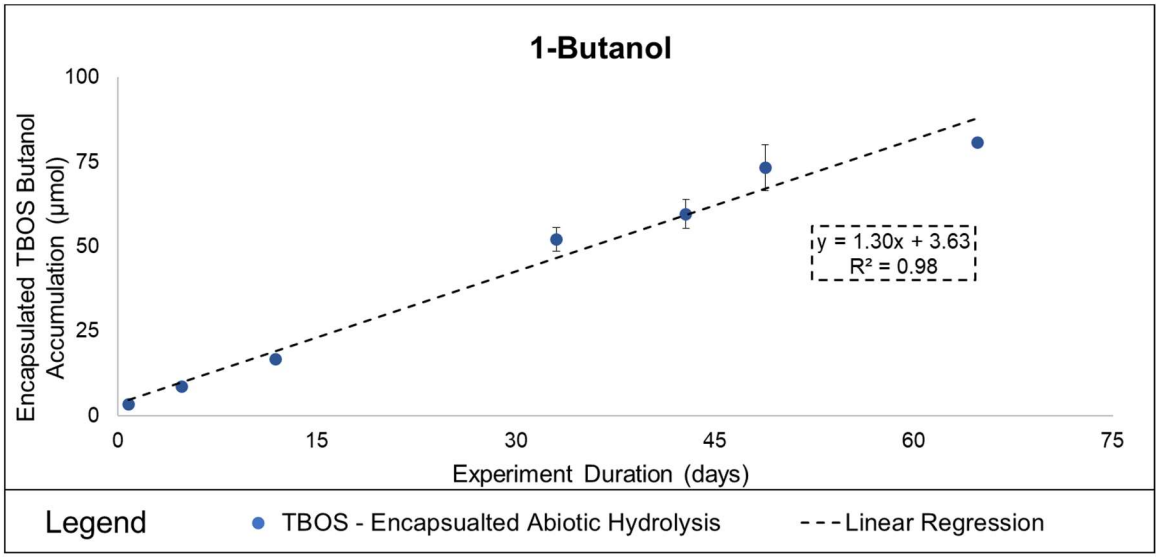

Figure 27. Measured 1-butanol masses in solution from the abiotic hydrolysis of gellan gum encapsulated TBOS. Total TBOS solution concentration of ~1500 mg/L and bead mass loading ~8% (w/w). Excel linear trend-line function fit to time-series and the black-dashed box represents the linear regression equation calculated by excel linear trend-line tool. Data points are averages between duplicate reactors and errors bars are 95% confidence intervals.

Table 14. Modeled abiotic hydrolysis rates used to predict the lifetime of gellan gum encapsulated TBOS and T_2BOS in reactors at total solution concentration ~1500 mg/L and bead mass loading ~8% (w/w) .

Treatment	Measured Initial BOS Mass (µmol)	Maximum Possible Butanol Release (µmol)	Butanol Production Rate (µmol/day)	Estimated Exhaustion of TBOS (years)
Suspended T_2BOS	476	1901	0.40	12.9
GG Encapsulated T_2BOS (8% w/w)	441	1763	0.03	169
GG Encapsulated TBOS (8% w/w)	479	1916	1.3	4.0

It can be seen from direct comparisons between substrate production rates between gellan gum encapsulated TBOS and T_2BOS, both encapsulated at mass loadings of ~8% and in solution at ~1500 mg/L, that TBOS hydrolyzes ~45 times more quickly (Table 14 and 15). This is an expected result due to previous research showing that the more sterically hindered the central silicate is by the leaving groups, the less access water has to hydrolysis sites [82,83] (Figure 28).

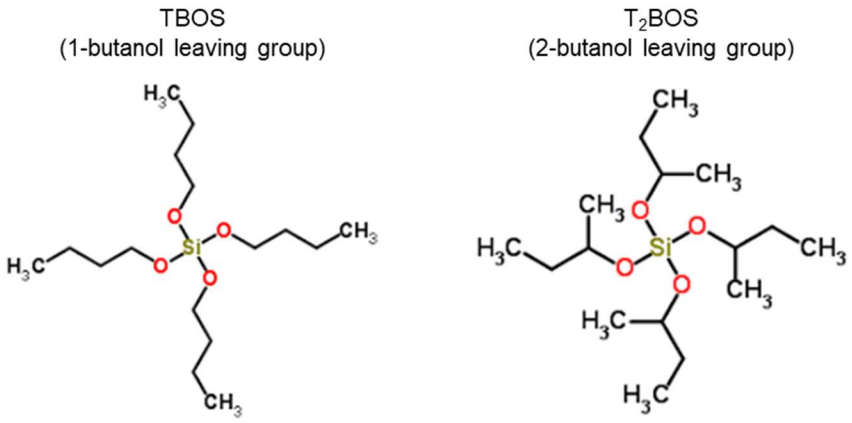

Figure 28. Chemical structure of TBOS and T_2BOS. Illustrating the greater steric hindrance of T_2BOS. Branched alcohols limit access to ester bonds and slow hydrolysis. [84]

4.5.4. Experimental Summary and Conclusions

For comparison, Table 15 below summarizes all abiotic hydrolysis rates presented in the above sections. The observed order of magnitude reduction in hydrolysis rates after encapsulation of both TBOS and T_2BOS is an important finding that may allow for more informed decisions to be made for the selection of SRSs in future applications of this technology. Observed differences in hydrolysis rates when SRSs were encapsulated at different mass loadings, as seen in row 2-3 of Table 15, may also provide a useful control over the rate of release of substrates. These controls might allow for the mitigation of excess substrate release leading to excess cellular growth and issues like well clogging or oxygen depletion. Also, as expected slight differences in leaving groups attached to orthosilicate compounds, 1- or 2-butanol, drastically altered the butanol production rate, slower for branched alcohols (Table 15).

Table 15. Summary of all collected SRS abiotic hydrolysis rates. All TBOS data presented in the first 4 rows, followed by T_2BOS data in row 5 and 6.

Treatment	Initial SRS Solution Conc. (mg/L)	Poisoned Cells Present	Measured Initial SRS (µmol)	Maximum Possible Butanol (µmol)	Butanol Production Rate (µmol/day)	Estimated Exhaustion of SRS (years)
Suspended TBOS	1000	No	312	1247	5.9	0.58
Alginate Encapsulated TBOS (5% w/w)	1000	No	326	1305	0.69	5.17
Alginate Encapsulated TBOS (30% w/w)	1000	No	324	1295	0.35	10.1
Gellan Gum encapsulated TBOS (8% w/w)	1500	Yes	479	1916	1.3	4.0
Suspended T_2BOS	1500	No	475	1901	0.40	12.9
GG Encapsulated T_2BOS (8% w/w)	1500	Yes	441	1763	0.03	169

Another important finding is the extended duration of possible substrate release ranging from several to hundreds of years (Table 15). The observed possible substrate production rate and duration provide supporting evidence that a single injection of co-encapsulated SRSs to the subsurface could produce low amounts of substrates over long periods of time, which could potentially drive contaminant remediation for a much longer period of time than current biostimulation or bioaugmentation applications. However, investigation into the kinetics of hydrolysis, cell substrate utilization, cell respiration, cell decay, and contaminant transformation will be necessary to better understand the desired rate of substrate release and duration.

In summary, it will be important to consider SRS selection and mass loading upon application of co-encapsulated beads to the subsurface, due to limited groundwater oxygen content. There will

be a strong desire to utilize oxygen as efficiently as possible to maximize the amount of contaminant transformed per mass of oxygen utilized. The differences in hydrolysis rates observed between the two examined SRSs; after encapsulation of the two SRSs; and when the SRSs were encapsulated at different mass loadings should be investigated in future work.

Optimization was not the primary objective of this thesis and therefore, work proceeded with experimental analysis to meet the project objective of determining if SRS co-encapsulation could increase and extend cometabolic potential of co-encapsulated cells. However, it is suggested that future work should be conducted with the aim of developing a model to further understand the above hydrolysis process.

4.6. Proof of Concept: Co-Encapsulated Cell Cometabolic Transformation Longevity Study

4.6.1. Overview

This experiment was created under the most optimum conditions in an attempt to determine if ATCC 21198 co-encapsulated with SRSs, TBOS or T_2BOS, could be induced by or gain energy from SRS products, 1- and 2-butanol, such that transformation rates or capacities of initially encapsulated biomass was greater than similar biomasses of suspended cells without access to SRSs or substrates.

Gellan gum was selected as the encapsulation matrix due to observed superiority over alginate in resistance to enzymatic degradation and long-term durability (Section 4.3 and Appendix C). In previous experiments, microbial consumption of alginate led to alginate bead instability, issues determining if cellular respiration was due to consumption of the encapsulation matrix or released SRS products, and caused encapsulated SRSs to be released to solution (Appendix C). In contrast to this, ATCC 21198 was not observed to have the ability to consume gellan gum, and it had been

observed that gellan gum macro-beads remained stable for over 120 days while shaking at ~100rpm on a shaker table, whereas, alginate macro-beads did not (Section 4.3) (Figure 21).

For this experiment cylindrical gellan gum macro-beads containing ATCC 21198 and TBOS/T_2BOS were created with biomass loadings of ~0.5mg_{TSS}/g_{bead} and SRS mass loadings of ~8% (w/w) SRS. Both SRSs were examined within this experiment to observe the difference between SRSs producing a non-inducing growth substrate, 1-butanol, and an inducing growth substrate, 2-butanol, and the effect of different substrate production rates on substrate utilization and oxygen consumption.

Two grams of beads were added to reactors, created as presented in section 3.6.2, to achieve final cell concentrations of ~10mg_{TSS}/L and SRS concentrations of ~1500 mg/L. The initial cell concentration within reactors was designed to directly compare to previous encapsulated cell experiments (Section 4.3, Appendix C), and the initial SRS concentrations to compare to encapsulated abiotic hydrolysis work conducted with TBOS and T_2BOS (Section 4.5.3). The abiotic hydrolysis work presented within section 4.5.3, was conducted using the same batch of beads created within this experiment but with an addition of sodium azide to reactors to ensure added ATCC 21198 did not survive. Data from abiotic hydrolysis experiments using the same batches of beads are presented with active reactor data to provide comparisons between observed respiration in active bottles and observed substrate, 1- and 2-butanol, production in poisoned bottles.

An abiotic control with no addition of beads ensured transformation of added CoCs was biotic. Suspended cell controls, illustrated the effect of co-encapsulation on initial and long-term cell viability, as measured via CoC transformation rates and capacities. Reactors were created in duplicate or triplicate. A summary of the treatments examined within the experiment are presented in Table 16.

All reactors were spiked initially with the chosen CoC mixture at environmentally relevant aqueous concentrations, 1,1,1-TCA (~250ppb), *c*DCE(~250ppb), and 1,4-D(~800ppb). All data are presented on a total mass basis within reactors calculated via Henry's law (Equation 1). Successive spikes of contaminants were made to reactors, over ~90days, after the majority of contaminants were transformed. The concentration of subsequent spikes were doubled in an attempt to challenge cell transformation capacities. Respiration data (O_2/CO_2), substrate data (1-/2-butanol), and contaminant data (1,1,1-TCA/*c*DCE/1,4-D) were monitored as necessary according to methods presented in section 3.2.1.

Table 16. Summary of treatments for: Co-Encapsulated Cell Cometabolic Transformation Longevity Study

Treatment	Abbrev.	Number of Reactors	Reactor Contents			
			Beads (2g)	SRS (TBOS/T_2BOS)	Cells (1mg$_{TSS}$)	CoCs
Abiotic Control	AC	1	--	--	--	✓
Suspended Cell Remediation Control	SC	2	✓	--	✓	✓
Co-encapsulated TBOS/ATCC 21198	CET	2	✓	✓	✓	✓
Co-encapsulated T_2BOS/ATCC 21199	CET_2	3	✓	✓	✓	✓

The data collected over the duration of this experiment have been separated, and are presented below, based on the model SRS that was encapsulated. Control reactor data (AC & SC) are presented initially with analysis of cellular viability post encapsulation. Control data are followed by a comparison to reactors containing cells co-encapsulated with TBOS (CET), a comparison to reactors containing cells co-encapsulated with T_2BOS (CET_2), a data summary section concluding

data presentation, and finally a summary and conclusion section for this experiment, which will conclude the results chapter within this thesis.

4.6.2. Experimental Set-up and Control

i. Initial Cellular Viability

To understand the effect of co-encapsulation on cell viability, initial CoC transformation rates from the first addition of contaminants were compared visibly between suspended and both co-encapsulated treatments (Figure 29). It became necessary to present all time-series data separately, as duplicates diverge at times for reasons explained below.

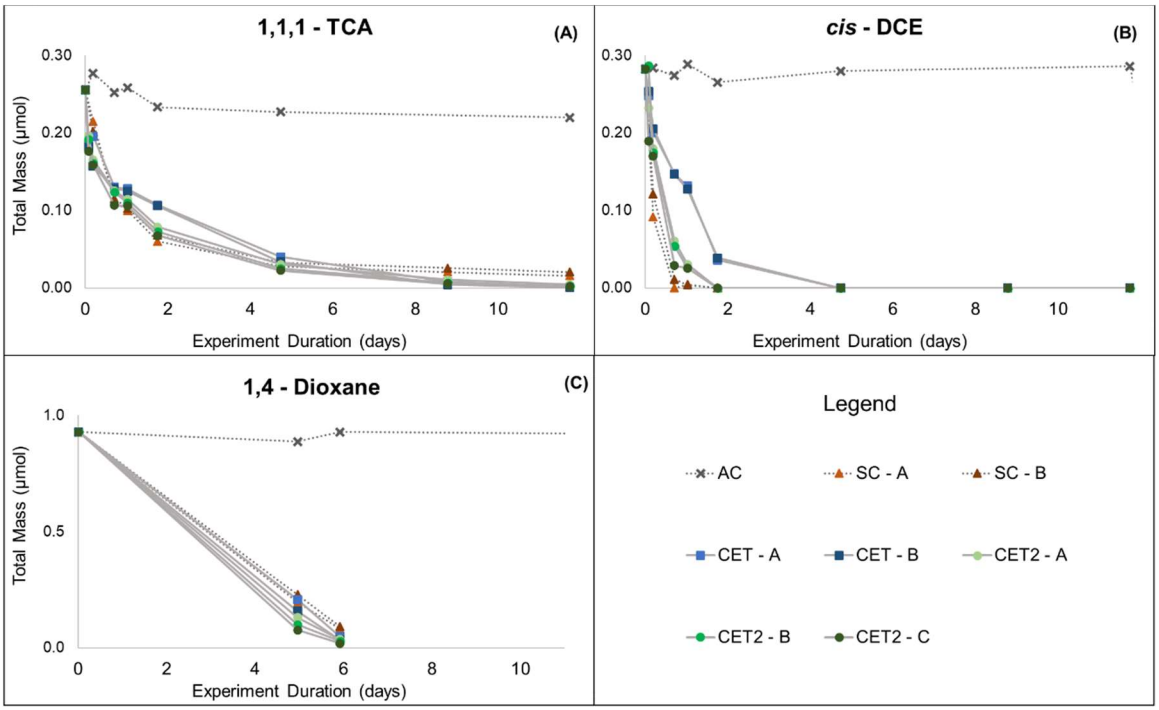

Figure 29. Initial contaminant transformation data comparison between suspended and co-encapsulated ATCC 21198. (AC) – Abiotic control. (SC) – Suspended cell control reactors. (CET) Cells co-encapsulated with 8% (w/w) TBOS. (CET_2) Cells co-encapsulated with 8% (w/w) T_2BOS. Alphabetical designations (A,B,C) are used to signify replicate reactors. AC has a single reactor, SC and CET treatments have duplicate reactors, and CET_2 has triplicate reactors.

Using the initial transformation rates of contaminants as a proxy for cell viability indicates that encapsulated cells are minimally effected by the co-encapsulation process (Figure 29). The

lagged transformation of *c*DCE and to a lesser extent 1,1,1-TCA in reactors containing ATCC 21198 co-encapsulated with TBOS (CET) in comparison to suspended cells does indicate cells may have been slightly impaired initially. Transformation rates for cells co-encapsulated with T_2BOS, compare well with suspended cells. These data in comparison to data presented in section 4.2 and Appendix C illustrate advancements made to encapsulation processes. Initial abiotic control data show minimal decrease in contaminant masses, indicating transformation of contaminants is due to the addition of ATCC 21198 and microbial contamination is not present within the AC at the inception of this experiment.

ii. Complete Control Data Time-series

Abiotic control reactors received a single addition of contaminants that was monitored over ~60 days. At ~ 60 days, contaminant masses were doubled in CET reactors to challenge cells ability to transform higher masses of contaminants. To follow these data the contaminant masses within control reactors were also doubled at ~60 days (Figure 30). Long-term suspended cell remediation-control reactors (SC) were used as a control to provide information about the possible rate, duration, and capacity of CoC transformation by a microbial biomass equivalent to that encapsulated within beads, though with no access to substrates.

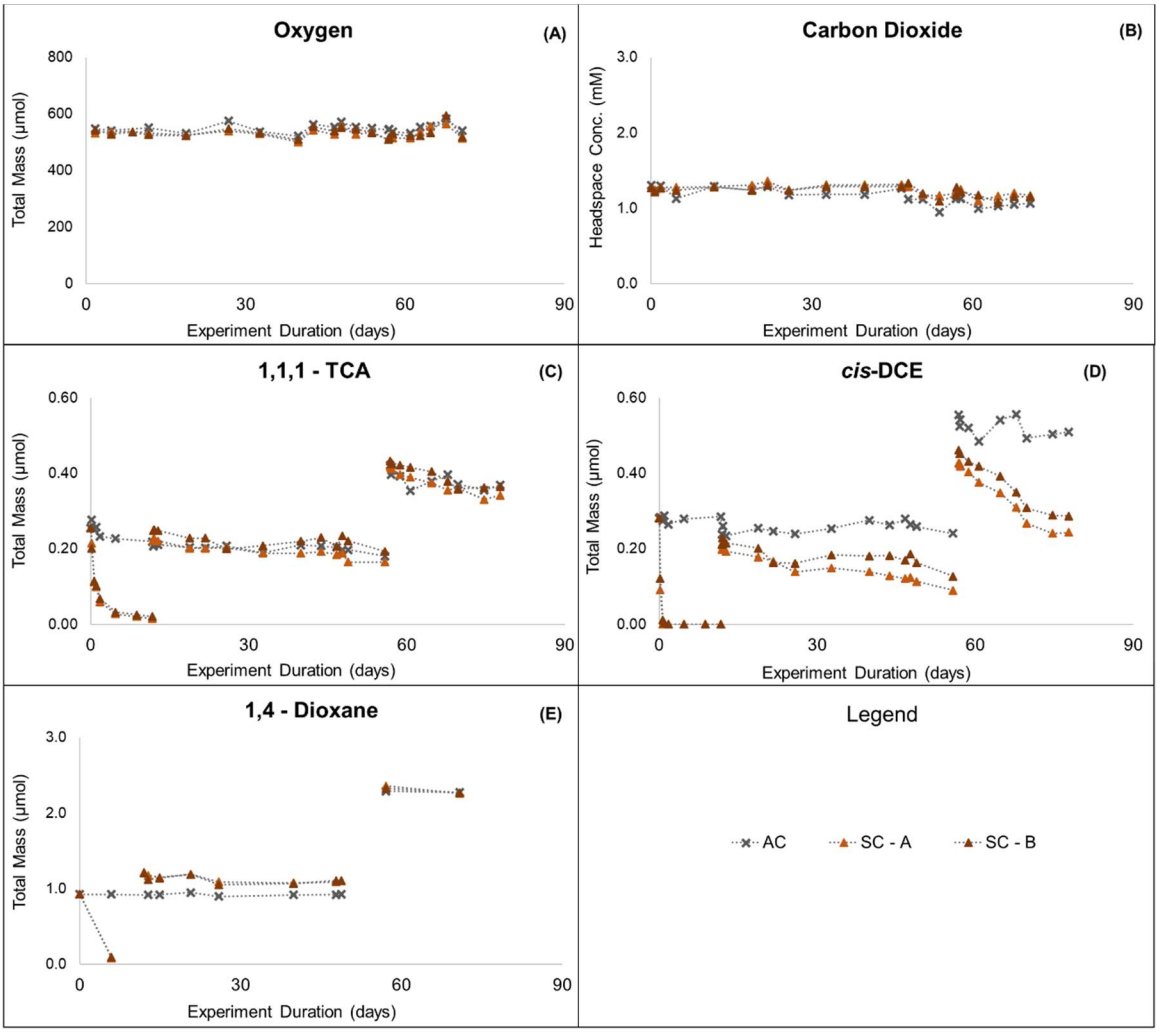

Figure 30. Control reactor respiration data (A and B) and contaminant data (C-E). (AC) – Abiotic control. (SC) – Suspended cell control reactors. Alphabetical designations (A,B,C) are used to signify replicate reactors. AC has a single reactor, SC have duplicate reactors

As seen in figure 30 (C-E) suspended cells rapidly transformed the entire mass of all contaminants within the initial spike, however, transformation of successive contaminant spikes was not observed for 1,1,1-TCA or 1,4-D and drastically reduced for *c*DCE. Suspended cells transformed a minimal percent of contaminants in both the second and third contaminant additions. Abiotic reactors behaved as expected, showing no change in initial contaminant masses, and upon

addition of more contaminants at ~60 days, masses fluctuate but remain at ~twice the original values.

These data illustrate the transformation capacity of ATCC 21198 biomass added to suspended cell reactors was likely met after the first addition of contaminants, and without a growth substrate or an inducing compound within reactors, the cells were not able to maintain cometabolic transformation activity. These reactors directly replicate suspended cell reactors monitored and presented in section 4.3. The contrast between suspended cell transformation duration and capacity observed within the two data sets is suggested to be due to possible differences within biomass growth conditions, where slight differences in growth conditions can cause a batch of cells to store more or less energy per weight of biomass [115]. This may be the reason for higher transformation capacities observed within suspended cell reactors in section 4.3. However, the suspended cell data presented above provide a benchmark for comparison to co-encapsulated cell reactors (CET and CET_2 treatments) in the following sections.

4.6.3. ATCC 21198 Co-encapsulated with TBOS

i. Data Presentation Overview

Figure 31 presents respiration data (O_2/CO_2), cometabolic transformation data (1,1,1-TCA/*c*DCE/1,4-D), and substrate data (1-butanol) collected for CET reactors A and B along with control reactor data collected during the same period. Figure 31 (A-B) contain respiration data. As in previous experiments when O_2 was depleted, due to cellular respiration, the headspace oxygen was refreshed to ensure cometabolism proceeded. Breaks in timeseries connection lines signify times at which O_2 additions were made to reactors. It is apparent from the repetitive decrease in O_2 and constant increase in CO_2 within CET reactors in comparison to suspended control reactors that cellular respiration is occurring within CET reactors. Though additions of O_2 were consistently made to CET reactors to maintain aerobic conditions, reactor CET-B went anoxic around day 30-

45 and after day 65 (Figure 31 A). The lack of O_2 caused transformation to cease during these periods (Figure 31 C-E) . In Figure 31 (B), CO_2 data are presented in terms of measured headspace concentrations due to speciation of CO_2 in the aqueous phase as carbonates and the lack of pH measurements throughout the experiment. Four additions of the chosen CoC mixture were made to CET reactors, three at standard aqueous concentrations (Section 4.6.1) and one with double concentrations made on days 0, 12, 33, and 57, respectively (Figure 31 C-E). Figure 31 (F) presents abiotic 1-butanol production data collected for poisoned co-encapsulated TBOS beads (presented in section 4.5.3), signified by open data points with red connecting lines, superimposed over measurements of 1-butanol within active CET reactors.

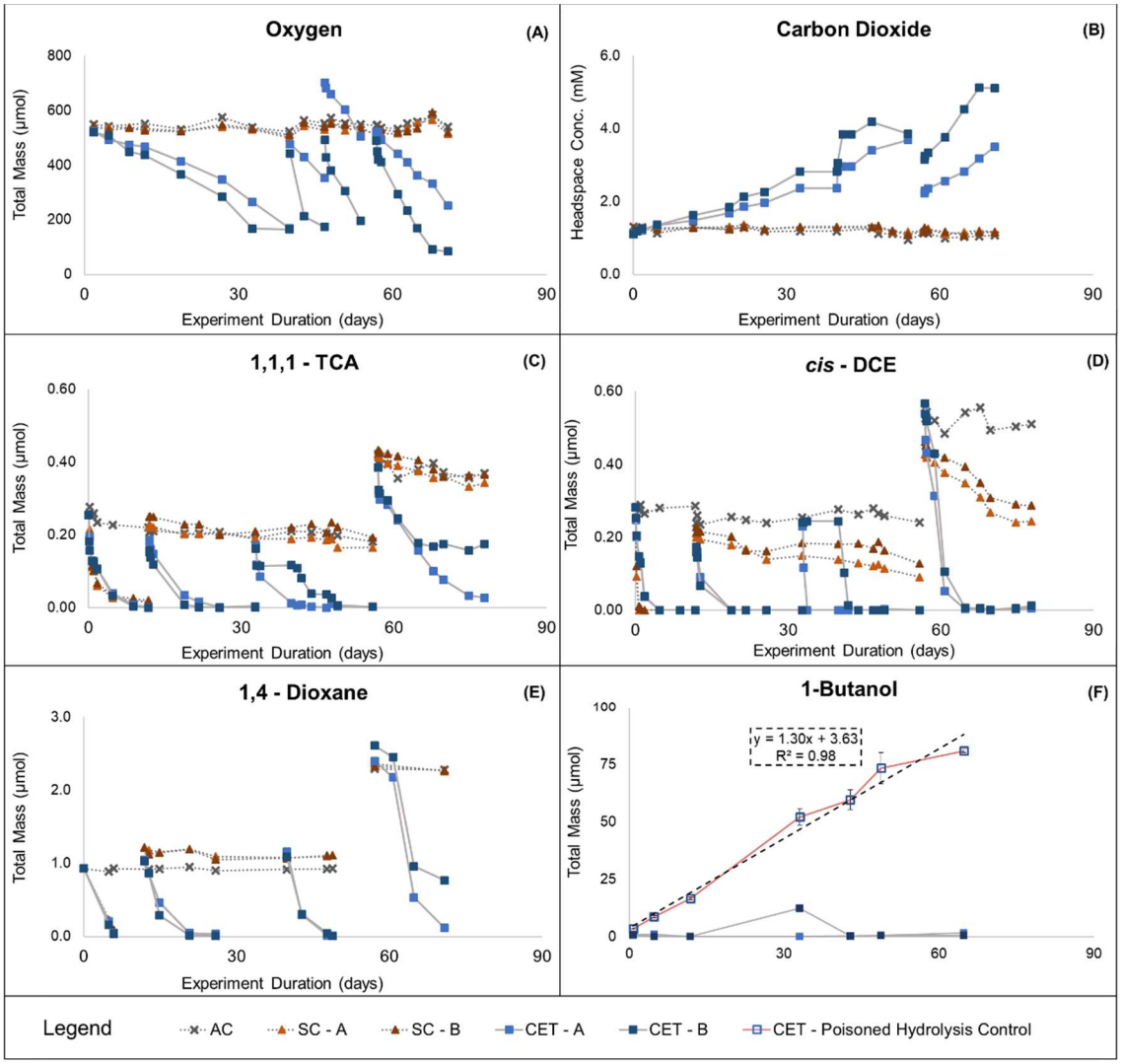

Figure 31. TBOS Co-Encapsulated Cell Cometabolic Transformation Longevity Study. (A-B) Respiration data. O_2 measurements reported at ~180µmol are assumed to be near zero due to vacuum created within reactors (see Section 3.2.1 pg 32). (C-E) Contaminant transformation data. Breaks in time-series connection lines signify successive additions. (F) TBOS 1-butanol production data. Data points with error bars are averages between duplicate reactors and errors bars are 95% confidence intervals. (AC) – Abiotic control. (SC) – Suspended cell control reactors. (CET) Cells co-encapsulated with 8% (w/w) TBOS. Alphabetical designations (A,B,C) are used to signify replicate reactors. AC has a single reactor, SC and CET treatments have duplicate reactors.

ii. Respiration Data

Respiration data collected for CET reactors suggest that microbes are highly active in comparison to suspended cell reactors, as shown by gradual O_2 depletion over the first ~40 days

followed by continued utilization of successive additions of O_2 made on days 40, 47, and 57 (Figure 31 A-B). The first and second additions of O_2, on days 40 and 47, were made via injection of pure O_2 to CET reactor headspaces through septa. For the last headspace refresh at ~57days all reactors including controls were opened to alleviate any vacuum created by repeated gas sampling, and to reduce headspace CO_2 concentrations within CET reactors, a reduction of CO_2 headspace concentration in CET reactors can be seen at ~57days (Figure 31 B).

The rate at which O_2 was utilized within CET reactors increased by 3-7 times from the initial observed rate to the rate observed after the first addition of O_2, however, in subsequent additions, the rate remained fairly constant (Table 17). The observed increase in O_2 consumption rate indicates that microbial growth likely occurred within CET reactors and the following plateauing of rates in subsequent additions suggests a pseudo steady-state biomass level may have been reached within reactors. With unlimited O_2 supply the linear substrate production rate of encapsulated TBOS will control the microbial population and oxygen consumption rate by providing a slow but steady source of substrate.

Table 17. O_2 utilization rates within CET reactors calculated via linear regression of time-series data presented in Figure 31 A. Method of O_2 addition to CET reactors presented.

O_2 Addition	**Method**	**Time of Addition (days)**	**Estimated O_2 Utilization Rate (µmol/day)**	
			CET - A	**CET - B**
0	Initial O_2	0	6.0	9.2
1	Pure O_2 Addition 1	40	18.6	38.1
2	Pure O_2 Addition 2	47	23.1	40.5
3	Atmosphere Headspace Equilibration	57	18.3	34.5

The observed O_2 utilization in CET reactors is due to cellular utilization of 1-butanol released from the hydrolysis of encapsulated TBOS. Of note is the elevated O_2 consumption rate observed

for CET reactor B in comparison to CET - A. This is assumed to be due to a greater 1-butanol release rate within reactor B. This is difficult to confirm because measurements of 1-butanol within active reactors were typically below the detection limit likely due to highly active microbial communities immediately consuming released 1-butanol (Figure 31 F).

One line of evidence confirming that the production of 1-butanol from encapsulated TBOS is driving O_2 utilization within CET reactors is the comparison between oxygen and substrate data in Figure 31 (A and F), where just after ~ 30 days, reactor CET-B went anoxic. The anoxic period in reactor CET – B can be seen by the stagnant O_2 data at ~30days, which was also observed to hinder transformation of contaminants in this reactor at this time. Just after the reactor went anoxic 1-butanol was measured and detected at an elevated mass in solution. After O_2 was refreshed 1-butanol decreased back below the detection limit, providing evidence that O_2 utilization within these reactors is due to cellular oxidation of 1-butanol released from encapsulated TBOS (Figure 31 A and F).

Stoichiometric analysis were used to provide another line of evidence confirming that O_2 consumption and CO_2 production was due to cellular utilization of 1-butanol released from TBOS. Using the measured mass of O_2 consumed within CET reactors at ~70 days, a estimate was made of the amount of 1-butanol that could have been oxidized to CO_2 and water according to equation 3. The estimated mass of 1-butanol oxidized was compared to the mass of 1-butanol that would be predicted to accumulate in reactors based on measured abiotic hydrolysis rates for gellan gum encapsulated TBOS, determined in section 4.5.3 and presented over active reactor data in Figure 31 F (Table 18).

Table 18. Estimated mass of 1-butanol consumed based on stoichiometric relationship of 1-butanol oxidation to CO_2 and water using measured amount of O_2 utilized versus the predicted amount of 1-butanol that would be predicted to be released by measured abiotic production rates.

Predicted Butanol Consumption (µmol)		**Predicted Butanol Production (µmol)**
CET - A	**CET - B**	
156.6	220.5	92.0

The predicted amount of 1-butanol consumed within reactors CET A and B, as estimated by the amount of O_2 utilized at 70 days, are on average ~2 times greater than the amount of 1-butanol that would be predicted to have hydrolyzed at 70 days based on the modeled abiotic linear rate (Table 18).

The elevated oxygen utilization within these reactors may be due to increased release of 1-butanol from microbial enzymatic hydrolysis of encapsulated TBOS. Previous research has shown that certain microbes are capable of biotically hydrolyzing orthosilicate compounds in order to access the attached alcohols more quickly than abiotic processes allow [80]. Even if TBOS is hydrolyzing at double the rate estimated in abiotic reactors, calculations indicate that the mass of encapsulated TBOS could still provide substrates for over 2 years.

A competing theory for the elevated O_2 utilization and CO_2 production in CET reactors, in relation to amount of 1-butanol that is predicted to have been produced by abiotic hydrolysis rates, is that encapsulated cultures respire more oxygen per mass of substrate than suspended cultures [89]. However, in either case, oxygen is being consumed rapidly due to 1-butanol release, which for this technology to be successful should translate to growth of induced microbial cells capable of transforming large quantities of contaminants.

iii. Contaminant Transformation Observations

From respiration data in CET reactors it is apparent that the biomass is active and TBOS hydrolysis is supporting elevated microbial populations. CoC mixture data illustrate that observed

microbial activity translated into high levels of cometabolic transformation activity (Figure 31 C-E). To date CET reactors have received and transformed 4 additions of CoCs, 3 at standard masses and one double mass addition; in contrast, suspended cell control reactors that contained a similar initial biomass have transformed only a single addition of CoCs.

As seen in Figure 31 (C-E), transformation rates within CET reactors of 1,1,1-TCA, *c*DCE, and 1,4-D have not slowed appreciably in comparison to the initial transformation rates observed. In comparison to suspended cells, ATCC 21198 utilizing 1-butanol released from co-encapsulated TBOS has maintained much greater cometabolic activity over the 3 month period. Of note, is the lag in transformation of contaminants observed in reactor CET-B just after the third contaminant addition, ~30days. As noted above, this is when this reactor was anoxic. The absence of O_2 is consistent with the observed lack of transformation of CoCs. After the addition of O_2 ~45 days, CoC transformation proceeds at rates similar to reactor CET-A.

The observations of retained transformation rates and continued cellular activity suggest that co-encapsulated cultures utilizing 1-butanol released from encapsulated TBOS are able to maintain cellular populations similar to or greater than what was added to reactors, and that cells growing on low concentrations of 1-butanol are able to produce and maintain cometabolic enzymes. Previous data have suggested that growth of ATCC 21198 on 1-butanol does not induce cometabolic enzymes [51]. However, similar studies have provided evidence that cometabolic enzymes may be induced by the presence of contaminants themselves and potentially by a starvation mechanism within cells [51,52]. Induction through starvation is suggested to be due to cellular upregulation of non-specific monooxygenase enzymes in an attempt to scavenge any available carbon. The data collected in CET reactors indicate that 1-butanol aqueous concentrations are kept low by immediate cellular utilization and the relatively slow hydrolysis of TBOS. The cometabolic activity of ATCC 21198 is maintained while the aqueous concentrations of 1-butanol

are low. This may suggest that cells are induced by a pseudo-starvation mechanism, although induction may also be occurring from the presence of mixed contaminants as seen in [52].

This experiment suggests that cellular utilization of co-encapsulated SRS products increased cell survivability, overall activity, and contaminant transformation capacity of initially augmented biomass over a period of ~70 days. In conclusion, these results provide initial evidence that co-encapsulation of cometabolizing cultures and LNAPL SRCs that produce alcohols can provide for long-term cometabolic activity.

4.6.4. ATCC 21198 Co-encapsulated with T_2BOS

i. Data Presentation Overview

Figure 32 presents respiration data (O_2/CO_2), cometabolic transformation data (1,1,1-TCA/*c*DCE/1,4-D), and substrate data (1-butanol) collected for CET_2 reactors A, B, and C along with control reactor data collected during the same period. Figure 32 (A-B) contain respiration data. Unlike CET reactors, CET_2 reactors do not appear to be more active than suspended cell controls, and therefore, no additions of O_2 were made to the headspaces of CET_2 reactors. In Figure 32 (B), CO_2 data are presented in terms of measured headspace concentrations due to speciation of CO_2 in carbonate system in the aqueous phase and lack of pH measurements throughout experiment. CET_2 reactors received three additions of the chosen CoC mixture at standard concentrations similar to CET reactors, on days 0, 12, and 47 (Figure 32 C-E). Figure 32 (F) presents abiotic 2-butanol production data collected for poisoned co-encapsulated TBOS beads (presented in section 4.5.3), signified by open data points with red connecting lines, superimposed over measurements of 2-butanol in solution within active CET_2 reactors.

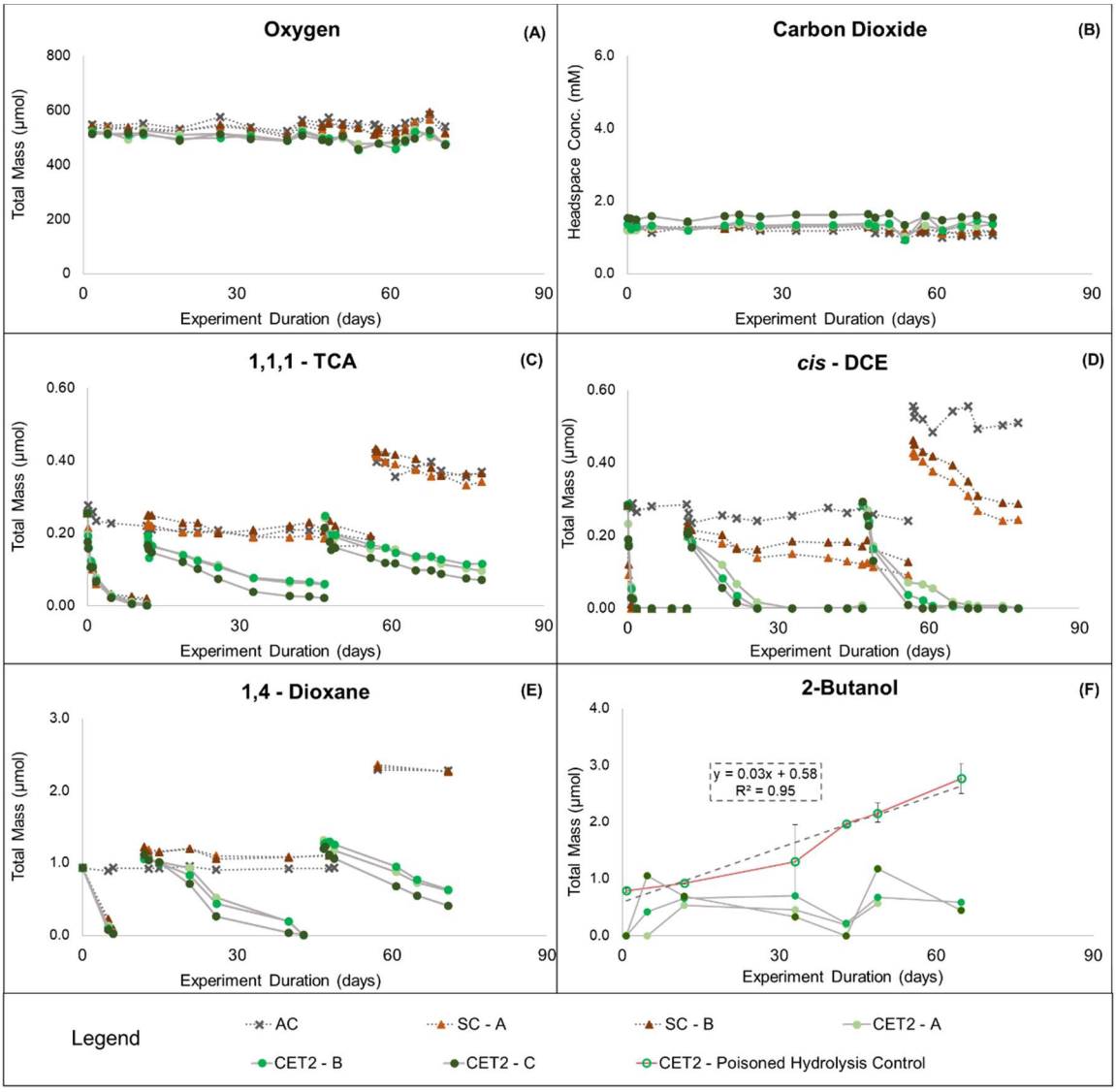

Figure 32. T_2BOS Co-Encapsulated Cell Cometabolic Transformation Longevity Study. (A-B) Respiration data. O_2 measurements reported at ~180µmol are assumed to be near zero due to vacuum created within reactors (see Section 3.2.1 pg 32). (C-E) Contaminant transformation data. Breaks in time-series connection lines signify successive additions. (F) Encapsulated T_2BOS 2-butanol production data. Data points with error bars are averages between duplicate reactors and errors bars are 95% confidence intervals. (AC) – Abiotic control. (SC) – Suspended cell control reactors. (CET_2) Cells co-encapsulated with 8% (w/w) T_2BOS.

ii. Respiration Data

Visual observation of the respiration data collected for CET_2 reactors show little to no evidence of increased cellular activity in relation to suspended or abiotic reactors over the entire ~70 day period (Figure 32 A-B). However, by calculating slopes from the linear regression of all

data points in each time-series and averaging the calculated slopes within treatments, it was determined that relative to suspended and abiotic controls, O_2 with CET_2 reactors has decreased and CO_2 has accumulated (Table 19).

Table 19. Averages of linear regression slopes for time-series 0-70 days in each treatment bounded by 95% confidence intervals. Positive O_2 utilization rate corresponds to a measured decrease in O_2, whereas, positive CO_2 production rates correspond to a measured increase in CO_2.

Treatment	Abbreviation	O_2 Utilization Rate (µmol/day)	CO_2 Production Rate (µMol/day)
Abiotic Control	AC	-0.04 ± N/A	-3.25 ± N/A
Suspended Cell Remediation Control	SC	0.09 ± 0.02	-1.42 ± 0.27
C-encapsulated T_2BOS/ATCC 21198	CET_2	0.48 ± 0.003	0.37 ± 0.54

Though it did not appear, visibly, that CET_2 reactors were more active than either control treatments, the data presented in Table 19 provides evidence that respiration was occurring within CET_2 reactors. The contrast between CET and CET_2 respiration data could have been predicted by the drastic difference in abiotic hydrolysis rates observed between TBOS and T_2BOS (Table 15).

To support these findings, Figure 32 (F) shows that by ~70 days poisoned co-encapsulated T_2BOS is predicted to have produced ~2.2µmol of 2-butanol, which would require ~13µmol of O_2 to oxidize, according to equation 3. From the predicted O_2 utilization rate estimated above, ~18µmol of oxygen has been consumed in CET_2 reactors at 70 days. The similarity between the measured O_2 consumption and 2-butanol production estimates suggests that the observed utilization of O_2 could be due to microbial consumption of 2-butnaol being slowly hydrolyzed from encapsulated T_2BOS.

While this analysis indicates that some cellular activity is likely occurring within CET_2 reactors in comparison to suspended cell controls, the amount is minimal in comparison to cells in

CET reactors, consuming 1-butanol released from co-encapsulated TBOS. Therefore, these data indicate that cell biomass has likely not increased in CET_2 reactors but may have diminished due to endogenous decay exceeding cell growth with prolonged incubation.

iii. Contaminant Transformation Observations

Respiration data within the CET_2 treated reactors indicate that there is minimal cellular activity. However, three consecutive additions of the chosen CoC mixture have been added to and transformed by CET_2 reactors, all at levels similar to CET reactors. CET_2 reactors have degraded the majority of all contaminants added, with the exception of 1,1,1-TCA, which is known to have the lowest transformation rate of the mixture (Figure 32 C-E).

In contrast to suspended cells, upon addition of the second spike of contaminants, CET_2 reactors continued to transform all CoCs at appreciable rates, whereas, suspended cells did not transform measureable amounts of 1,1,1-TCA or 1,4-D when compared to the abiotic control, though slow transformation of *c*DCE may be occurring in suspended cell reactors.

These data indicate that in CET_2 reactors, the presence of T_2BOS, and likely the slow release and consumption of 2-butanol, has increased encapsulated cell survivability and transformation capacity in comparison to suspended cells. This is likely due to the slow rate of release of the inducing primary growth substrate providing some energy for cellular growth or potentially cell and enzyme maintenance. In either case, the encapsulated cultures cometabolic transformation potential has been maintained for over 70 days with minimal increase in oxygen demand when compared with free suspended cells that lost the majority of cometabolic transformation potential prior to day 12. The low oxygen demand observed in CET_2 reactors, in comparison to the mass of contaminants transformed, is a very positive outcome, since O_2 will likely be the limiting factor in contaminated aquifers.

4.6.5. Co-encapsulated TBOS and T_2BOS Data Comparison

ATCC 21198 co-encapsulated with TBOS showed highly elevated levels of cellular respiration, which corresponded directly to a large increase in cometabolic transformation capacity of the initially augmented biomass. Transformation capacities of cells in CET reactors were at least 4 times greater than cells suspended directly in media (Table 20). In addition, it was observed that CET reactors did not experience any appreciable decrease in transformation rates in successive contaminant spikes, as was seen in suspended and encapsulated cell reactors without SRSs presented in section 4.3 (Figure 33).

A period of anoxic conditions in reactor CET-B provided evidence that cellular respiration was due to microbial consumption 1-butanol, produced through the hydrolysis of encapsulated TBOS. Also, the increase in rate at which oxygen was consumed in consecutive additions indicated microbial biomass growth. O_2 utilization rates did visibly plateau after the second O_2 addition, which was likely controlled by the hydrolysis rate of encapsulated TBOS (Table 17). Also, it was shown that TBOS was likely hydrolyzing more quickly within active reactors than in abiotic reactors, and as such the conclusion was drawn that ATCC 21198 may have the ability to biotically hydrolyze TBOS.

ATCC 21198 co-encapsulated with T_2BOS showed only very slight increases in cellular respiration in comparison to suspended cells, and, not nearly to the same degree as TBOS co-encapsulated cells (Table 20). This results from the hydrolysis rate of encapsulated T_2BOS being ~40 times less in comparison to encapsulated TBOS (Table 15). In spite of the low amount of estimated substrate produced and minimal O_2 utilized within CET_2 reactors, much higher transformation rates and capacities in CET_2 reactors were observed when compared to suspended cultures over the duration of this experiment (Table 20). Calculated transformation capacities of cells in CET_2 reactors were at least 2 times greater than suspended cells (Table 20). However,

transformation rates in CET_2 reactors were slower than in CET reactors (Figure 33). The observed slower transformation rates within CET_2 reactors are less desirable than the higher transformation rates in CET reactors, however, an important consideration upon application of the designed technology will be oxygen mass consumed per mass of contaminant transformed.

Figure 33 and Table 20 illustrate the contrast between contaminant transformation rates and capacities and oxygen consumption observed within CET and CET_2 reactors. CET reactors were able to transform ~2 times the amount of contaminants that CET_2 reactors were at ~70 days, though CET reactors consumed ~35 times the amount of oxygen. However, from Figure 33 it is apparent from zero slowing in transformation rates over the ~ day period that CET reactors could likely have transformed more contaminants than were added. Therefore, a direct comparison between the amount of contaminants transformed to the amount of O_2 utilized between CET and CET_2 reactors may not be representative. However, the amount of O_2 consumed and contaminants transformed are presented in Table 20 to illustrate the contrast between the two co-encapsulation scenarios.

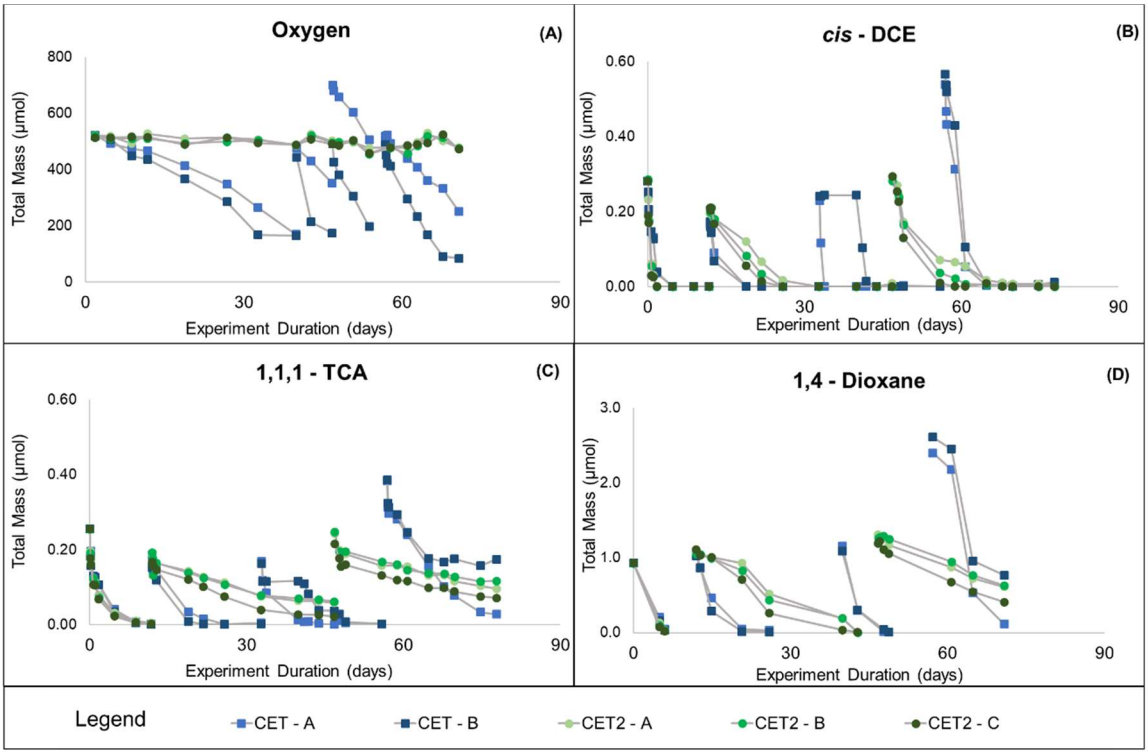

Figure 33. TBOS and T_2BOS Co-Encapsulated Cell Cometabolic Transformation Longevity Study. (CET) Cells co-encapsulated with 8% (w/w) TBOS. (CET_2) Cells co-encapsulated with 8% (w/w) T_2BOS. (A) Oxygen data contrasting CET and CET_2 treatments. Reactor CET-B went anoxic ~days 30-45 and from day 65 on, seen in O_2 data and lack of O_2 also caused transformation to cease during these periods. (B-D) Contaminant transformation data. Four additions of CoCs were made to CET reactors and three to CET_2 reactors. CET transformation rates ae visibly greater. Breaks in time-series connection lines signify successive additions.

Table 20. All masses reported have been estimated over a 70 day period. The mass of butanol produced was estimated based on measured poisoned encapsulated SRS reactors. O_2 consumption for AC, SC, and CET_2 reactors was based on estimated O_2 utilization rates presented in Table xx and is an averaged of the measured O_2 utilized in CET reactors. Total contaminant transformation masses are average measured values between treatments.

Treatment	Estimated Butanol Produced (µmol)	Estimated Oxygen Consumed (µmol)	Total Mass of Contaminant Transformed (µmol)		
			1,1,1 - TCA	*c*DCE	1,4 - Dioxane
AC - Abiotic Control	N/A	N/A	0.13	0.09	0.02
SC - Suspended Cell Controls	N/A	6.3	0.36	0.49	1.03
CET - Cells Co-encapsulated with TBOS	91	1131.2	0.87	1.23	5.08
CET_2 - Cells Co-encapsulated with T_2BOS	2.1	33.6	0.53	0.77	2.67

4.6.6. Gellan Gum Co-encapsulated ATCC 21198 Summary and Conclusions

ATCC 21198 co-encapsulated with both model SRSs was observed to have the ability to transform greater masses of contaminants than suspended cells over the duration of this experiment (Table 20). Cells in CET reactors transformed ~4 times the total mass of CoCs as suspended cells, while CET_2 reactors transformed ~2 time the mass of contaminants as suspended cells. The greater transformation capacities was shown to be due to energy gained from cellular utilization of the slow hydrolysis of substrates from co-encapsulated SRSs. Also both systems have ample SRCs to continue to promote longer-term contaminant transformation.

Though both co-encapsulated treatments were observed to have retained much greater cometabolic transformation potential than suspended cultures, it was observed that cells co-encapsulated with TBOS maintained higher cometabolic transformation rates and transformed ~2 times the total mass of CoCs as cells co-encapsulated with T_2BOS. However, cells co-encapsulated with TBOS required ~35 times more oxygen than cells co-encapsulated with T_2BOS.

These data illustrate the tradeoff and balance that will need to be maintained between substrate hydrolysis, oxygen consumption, and contaminant transformation. These parameters will be heavily influenced by the rate of SRS hydrolysis or substrate production, substrate utilization, and the degree of cometabolic enzyme induction. Therefore, it is suggested, that future work be focused on understanding the kinetics behind the developed technology in order to develop a model that includes hydrolysis rates, cellular growth and utilization of substrates, oxygen consumption, and contaminant transformation. This model might be used to optimize the technology and could be used to address and mitigate issues including excess cellular growth and oxygen depletion in the subsurface prior to application.

CHAPTER 5: CONCLUSIONS

Initially, it was suggested that encapsulation of microbes prior to bioaugmentation of contaminated aquifers may improve current bioremediation techniques by providing benefits to augmented cultures including protection from toxic substances, ambient stressors like temperature and pH, and predation by protozoa. Also, encapsulation provides a method to obtain and maintain localized high cell densities, mitigate biofilm production and aquifer clogging, and increase transport distance of cells through subsurface porous media. The results of previous research provide strong evidence that encapsulation of microbes may provide the above benefits [12–14,85–87]. However, the overarching hypothesis of this thesis was that if it were possible to include SRSs within an encapsulation matrix with cometabolically active cultures, then co-encapsulated cells would be afforded addition benefits and many issues with current bioaugmentation techniques could be mitigated.

It was hypothesized that co-encapsulated SRSs could produce an exclusive controlled source of inducing growth substrate that would support the co-encapsulated microbial populations, extend the remediation duration, and increase the transformation capacity of initially augmented cultures. In addition to supporting a targeted microbial species, it was suggested that the inclusion of an SRS would mitigated issues with current bioaugmentation methods that result in excess cellular growth, oxygen depletion, and the need for recurring low concentration injections of gaseous substrates. A large portion of the work conducted and presented above was aimed at developing methods such that the proposed co-encapsulation technology could be tested at the lab scale.

This work started by developing methods for the successful encapsulation of the model cometabolizing culture *Rhodococcus Rhodochrous* ATCC 21198 in alginate and gellan gum hydrogel beads. Initially, encapsulated cultures experienced a ~60% reduction in substrate

utilization rates, which was shown to translate into a large reduction in cells ability to transform CoCs over extended periods of time (Appendix C). However, after method optimization ATCC 21198 was successfully encapsulated in spherical alginate macro-beads (~2mm in diameter), cylindrical gellan gum macro-beads (~2mm in height by ~2mm in diameter) and spherical gellan gum micro-beads (~10-100µm in diameter) with little effect on short-term substrate utilization or long-term cellular cometabolic transformation potential, when compared to suspended cultures (Section 4.2-3).

From long-term experiments, it was discovered that suspended and encapsulated ATCC 21198 could maintain cometabolic transformation potential for extended periods of time, over 120 days. In addition to this, it was confirmed that alginate beads were less resistant to break-down than gellan gum [97,108]. ATCC 21198 had the ability to oxidize a portion of the alginate matrix. The energy gained by consumption of alginate resulted in a cometabolic activity compared to suspended and gellan gum-encapsulated cells. However, the observed consumption of the alginate matrix was associated with a large oxygen demand and also led to bead instability after several months. In contrast to alginate, gellan gum was not accessible as a carbon source for ATCC 21198 nor a contaminant microbe. This provides evidence that upon application of this technology in a natural system, gellan gum will be more successful, due to increased durability, and less oxygen demand will be associated with the encapsulation matrix (Section 4.3).

After microbial encapsulation was optimized, methods were developed to encapsulate two model LNAPL SRSs, TBOS and T_2BOS, in both alginate and gellan gum hydrogel beads. Mass loadings were achieved above what had been observed previously with other LNAPL oils, ~30% (w/w) and ~8% (w/w) for alginate and gellan gum, respectively [114]. Long-term experiments provided evidence that encapsulated SRSs could be held within beads for extended periods, over ~80days, and abiotic hydrolysis experiments conducted with encapsulated SRSs, showed that after

encapsulation hydrolysis rates of both TBOS and T_2BOS were reduced by an order of magnitude in comparison to suspended SRSs. In addition to the observed reduction in hydrolysis rates after encapsulation, it was shown that the mass loading of LNAPL SRSs within beads might affect the rate at which encapsulated SRSs hydrolyze and produce substrates. It was found that TBOS encapsulated at 5% (w/w) hydrolyzed at twice the rate of TBOS encapsulated at 30% (w/w) (Table 13), indicating that it may be possible to tune the hydrolysis rate of encapsulated SRSs by adjusting the amount of SRS entrapped within beads.

The above phenomena, demonstrated within this thesis, in combination with the known difference in hydrolysis rates between SRS compounds may provide valuable controls over substrate production rates. Engineered controls over substrate release alone might benefit current bioremediation techniques through the ability to make a single high concentration injection of SRSs that would provide a long-term timed production of IGS. For example, it was predicted from the measured hydrolysis rates and an assumed bead mass loading of 10 % SRS (w/w) that over 90 mg of cells could be generated and SRSs could provide substrates for several to hundreds of years. This demonstrates the potential for this technology to solve issues encountered with current growth substrates, such as, the need for recurring injections of currently used gaseous substrates due to low solubility, excess cellular growth from injection of elevated concentrations of IGSs, and oxygen depletion due to excess cellular utilization of substrates.

The capstone work of this thesis utilized methods developed above, in combination, to co-encapsulate ATCC 21198 with LNAPL SRSs in gellan gum macro-beads with little effect on cellular viability. It was determined from long-term experiments that co-encapsulated cultures could utilize SRS products within beads prior to any build up in solution, indicating that substrate utilization rates were greater than substrate production rates and that all substrates were likely being utilized by the target encapsulated culture. Results from long-term studies also confirmed that the

energy gained by cometabolizing cultures from SRS products could support cometabolically active microbial populations for extended durations, over 70 days.

The purpose of this thesis was realized when it was determined that the utilization of released 1- and 2-butanol from co-encapsulated TBOS and T_2BOS increased the survivability, overall activity, and contaminant transformation rate and capacity of initially augmented biomass. However, differences in hydrolysis rates of the examined orthosilicate compounds led to the observation of a major tradeoff between the substrate production and utilization rate, oxygen demand, and cellular contaminant transformation capacities and rates. It was observed that higher substrate production rates could support greater microbial populations, which were able to transform contaminants at higher rates, though increased substrate utilization led to elevated oxygen demand. Oxygen is necessary but limited resource in the subsurface and upon application of this technology may be the limiting factor, and therefore, slower substrate production rates may prove to be more efficient in the long-term transformation of contaminants. The findings below highlight the important discoveries made during long-term co-encapsulation experiments.

- Gellan gum is more durable and resistant to break-down than alginate and results gathered suggest that gellan gum will be a more successful encapsulation matrix upon application of the developed technology. Also, creation of gellan gum micro-beads ~10-100µm in diameter provide positive evidence that this technology can be scaled down.

- Cells co-encapsulated with TBOS were observed to transform each contaminant in a mixture of 1,1,1-TCA, *c*DCE, and 1,4-D at rates similar to initially augmented biomass for as long as ~70 days; whereas, suspended cells cometabolic transformation potential was drastically reduced before ~12days. Also, cells co-encapsulated with TBOS transformed ~4 times more contaminants that suspended cells after over 70 days, and could likely have transformed a higher mass of CoCs.

- Cells co-encapsulated with T_2BOS were observed to transform each contaminant in a mixture of 1,1,1-TCA, *c*DCE, and 1,4-D at appreciable rates for as long as ~70 days. Transformation rates observed in cells co-encapsulated with T_2BOS were not maintained as well as cells co-encapsulated with TBOS, however, T_2BOS cells did transform ~2 times more contaminants than suspended cells after 70 days, and will likely continue to transform contaminants with continued incubation.

- Although contaminant transformation rates were observed to be higher in reactors containing ATCC 21198 co-encapsulated with TBOS than T_2BOS and around twice the total mass of contaminants were transformed in TBOS reactors, the amount of O_2 utilized over a 70 day period within TBOS reactors was ~35 times more than in T_2BOS reactors. This illustrates the tradeoff between transformation rate and oxygen utilization efficiency. These data suggest that the co-encapsulated system containing a SRS that produces a known inducing substrate at a very slow rate may be much more efficient at treating CoCs.

In summary, it was determined that:

1. LNAPL SRCs that hydrolyze to produce substrates known to induce cometabolizing cultures can be successfully encapsulated for extended periods of time in beads made from the natural polysaccharide hydrogels alginate and gellan gum.
2. Encapsulated LNAPL SRS products can be consumed by co-encapsulated ATCC 21198 and utilized for cellular growth and cometabolic enzyme production prior to diffusion from beads.
3. Encapsulated cellular utilization of SRS products increased cell survivability, activity, and cometabolic transformation rates and capacities.

The summarized results above confirm the overarching hypothesis investigated throughout this thesis and provide strong evidence that the developed technology could successfully be used to provide an exclusive controlled source of IGS that can be utilized by co-encapsulated cells to support encapsulated microbial populations and extend the remediation duration, and increase the transformation capacity of initially augmented cultures. As optimization was not the objective of this thesis, prior to concluding, discussion of possible future work that could drastically improve this technology, before application, is presented below.

CHAPTER 6: FUTURE WORK

The technology within this thesis was developed as an overarching proof of concept, and therefore, it is suggested that future work be conducted with the aim of understanding the basic kinetics of the overarching system. Future work should be focused on developing a model including parameters such as SRS hydrolysis rate, cell substrate utilization rate, cell respiration, cell growth and decay, and contaminant transformation in order to further understand and optimize the system prior to application.

The discoveries made within this thesis were made at the macro-bead scale, ~2mm, and the proposed technology is suggested to be on the micron-scale such that beads can be transported through porous media. The successes with macro-beads have led to concepts for use at the macro-scale such as in reactive barrier systems or above ground bioreactors, which could be the focus of future work. However, micron scale beads, ~10-40μm in diameter, would be necessary for the desired application of co-encapsulated micro-beads to contaminant subsurface. The successful encapsulation of ATCC 21198 in micro-beads, ranging in size from ~10-100μm, does suggest that the developed technology can be downscaled such that the beads can be transported successfully through porous aquifer media [15]. However, little success was achieved in attempts to create micro-beads containing both SRSs and microbes. It is therefore suggested that future work focus on developing techniques for micro-encapsulation of LNAPL SRSs and active microbial cultures. This may be possible through development of double emulsion techniques as illustrated in [116–118] in which oils were successfully encapsulated in micron-scale gel beads.

This thesis also focused on a single group of potential SRSs, LNAPL orthosilicate compounds, though all observations made with these compounds were not fully understood; such as the phenomena of slower hydrolysis rates when TBOS was encapsulated within alginate at

higher mass loadings (Section 4.5). This observed phenomenon could provide a useful control over substrate production rates and should be a focus of future work. Future work should also focus on investigating other potential SRS compounds that may hydrolyze at different rates or produce more favorable substrates such as organic esters, other LNAPL orthosilicates, or LNAPL essential oils that have been shown to induce cometabolizing cultures [77].

Another important consideration is that all of the work within this thesis was conducted on "clean systems" or pure culture systems. Investigation into how well co-encapsulated cells would perform in microcosm or column studies with native microbes present would be useful to make further predictions about the successful application of this technology in a field scale setting. Also, this thesis focused on a single mixture of contaminants that ATCC 21198 was able to transform, though it is known that ATCC 21198 is much less capable of degrading TCE. Therefore, it is suggested that future work be focused on adapting the developed technology such that other model cometabolizing microbial species capable of transformation of other common groundwater contaminants, like TCE, can be encapsulated and co-encapsulated in hydrogel beads, with appropriate SRSs.

CHAPTER 7: REFERENCES

1. Squillace, P. J., Scott, J. C., Moran, M. J., Nolan, B. T. & Kolpin, D. W. VOCs, pesticides, nitrate, and their mixtures in groundwater used for drinking water in the United States. *Environ. Sci. Technol.* 36, 1923–1930 (2002).
2. Zogorski, J. S. *The Quality of our nation's waters: volatile organic compounds in the nation's ground water and drinking-water supply wells*. (U.S. Geological Survey, 2006).
3. NIOSH. CDC - Organic Solvents - NIOSH Workplace Safety and Health Topic. (2013). Available at: https://www.cdc.gov/niosh/topics/organsolv/default.html. (Accessed: 8th August 2018)
4. Anderson, R. H., Anderson, J. K. & Bower, P. A. Co-occurrence of 1,4-dioxane with trichloroethylene in chlorinated solvent groundwater plumes at US Air Force installations: Fact or fiction. *Integr. Environ. Assess. Manag.* 8, 731–737 (2012).
5. ATSDR. *Toxicological Profile for 1,4-Dioxane*. (Agency for Toxic Substances and Disease Registry (ASTDR), 2012).
6. Hand, S., Wang, B. & Chu, K.-H. Biodegradation of 1,4-dioxane: Effects of enzyme inducers and trichloroethylene. *Sci. Total Environ.* 520, 154–159 (2015).
7. Frascari, D., Zanaroli, G. & Danko, A. S. In situ aerobic cometabolism of chlorinated solvents: A review. *J. Hazard. Mater.* 283, 382–399 (2015).
8. Semprini, L. Strategies for the aerobic co-metabolism of chlorinated solvents. *Curr. Opin. Biotechnol.* 8, 296–308 (1997).
9. Azizian, M. F., Istok, J. D. & Semprini, L. Evaluation of the in-situ aerobic cometabolism of chlorinated ethenes by toluene-utilizing microorganisms using push–pull tests. *J. Contam. Hydrol.* 90, 105–124 (2007).
10. Connon, S. A. *et al.* Bacterial community composition determined by culture-independent and -dependent methods during propane-stimulated bioremediation in trichloroethene-contaminated groundwater. *Environ. Microbiol.* 7, 165–178 (2005).
11. Semprini, L., Ely, R. L. & Lang, M. M. Modeling of Cometabolism for the in situ Biodegradation of Trichloroethylene and Other Chlorinated Aliphatic Hydrocarbons. *Fundamentals and Applications of Bioremediation* (2017). doi:10.1201/9780203755389-4
12. Moslemy, P., Neufeld, R. J. & Guiot, S. R. Biodegradation of gasoline by gellan gum-encapsulated bacterial cells. *Biotechnol. Bioeng.* 80, 175–184 (2002).
13. Petrich, C. R., Stormo, K. E., Ralston, D. R. & Crawford, R. L. Encapsulated Cell Bioremediation: Evaluation on the Basis of Particle Tracer Tests. *Groundwater* 36, 771–778 (1998).
14. Cassidy, M. Environmental Applications of Immobilized Microbial Cells: A Review. (1996).
15. Moslemy, P., Neufeld, R. J., Millette, D. & Guiot, S. R. Transport of gellan gum microbeads through sand: an experimental evaluation for encapsulated cell bioaugmentation. *J. Environ. Manage.* 69, 249–259 (2003).
16. Kurz, M. D. & Olson, E. S. *Subtask 1.16-Slow-Release Bioremediation Accelerators*. (University Of North Dakota, 2006).
17. Lin, C.-W., Wu, C.-H., Tang, C.-T. & Chang, S.-H. Novel oxygen-releasing immobilized cell beads for bioremediation of BTEX-contaminated water. *Bioresour. Technol.* 124, 45–51 (2012).

18. Trevors, J. T., Elsas, J. D. van, Lee, H. & Wolters, A. C. Survival ofalginate-ecapsulated <Emphasis Type="Italic">Pseudomonas fluorescens</Emphasis> cells in soil. *Appl. Microbiol. Biotechnol.* 39, 637–643 (1993).
19. Luo, Y., Zhang, B., Whent, M., Yu, L. (Lucy) & Wang, Q. Preparation and characterization of zein/chitosan complex for encapsulation of α-tocopherol, and its in vitro controlled release study. *Colloids Surf. B Biointerfaces* 85, 145–152 (2011).
20. Hosseini, S. F., Zandi, M., Rezaei, M. & Farahmandghavi, F. Two-step method for encapsulation of oregano essential oil in chitosan nanoparticles: Preparation, characterization and in vitro release study. *Carbohydr. Polym.* 95, 50–56 (2013).
21. M.A. Maupin *et al. Estimated Use of Water in the United States in 2010*. (USGS, 2014).
22. NPDWR. *National Primary Drinking Water Regulations*. (US Department of the Interior, US Geological Survey, 2005).
23. Doherty, R. E. A History of the Production and Use of Carbon Tetrachloride, Tetrachloroethylene, Trichloroethylene and 1,1,1-Trichloroethane in the United States: Part 1—Historical Background; Carbon Tetrachloride and Tetrachloroethylene. *Environ. Forensics* 1, 69–81 (2000).
24. Gabriel, C. L. influence of New Solvents on Development of Chemical Industries. *News Ed. Am. Chem. Soc.* 19, 131–134 (1941).
25. EPA. The Plain Engilish Guide to the Clean Air Act. (2007).
26. List -10, C. *Contaminants at CERCLIS SITES (List-10)*. (United States Environmental Protection Agency (USEPA), 2013).
27. Mohr, T. K. G. Environmental Investigation and Remediation: 1,4-Dioxane and other Solvent Stabilizers. *CRC Press* (2010). Available at: https://www.crcpress.com/Environmental-Investigation-and-Remediation-14-Dioxane-and-other-Solvent/Mohr-Stickney-DiGuiseppi/p/book/9781566706629. (Accessed: 9th August 2018)
28. Brautbar, N. & Williams, J. Industrial solvents and liver toxicity: Risk assessment, risk factors and mechanisms. *Int. J. Hyg. Environ. Health* 205, 479–491 (2002).
29. Huang, B., Lei, C., Wei, C. & Zeng, G. Chlorinated volatile organic compounds (Cl-VOCs) in environment — sources, potential human health impacts, and current remediation technologies. *Environ. Int.* 71, 118–138 (2014).
30. Liu, C. & Ball, W. P. Back diffusion of chlorinated solvent contaminants from a natural aquitard to a remediated aquifer under well-controlled field conditions: predictions and measurements. *Ground Water* 40, 175–184 (2002).
31. Zhang, S., Mao, G., Crittenden, J., Liu, X. & Du, H. Groundwater remediation from the past to the future: A bibliometric analysis. *Water Res.* 119, 114–125 (2017).
32. Gossett, J. M. Measurement of Henry's law constants for C1 and C2 chlorinated hydrocarbons - Environmental Science & Technology (ACS Publications). (1987). Available at: https://pubs.acs.org/doi/abs/10.1021/es00156a012. (Accessed: 9th August 2018)
33. Horvath, A. L., Getzen, F. W. & Maczynska, Z. IUPAC-NIST Solubility Data Series 67. Halogenated Ethanes and Ethenes with Water. *J. Phys. Chem. Ref. Data* 28, 395–627 (1999).
34. Semprini, L. In situ bioremediation of chlorinated solvents. *Environ. Health Perspect.* 103, 101–105 (1995).
35. Mackay, D. M. *et al.* A controlled field evaluation of continuous vs. pulsed pump-and-treat remediation of a VOC-contaminated aquifer: site characterization, experimental setup, and overview of results. *J. Contam. Hydrol.* 41, 81–131 (2000).

36. Bankston, J. L., Sola, D. L., Komor, A. T. & Dwyer, D. F. Degradation of trichloroethylene in wetland microcosms containing broad-leaved cattail and eastern cottonwood. *Water Res.* 36, 1539–1546 (2002).
37. Anderson, J. E. & McCarty, P. L. Transformation yields of chlorinated ethenes by a methanotrophic mixed culture expressing particulate methane monooxygenase. *Appl. Environ. Microbiol.* 63, 687–693 (1997).
38. Mahendra, S. & Alvarez-Cohen, L. Kinetics of 1,4-Dioxane Biodegradation by Monooxygenase-Expressing Bacteria. *Environ. Sci. Technol.* 40, 5435–5442 (2006).
39. Arp, D. J., Yeager, C. M. & Hyman, M. R. Molecular and cellular fundamentals of aerobic cometabolism of trichloroethylene. *Biodegradation* 12, 81–103 (2001).
40. Kim, S., Hwang, J., Chung, J. & Bae, W. Enhancing trichloroethylene degradation using non-aromatic compounds as growth substrates. *J. Hazard. Mater.* 275, 99–106 (2014).
41. Morono, Y., Unno, H. & Hori, K. Correlation of TCE cometabolism with growth characteristics on aromatic substrates in toluene-degrading bacteria. *Biochem. Eng. J.* 31, 173–179 (2006).
42. Ensign, S. A., Hyman, M. R. & Arp, D. J. Cometabolic degradation of chlorinated alkenes by alkene monooxygenase in a propylene-grown Xanthobacter strain. *Appl. Environ. Microbiol.* 58, 3038–3046 (1992).
43. Tyagi, M., da Fonseca, M. M. R. & de Carvalho, C. C. C. R. Bioaugmentation and biostimulation strategies to improve the effectiveness of bioremediation processes. *Biodegradation* 22, 231–241 (2011).
44. Elango, V., Kurtz, H. D. & Freedman, D. L. Aerobic cometabolism of trichloroethene and cis-dichloroethene with benzene and chlorinated benzenes as growth substrates. *Chemosphere* 84, 247–253 (2011).
45. Yeager, C. M., Arthur, K. M., Bottomley, P. J. & Arp, D. J. Trichloroethylene degradation by toluene-oxidizing bacteria grown on non-aromatic substrates. *Biodegradation* 15, 19–28 (2004).
46. Johnson, E. L., Smith, C. A., O'Reilly, K. T. & Hyman, M. R. Induction of Methyl Tertiary Butyl Ether (MTBE)-Oxidizing Activity in Mycobacterium vaccae JOB5 by MTBE. *Appl. Environ. Microbiol.* 70, 1023–1030 (2004).
47. McCarty, P. L. In situ bioremediation of chlorinated solvents. *Curr. Opin. Biotechnol.* 4, 323–330 (1993).
48. McCarty, P. L. Biotic and Abiotic Transformation of Chlorinated Solvents in Ground Water. In: Remediation technology development forum intrinsic remediation project at Dover Air Force Base, Delaware. in *Symposium on Natural Attenuation of Chlorinated Organics in Ground Water* 95 (1997).
49. Pant, P. & Pant, S. A review: Advances in microbial remediation of trichloroethylene (TCE). *J. Environ. Sci.* 22, 116–126 (2010).
50. Li, M. *et al.* Hindrance of 1,4-dioxane biodegradation in microcosms biostimulated with inducing or non-inducing auxiliary substrates. *Water Res.* 112, 217–225 (2017).
51. Personal Communication Hyman, M. Personal Communication 2018. (2018).
52. McClay, K., Streger, S. H. & Steffan, R. J. Induction of toluene oxidation activity in Pseudomonas mendocina KR1 and Pseudomonas sp. strain ENVPC5 by chlorinated solvents and alkanes. *Appl Env. Microbiol* 61, 3479–3481 (1995).
53. Hopkins, G. D. & McCarty, P. L. Field Evaluation of in Situ Aerobic Cometabolism of Trichloroethylene and Three Dichloroethylene Isomers Using Phenol and Toluene as the Primary Substrates. *Environ. Sci. Technol.* 29, 1628–1637 (1995).

54. Mahendra, S., Grostern, A. & Alvarez-Cohen, L. The impact of chlorinated solvent co-contaminants on the biodegradation kinetics of 1,4-dioxane. *Chemosphere* 91, 88–92 (2013).
55. Stroo, H. F., Leeson, A. & Ward, C. H. *Bioaugmentation for Groundwater Remediation*. (Springer Science & Business Media, 2012).
56. Semprini, L., Dolan, M., Mathias, M., Hopkins, G. & McCarty, P. Bioaugmentation of butane-utilizing microorganisms for the in situ cometabolic treatment of 1,1-dichloroethene, 1,1-dichloroethane, and 1,1,1-trichloroethane - ScienceDirect. Available at: https://www.sciencedirect.com/science/article/pii/S1164556307000295. (Accessed: 1st September 2018)
57. Westmeier, F. & Rehm, H. J. Biodegradation of 4-chlorophenol by entrapped<Emphasis Type="Italic">Alcaligenes</Emphasis> sp. A 7-2. *Appl. Microbiol. Biotechnol.* 22, 301–305 (1985).
58. Hamamura, N., Page, C., Long, T., Semprini, L. & Arp, D. J. Chloroform Cometabolism by Butane-Grown CF8, Pseudomonas butanovora, and Mycobacterium vaccae JOB5 and Methane-Grown Methylosinus trichosporium OB3b. *Appl Env. Microbiol* 63, 3607–3613 (1997).
59. Burback, B. L. & Perry, J. J. Biodegradation and biotransformation of groundwater pollutant mixtures by Mycobacterium vaccae. *Appl. Environ. Microbiol.* 59, 1025–1029 (1993).
60. Vanderberg, L. A. & Perry, J. J. Dehalogenation by Mycobacterium vaccae JOB-5: role of the propane monooxygenase. *Can. J. Microbiol.* 40, 169–172 (1994).
61. Chu, K.-H., Mahendra, S., Song, D., Conrad, M. & Alvarez-Cohen, L. Stable Carbon Isotope Fractionation during Aerobic Biodegradation of Chlorinated Ethenes - Environmental Science & Technology (ACS Publications). Available at: https://pubs.acs.org/doi/abs/10.1021/es035238c. (Accessed: 6th September 2018)
62. Wackett, L. P., Brusseau, G. A., Householder, S. R. & Hanson, R. S. Survey of microbial oxygenases: trichloroethylene degradation by propane-oxidizing bacteria. *Appl Env. Microbiol* 55, 2960–2964 (1989).
63. Cappelletti, M., Frascari, D., Zannoni, D. & Fedi, S. Microbial degradation of chloroform. *Appl. Microbiol. Biotechnol.* 96, 1395–1409 (2012).
64. Oldenhuis, R., Vink, R. L., Janssen, D. B. & Witholt, B. Degradation of chlorinated aliphatic hydrocarbons by Methylosinus trichosporium OB3b expressing soluble methane monooxygenase. *Appl. Environ. Microbiol.* 55, 2819–2826 (1989).
65. Hylckama, V. J. V., Koning, W. D. & Janssen, D. B. Effect of Chlorinated Ethene Conversion on Viability and Activity of Methylosinus trichosporium OB3b. *Appl Env. Microbiol* 63, 4961–4964 (1997).
66. Tsien, H. C., Brusseau, G. A., Hanson, R. S. & Waclett, L. P. Biodegradation of trichloroethylene by Methylosinus trichosporium OB3b. *Appl Env. Microbiol* 55, 3155–3161 (1989).
67. Hatzinger, P. B. & Lippincott, D. *Field Demonstration of Propane Biosparging for In Situ Remediation of N-Nitrosodimethylamine (NDMA) in Groundwater*. (CB and I Federal Services Lawrenceville United States, CB and I Federal Services Lawrenceville United States, 2015).
68. Smith, C. A. & Hyman, M. R. Oxidation of gasoline oxygenates by closely related non-haem-iron alkane hydroxylases in Pseudomonas mendocina KR1 and other n-octane-utilizing Pseudomonas strains: Ether oxygenate biodegradation by alkane hydroxylases. *Environ. Microbiol. Rep.* 2, 426–432 (2010).

69. Rolston, H. M. Experimental demonstration and modeling of aerobic cometabolism of 1, 4-dioxane by isobutane-utilizing microorganisms in aquifer microcosms. (2017).
70. Chen, W. Activity-Based Protein Profiling of Alkane-Oxidizing Monooxygenases in Rhodococcus rhodochrous ATCC 21198. (2016).
71. Thankitkul, S. Kinetic Analysis and Modeling Cometabolic Transformation of CAHs by R. Rhodochrous ATCC 21198. (2016).
72. Rolston, H. M., Semprini, L., Thankitkul, S., Azizian, M. & Hyman, M. R. Kinetic Studies of the Cometabolism of 1,4-DIOXANE and Chlorinated Aliphatic Hydrocarbon Mixtures by Rhodococcus Rhodochrous Grown on Isobutane. *AGU Fall Meet. Abstr.* 23, H23C–1556 (2016).
73. Kim, Y., Istok, J. D. & Semprini, L. Single-well, gas-sparging tests for evaluating the in situ aerobic cometabolism of cis-1,2-dichloroethene and trichloroethene. *Chemosphere* 71, 1654–1664 (2008).
74. Lippincott, D. *et al.* Bioaugmentation and propane biosparging for in situ biodegradation of 1, 4-dioxane. *Groundw. Monit. Remediat.* 35, 81–92 (2015).
75. ATSDR. *Toxicological profile for phenol*. (Agency for Toxic Substances and Disease Registry (ASTDR), 2000).
76. ATSDR. *Toxicological Profile for Toluene*. (Agency for Toxic Substances and Disease Registry (ASTDR), 2004).
77. Suttinun, O., Müller, R. & Luepromchai, E. Trichloroethylene cometabolic degradation by Rhodococcus sp. L4 induced with plant essential oils. *Biodegradation* 20, 281–291 (2009).
78. Personal Communication Murnane, R. Personal Communication 2018. (2018).
79. Moslemy, P., Guiot, S. R. & Neufeld, R. J. Production of size-controlled gellan gum microbeads encapsulating gasoline-degrading bacteria. *Enzyme Microb. Technol.* 30, 10–18 (2002).
80. Vancheeswaran, S., Halden, R. U., Williamson, K. J., Ingle, J. D. & Semprini, L. Abiotic and Biological Transformation of Tetraalkoxysilanes and Trichloroethene/cis -1,2-Dichloroethene Cometabolism Driven by Tetrabutoxysilane-Degrading Microorganisms. *Environ. Sci. Technol.* 33, 1077–1085 (1999).
81. Yu, S. Kinetic and modeling investigations of the anaerobic reductive dechlorination of chlorinated ethylenes using single and binary mixed cultures and silicon-based organic compounds as slow-release substrates. (2003).
82. Arkles, B., Steinmetz, J. R., Zazyczny, J. & Mehta, P. Factors contributing to the stability of alkoxysilanes in aqueous solution. *J. Adhes. Sci. Technol.* 6, 193–206 (1992).
83. Osterholtz, F. D. & Pohl, E. R. Kinetics of the hydrolysis and condensation of organofunctional alkoxysilanes: a review. *J. Adhes. Sci. Technol.* 6, 127–149 (1992).
84. Tetra-sec-butyl orthosilicate | C16H36O4Si | ChemSpider. Available at: http://www.chemspider.com/Chemical-Structure.83945.html. (Accessed: 24th August 2018)
85. Tan, S. M., Heng, P. W. S. & Chan, L. W. Development of Re-Usable Yeast-Gellan Gum Micro-Bioreactors for Potential Application in Continuous Fermentation to Produce Bio-Ethanol. *Pharmaceutics* 3, 731–744 (2011).
86. Dwyer, D. F., Krumme, M. L., Boyd, S. A. & Tiedje, J. M. Kinetics of Phenol Biodegradation by an Immobilized Methanogenic Consortium. *Appl. Environ. Microbiol.* 52, 345–351 (1986).
87. Mandal, S., Puniya, A. K. & Singh, K. Effect of alginate concentrations on survival of microencapsulated Lactobacillus casei NCDC-298. *Int. Dairy J.* 16, 1190–1195 (2006).

88. Hall, B. M., McLoughlin, A. J., Leung, K. T., Trevors, J. T. & Lee, H. Transport and survival of alginate-encapsulated and free lux-lac marked Pseudomonas aeruginosa UG2Lr cells in soil. *FEMS Microbiol. Ecol.* 26, 51–61 (1998).
89. Gosmann, B. & Rehm, H. J. Oxygen uptake of microorganisms entrapped in Ca-alginate. *Appl. Microbiol. Biotechnol.* 23, 163–167 (1986).
90. Hiemstra, H., Dijkhuizen, L. & Harder, W. Diffusion of oxygen in alginate gels related to the kinetics of methanol oxidation by immobilized Hansenula polymorpha cells. *Eur. J. Appl. Microbiol. Biotechnol.* 18, 189–196 (1983).
91. O'Reilly, K. T., Kadakia, R., Korus, R. A. & Crawford, R. L. Utilization of Immobilized-Bacteria to Degrade Aromatic Compounds Common to Wood-Treatment Wastewaters. *Water Sci. Technol.* 20, 95–100 (1988).
92. Chan, L. W., Lee, H. Y. & Heng, P. W. S. Mechanisms of external and internal gelation and their impact on the functions of alginate as a coat and delivery system. *Carbohydr. Polym.* 63, 176–187 (2006).
93. Smidsrod, O. Alginate as immobilization matrix for cells. (1990).
94. Bajpai, S. K. & Sharma, S. Investigation of swelling/degradation behaviour of alginate beads crosslinked with Ca2+ and Ba2+ ions. *React. Funct. Polym.* 59, 129–140 (2004).
95. Kühbeck, D. *et al.* Evaluation of the nitroaldol reaction in the presence of metal ion-crosslinked alginates. *New J. Chem.* 39, 2306–2315 (2015).
96. Lupo, B., Maestro, A., Porras, M., Gutiérrez, J. M. & González, C. Preparation of alginate microspheres by emulsification/internal gelation to encapsulate cocoa polyphenols. *Food Hydrocoll.* 38, 56–65 (2014).
97. Sanderson, G. R. (Kelco D. of M. and C., Bell, V. L. & Ortega, D. A comparison of gellan gum, agar, K-carrageenan, and algin. *Cereal Foods World USA* (1989).
98. Sugiura, S. *et al.* Size control of calcium alginate beads containing living cells using micro-nozzle array. *Biomaterials* 26, 3327–3331 (2005).
99. Uchiyama, H., Oguri, K., Nishibayashi, M., Kokufuta, E. & Yagi, O. Trichloroethylene degradation by cells of a methane-utilizing bacterium, Methylocystis sp. M, immobilized in calcium alginate. *J. Ferment. Bioeng.* 79, 608–613 (1995).
100. Paje, M. L., Marks, P. & Couperwhite, I. Degradation of benzene by a Rhodococcus sp. using immobilized cell systems. *World J. Microbiol. Biotechnol.* 14, 675–680 (1998).
101. Serp, D., Cantana, E., Heinzen, C., Stockar, U. V. & Marison, I. W. Characterization of an encapsulation device for the production of monodisperse alginate beads for cell immobilization. *Biotechnol. Bioeng.* 70, 41–53 (1999).
102. Gåserød, O., Sannes, A. & Skjåk-Bræk, G. Microcapsules of alginate–chitosan. II. A study of capsule stability and permeability. *Biomaterials* 20, 773–783 (1999).
103. Molzahn, P. Batch and Continuous Flow Column Studies of Methane Consumption and Methanol Production by Methylosinus Trichosporium OB3b and Methylomicrobium Buryatense 5GB1 Immobilized In Ca-Alginate and Agarose Hydrogels. (2016).
104. Nowack, B. & Briesen, J. M. V. Chelating agents in the environment. in *Biogeochemistry of chelating agents* 910, 1–18 (American Chemical Society, 2005).
105. Giavasis, I., Harvey, L. M. & McNeil, B. Gellan Gum. *Crit. Rev. Biotechnol.* 20, 177–211 (2008).
106. Doner, L. W. & Bécard, G. Solubilization of gellan gels by chelation of cations. *Biotechnol. Tech.* 5, 25–28 (1991).
107. Osmałek, T., Froelich, A. & Tasarek, S. Application of gellan gum in pharmacy and medicine. *Int. J. Pharm.* 466, 328–340 (2014).

108. Norton, S. Gellan Gum Gel As Entrapment Matrix for High Temperature Fermentation Processes: A Rheological Study. (1990).
109. Grasdalen, H. & Smidsrød, O. Gelation of gellan gum. *Carbohydr. Polym.* 7, 371–393 (1987).
110. Camelin, I. *et al.* Effect of chelatants on gellan gel rheological properties and setting temperature for immobilization of living bifidobacteria. *Biotechnol. Prog.* 9, 291–297 (1993).
111. Bettmann, H. & Rehm, H. J. Degradation of phenol by polymer entrapped microorganisms. *Appl. Microbiol. Biotechnol.* 20, 285–290 (1984).
112. Li, R. H., Altreuter, D. H. & Gentile, F. T. Transport characterization of hydrogel matrices for cell encapsulation. *Biotechnol. Bioeng.* 50, 365–373 (1996).
113. Hamid, S., Bae, W., Kim, S. & Amin, M. T. Enhancing co-metabolic degradation of trichloroethylene with toluene using *Burkholderia vietnamiensis* G4 encapsulated in polyethylene glycol polymer. *Environ. Technol.* 35, 1470–1477 (2014).
114. Soliman, E. A., El-Moghazy, A. Y., El-Din, M. S. M. & Massoud, M. A. Microencapsulation of Essential Oils within Alginate: Formulation and <i>in Vitro</i> Evaluation of Antifungal Activity. *J. Encapsulation Adsorpt. Sci.* 03, 48–55 (2013).
115. Hernández, M. A. *et al.* Biosynthesis of storage compounds by Rhodococcus jostii RHA1 and global identification of genes involved in their metabolism. *BMC Genomics* 9, 600 (2008).
116. Pradhan, M. & Rousseau, D. A one-step process for oil-in-water-in-oil double emulsion formation using a single surfactant. *J. Colloid Interface Sci.* 386, 398–404 (2012).
117. Liu, L. *et al.* Preparation of monodisperse calcium alginate microcapsules via internal gelation in microfluidic-generated double emulsions. *J. Colloid Interface Sci.* 404, 85–90 (2013).
118. Guzey, D. & McClements, D. J. Formation, stability and properties of multilayer emulsions for application in the food industry. *Adv. Colloid Interface Sci.* 128–130, 227–248 (2006).
119. Pubchem. Sodium alginate. Available at: https://pubchem.ncbi.nlm.nih.gov/compound/5102882. (Accessed: 21st August 2018)

CHAPTER 8: APPENDICIES

A. Encapsulated Cell Substrate Utilization Shelf Life Study

This experiment was created in an attempt to determine the storage potential of encapsulated microorganisms, in anticipation of the necessary storage and transport, prior to application. ATCC 21198 was encapsulated in alginate macro-beads via a rudimentary encapsulating method, presented in section 4.2.2, that was found to have reduced encapsulated cell substrate utilization rates by ~60%. This study focused on the retention of immediate substrate utilization by beads stored in a 155 mL glass Wheaton bottle filled as full as possible, to minimize an air headspace, with carbonate buffered Nanopure water at 4°C.

A single batch of beads was made and stored, from which beads were harvested and isobutane utilization tests were conducted as presented in section 3.6.1 to determine the substrate utilization after storage for 2, 6, and 18 weeks. Isobutane utilization rates were calculated via linear regression of the initial disappearance of isobutane and normalized to the added cell mass; presented as $\mu mol_{IB}/mg_{TSS}/day$. The calculated substrate utilization rates were compared to the initial substrate utilization rate of encapsulated cells to determine storage potential (Table 21) (Figure 34). Suspended cells were also stored, though as a concentrated cell slurry suspended in carbonate buffered Nanopure, which was harvested weekly to determine the storage potential of suspended cells in comparison to encapsulated. Abiotic controls were used to ensure isobutane disappearance was from consumption by the addition of ATCC 21198.

Table 21. Isobutane utilization rates calculated from data presented in Figure 34 after specified durations in storage at 4°C. Data presented as average utilization rates in units of $\mu mol_{IB}/mg_{TSS}/day$ bounded by 95% confidence intervals.

Storage Duration	Suspended ATCC 21198	Encapsulated ATCC 21198
Initial	38.5 ± 0.9	9.3 ± 0.9
2 Weeks	26.7 ± 1.5	7.1 ± 0.7
6 Weeks	11.1 ± 0.8	8.2 ± 1.0
18 Weeks	8.9 ± 1.4	5.1 ± 0.8

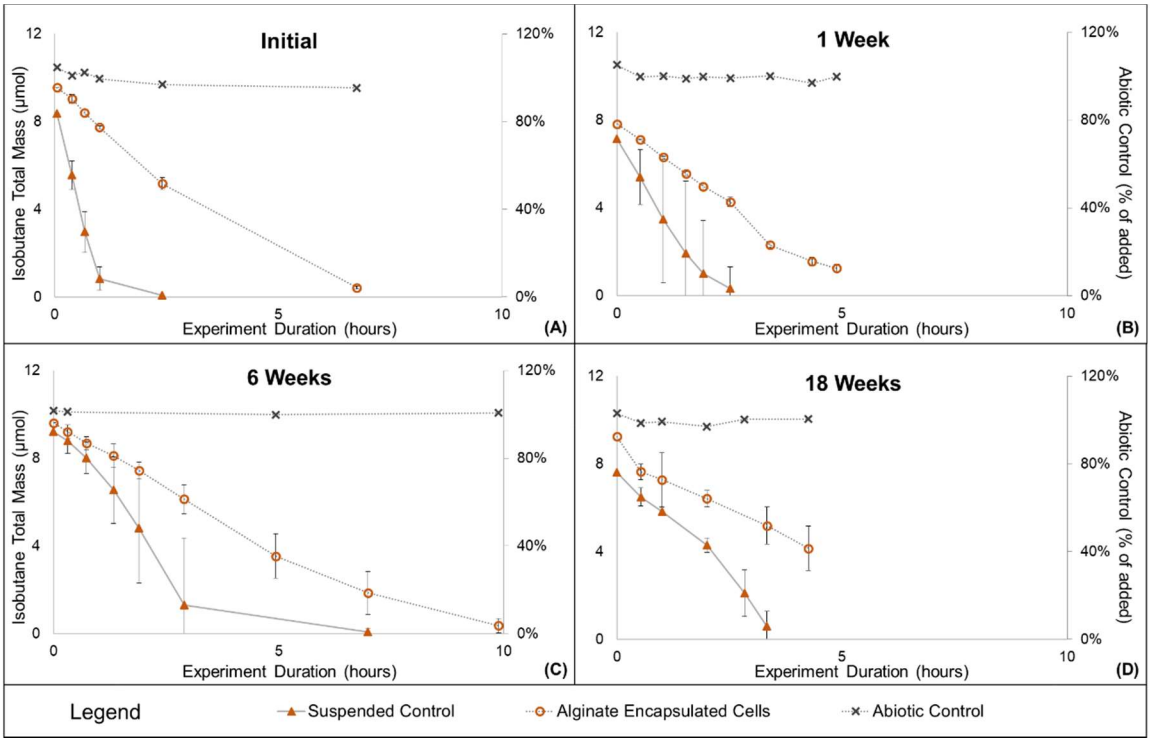

Figure 34. Isobutane utilization curves of similar biomasses of suspended and alginate encapsulated ATCC 2119 after specified durations in storage at 4°C. Storage duration specified in chart titles. Data are averages of duplicate reactors bounded by 95% confidence intervals for each point.

As seen from Figure 34 (A), alginate encapsulated cells had lagged initial substrate utilization rates just after encapsulation due to the encapsulation method used. However, it was determined that encapsulated cells retained ~55% of their initial substrate utilization rates after being in storage for as long as 18 weeks, whereas suspended cells substrate utilization rates were only 23% of initial

values. These data illustrate that encapsulated cultures can be stored for extended periods of time and retain a majority of their original substrate utilization activity. These findings help to paint a more clear picture of the path forward for the technology developed within this thesis, suggesting that bead creation can be conducted in a single location from which beads can be storage and transported to sites over several weeks.

B. Encapsulated Cell Contaminant Transformation Statistics

The amount of contaminants transformed by suspended, alginate encapsulated, and gellan gum encapsulated cells within section 4.3 appear to be visibly different, yet, calculated transformation capacities for the three treatments are relatively similar as presented in Table 12. To determine if the transformation capacity between treatments were statistically different, the Microsoft Data Analysis tool kit was used to perform a single factor analysis of variance ANOVA test on calculated 1,1,1-TCA transformation capacities for each reactor (Table 22).

Table 22. ANOVA analysis used to determine if any one of the examined treatments transformation capacities was statistically different from the other treatments.

Anova: Single Factor

Groups	Count	Sum	Average	Variance
Suspended	3	1.35	0.45	0.0013
Alginate	3	1.59	0.53	0.0005
Gellan Gum	3	1.32	0.44	0.0001

ANOVA

Source of Variation	SS	df	MS	F	P-value	F crit
Between Groups	0.0145	2	0.0073	11.09	0.0096	5.14
Within Groups	0.0039	6	0.0007			
Total	0.0185	8				

Table 22 presents the ANOVA test output, and the data illustrate that at least one transformation capacity observed within the treatments is different from the others, seen by $F>F_{crit}$ and the low P-value. Two-Sample t-Tests were then conducted to determine whether suspended, alginate encapsulated, or gellan gum encapsulated transformation capacities were statistically different from one another (Table 23). As stated in section 4.3, it was determined through these analysis that the transformation capacity for alginate encapsulated cells was statistically greater than that of both suspended and gellan gum encapsulated cells. Determined by two tail p-values <

0.05. Also, from Table 23 it can be seen that transformation capacities of suspended and gellan gum encapsulated cells do not differ significantly, p-value>>0.05.

Table 23. Two-sample t-Tests assuming unequal variances between all combinations of treatments. Output direction from Microsoft Data Analysis Toolkit.

	Suspended	Alginate
Mean	0.430	0.514
Variance	0.00095	0.00083
Observations	3	3
Hypothesized Mean Difference	0	
df	4	
t Stat	-3.452	
P(T<=t) one-tail	0.013	
t Critical one-tail	2.132	
P(T<=t) two-tail	0.026	
t Critical two-tail	2.776	

	Suspended	Gellan Gum
Mean	0.43	0.42
Variance	0.00095	0.00012
Observations	3	3
Hypothesized Mean Difference	0	
df	3	
t Stat	0.599	
P(T<=t) one-tail	0.296	
t Critical one-tail	2.353	
P(T<=t) two-tail	0.592	
t Critical two-tail	3.182	

	Alginate	Gellan Gum
Mean	0.51	0.42
Variance	0.00083	0.00012
Observations	3	3
Hypothesized Mean Difference	0	
df	3	
t Stat	5.343	
P(T<=t) one-tail	0.006	
t Critical one-tail	2.353	
P(T<=t) two-tail	0.013	
t Critical two-tail	3.182	

C. Proof of Concept: Alginate Co-Encapsulated Cell Cometabolic Transformation Longevity Study

C.1 Overview

This experiment was created in an attempt to provide proof of the concept that cometabolizing cultures could be induced by or gain energy from products of co-encapsulated SRSs. ATCC 21198 was encapsulated in alginate macro-beads via the rudimentary encapsulation method, presented in section 4.2.2, that was found to have reduced encapsulated cell substrate utilization rates by ~60%. Two batches of alginate macro-beads were created; one containing ATCC 21198 at a biomass loading of ~0.5 mg_{TSS}/g_{bead} alone and one containing ATCC 21198 co-encapsulated with TBOS at biomass loading of ~0.5 mg_{TSS}/g_{bead} and TBOS mass loading of ~5% (w/w).

Four grams of beads were added to each reactor to reach a final cell concentration of ~10 mg_{TSS}/L and when applicable TBOS concentration of ~1000 mg/L. Initial concentrations were designed to be comparable to the encapsulated cell cometabolism study and abiotic TBOS hydrolysis study presented in sections 4.3 and 4.5. Abiotic controls were used to ensure contaminant transformation was due to the addition of ATCC 21198, and in this experiment 4 grams of alginate beads, that were created without an addition of ATCC 21198, were added to abiotic controls to ensure the creation of beads was sterile and free from contamination. Reactors were spiked with the chosen CoC mixture; 1,1,1-TCA (~250ppb), *c*DCE (~250ppb), and 1,4-D(~500ppb); and were monitored over a period of ~200 days for respiration data (O_2/CO_2), substrate data (SRS/alcohols), and contaminant data (1,1,1-TCA, *c*DCE, and 1,4-D) according to methods presented in section 3.2.1.

A summary of the treatments examined within this experiment are presented in Table 24. Encapsulated cell remediation controls (EC) were created in order to determine if utilization of substrates produced by co-encapsulated TBOS in the co-encapsulated remediation reactors (CECR)

increased cells remediation potential in relation to cells encapsulated alone. Co-encapsulated substrate control reactors (CECS) were created such that substrate utilization could still be observed if the mass of contaminants added were to inhibit encapsulated cultures.

Table 24. Proof of Concept #1 reactor treatment summary.

Treatment Name	Abbreviation	Number of Reactors	Reactor Contents			
			Beads (4g)	Cells ($2mg_{TSS}$)	TBOS (624 µmol)	CoCs
Abiotic Control	AC	3	✓	--	--	✓
Encapsulated Cell Remediation Control	EC	3	✓	✓	--	✓
Co-encapsulated Cell Substrate Control	CECS	3	✓	✓	✓	--
Co-encapsulated Cell Remediation	CECR	3	✓	✓	✓	✓

C.2 Contaminant Transformation Observations

All reactors received only a single addition of contaminants due to minimal contaminant transformation over the duration of this experiment (Figure 35 C-E). The stark contrast between the cometabolism data presented in Figure 35 and data presented in section 4.3 for alginate-encapsulated cultures is likely due to the flawed encapsulation method used within this study having caused cell death prior to reactor creation. However, it is possible that to a lesser degree, that cells grown up under slightly different growth conditions may exhibit higher transformation durations and/or capacities due to the level of energy stored during growth [115].

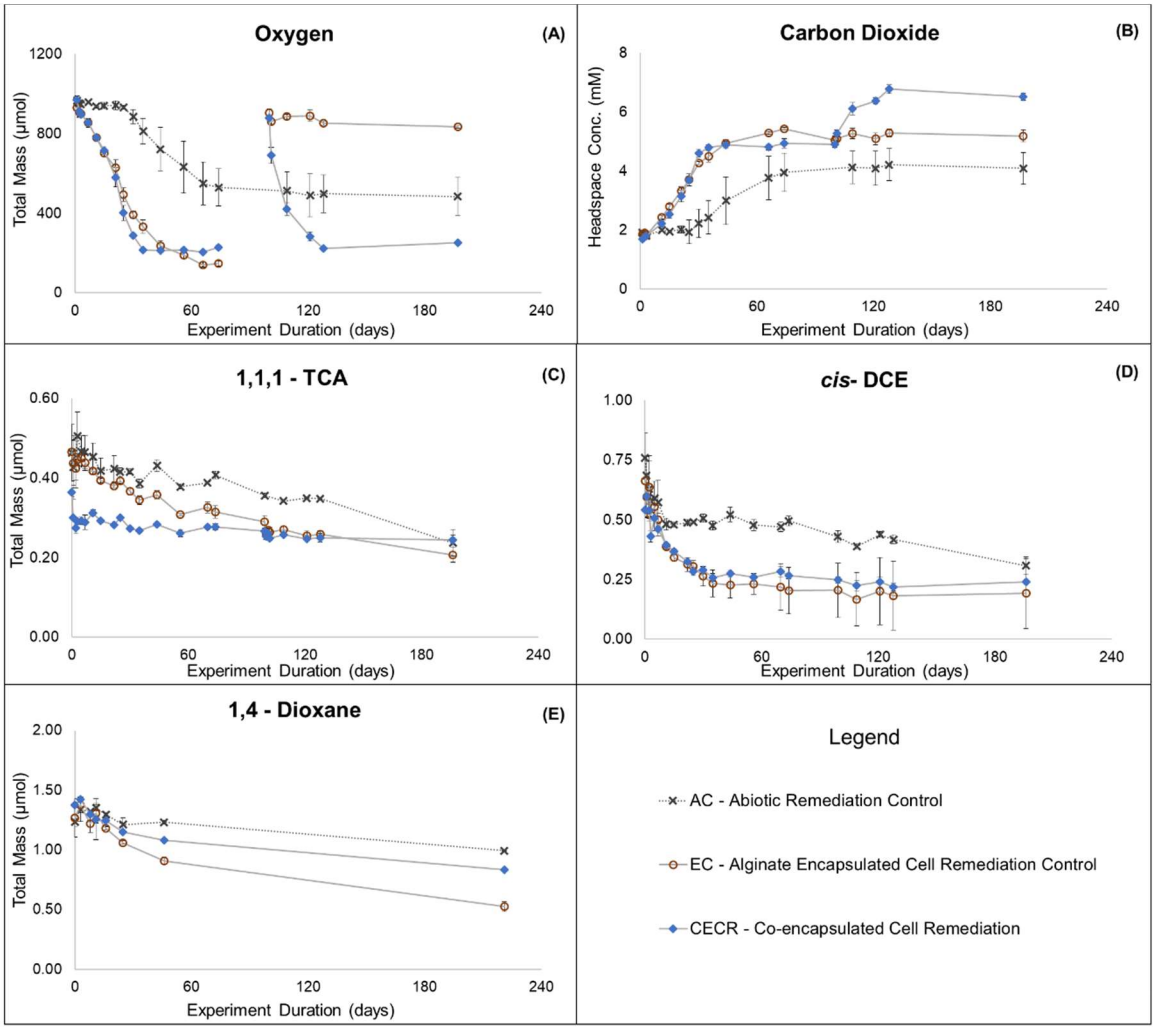

Figure 35. Long-term alginate encapsulated and co-encapsulated cell cometabolic transformation study. (A-B) Respiration data. O_2 measurements reported as ~180µmol is assumed to be near zero due to vacuum created within reactors (see Section 3.2.1 pg 32). CO_2 data are presented in terms of measured headspace concentrations due to speciation of CO_2 in carbonate system in the aqueous phase and lack of pH measurements throughout experiment. (C-E) Contaminant transformation data. A single contaminant addition was made to each reactor. Data points are averages between triplicate reactors in each treatment and errors bars are 95% confidence intervals.

Examining contaminant transformation data from the initial contaminant masses present in bottles to the final data point taken at ~200 days, suggests that there is not a significant difference, as determined by overlapping 95% confidence intervals, between cometabolically active treatments (EC/CECR) and the abiotic control, other than 1,4-dioxane. However, the majority of transformation observed in active treatments occurred over the first 60 days, whereas,

disappearance of contaminants within the abiotic controls happened after ~120 days (Figure 35). This suggests that low amounts ATCC 21198 were active upon addition to reactors, though the lack of transformation after 60 days suggests that cometabolizing cultures are no longer active or induced. Initial inactivation occurred during the encapsulation process and transformation likely halted due to transformation capacities of impaired cells being met and decay of cometabolic enzymes over the long-term experiment. The limited contaminant transformation observed in this experiment highlights the importance of the work conducted to optimize encapsulation methods, presented in section 4.2, such that cells maintain viability post-encapsulation and the reduction in remediation potential observed here is mitigated.

C.3 Cellular Respiration and SRS Observations

The above contaminant transformation data provide little to no evidence of growth or induction of ATCC 21198 by slowly releasing substrates. However, respiration and substrate data provide evidence that an aerobic microbe within these reactors was utilizing O_2 and producing CO_2, and therefore, consuming substrates (Figure 35). Figure 36 presents the same respiration data as Figure 35, though respiration time-series data for co-encapsulated cell reactors that did not received an addition of contaminants is included. Also, identifiers for the addition of O_2 is included.

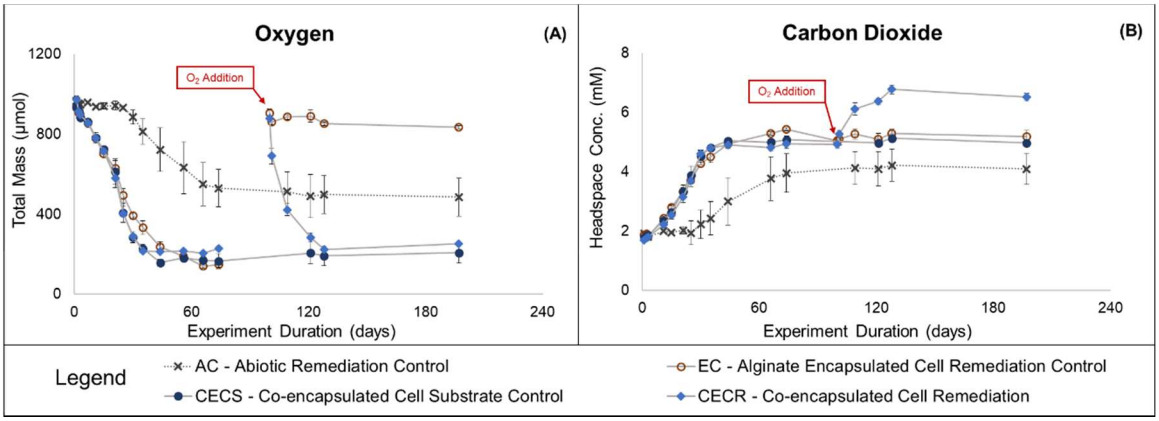

Figure 36. Long-term alginate encapsulated and co-encapsulated cell cometabolic transformation study. (A-B) Respiration data. O_2 measurements reported as ~180µmol is assumed to be near zero due to vacuum created within reactors (see Section 3.2.1 pg 32). CO_2 data are presented in terms of measured headspace concentrations due to speciation of CO_2 in carbonate system in the aqueous phase and lack of pH measurements throughout experiment. O_2 was refreshed at ~100 days in EC and CECR reactors. AC, EC, and CECR reactors contain CoC mixture, data presented in Figure 35. Data points are averages between triplicate reactors in each treatment and errors bars are 95% confidence intervals.

It can be seen from Figure 36 that in all reactors that received an addition of active alginate beads (EC, CECS, & CECR treatments), O_2 utilization and CO_2 production began immediately. Respiration data within alginate encapsulated and co-encapsulated reactors mimicked one another until ~25days, at which point oxygen consumption rates appeared to increase within all six co-encapsulated reactors (CECS & CECR).

Oxygen consumption within reactors containing ATCC 21198 encapsulated in alginate alone has been observed in previous experiments (Section 4.3). Respiration in these reactors is suggested to be due to enzymatic breakdown of the alginate matrix and microbial utilization of alginate as a carbon source. Due to issues with microbial contamination, as illustrated here from oxygen consumption in abiotic controls ~30 days and streak plating in section 4.3, it is difficult to determine whether ATCC 21198 or another microbial species is responsible for the consumption of alginate. However, respiration data was stagnant in the abiotic controls for over 30 days even though these reactors received an addition of alginate beads. This suggests that the alginate encapsulation method was sterile, and that the contamination within these bottles occurred after ~30days. The

lagged oxygen consumption within abiotic alginate containing controls (AC) provides evidence that immediate alginate consumption is correlated to the presence of ATCC 21198. This provides supporting evidence that ATCC 21198 may have the ability to utilize some portion of the alginate matrix as a growth substrate.

The increase in O_2 consumption within CECS and CECR reactors in comparison to EC reactors is suggested to be due to increased oxygen demand from the release of readily metabolized 1-butanol from encapsulated TBOS. The separation in respiration data between reactors containing encapsulated ATCC 21198 (EC) and co-encapsulated ATCC 21198 and TBOS was not drastic and oxygen was depleted before significant separation occurred, by ~50 days (Figure 37 A).

Generally, oxygen depletion is not desired because aerobic conditions are necessary for substrate utilization and contaminant transformation to proceed; however, the decision was made that reactors would not be refreshed with O_2 immediately. This was done in an attempt to allow 1-butanol to accumulate within reactors by maintaining a micro-aerobic or potentially anoxic condition in which cells could not oxidize released 1-butanol (Figure 37).

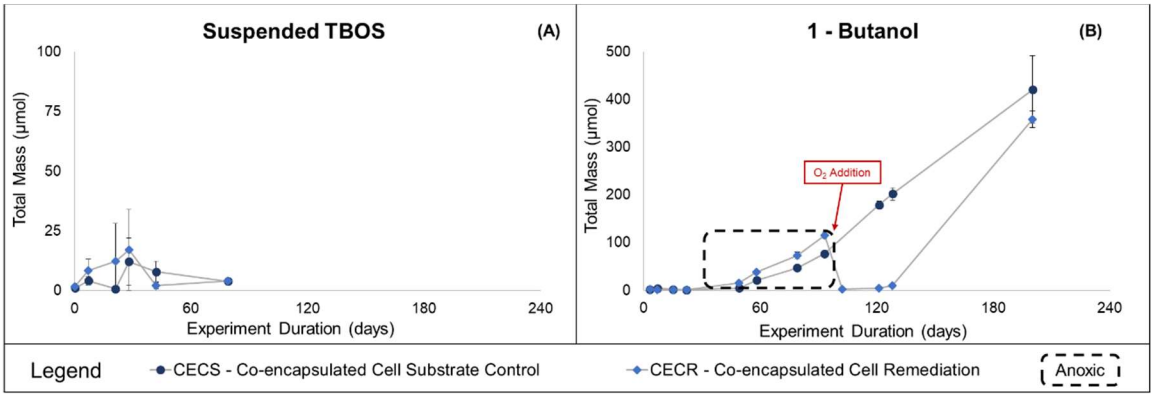

Figure 37. Long-term alginate co-encapsulated ATCC 21198 and TBOS slow release substrate data. (A) Measured TBOS concentrations within solution, ~312µmol encapsulated TBOS was added initially and <25 µmol was observed in solution at all times. (B) Measured 1-butanol accumulation during anoxic period. O_2 addition was made to CECR reactors at ~100 days at which point 1-butanol was observed to have been consumed. Data points are averages between triplicate reactors in each treatment and errors bars are 95% confidence intervals.

Figure 37 presents TBOS and 1-butanol substrate data collected for co-encapsulated cell reactors. During the anoxic condition maintained in co-encapsulated cell reactors from ~50-100 days (Figure 36), illustrated by the black dashed box in Figure 37, 1-butanol was observed to be accumulating over time within solution. An addition of oxygen was made to CECR reactors at ~100 days and 1-butanol concentrations were observed to have decreased back below the detection limit, which was attributed to cellular oxidation of released 1-butanol. No O_2 was added to CECS reactors and 1-butanol release rates were tracked over an extended duration (Figure 38). Figure 37 (A) illustrates that less than >25µmol TBOS, of the added ~312µmol, was observed in suspension at any time within all reactors. These data provide strong evidence that encapsulated SRSs remain entrapped within the alginate matrix for at least ~80days.

Figure 38 presents an enlarged graphic of CECS reactor with a calculated butanol release rate over the anoxic portion of the data. Table 25 presents a comparison between abiotic suspended and alginate encapsulated TBOS hydrolysis rates presented in section 4.3 and hydrolysis rates observed during the anoxic portion of this experiment.

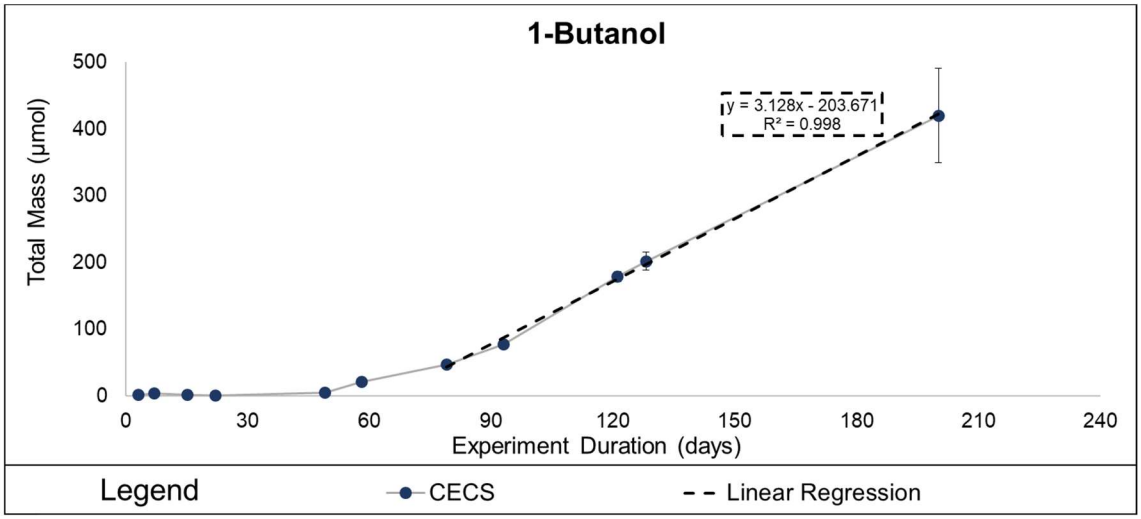

Figure 38. Butanol production data used as a proxy for TBOS hydrolysis, under non-aerobic conditions. Data points are averages between reactors and errors bars are 95% confidence intervals.

Table 25. Abiotic 1-butanol production rates calculated from measured butanol masses in solution. Abiotic TBOS hydrolysis data collected in section 4.3 presented above hydrolysis data observed within Co-encapsulated cell substrate control (CECS) reactors after oxygen was depelted.

Treatment	Initial Total SRS Solution Concentration (mg/L)	Non-Active Cells Present	Measured Initial SRS Mass (µmol)	Max Possible Butanol Release (µmol)	Butanol Production Rate (µmol/day)	Estimated Exhaustion of TBOS (years)
Suspended TBOS	1000	No	311.9	1247.4	5.91	0.58
Alginate Encapsulated TBOS (5% w/w)	1000	No	326.2	1304.7	0.69	5.17
Alginate Co-encapsulated TBOS (5% w/w)	1000	Yes	312	1248	3.13	1.09

As expected, the observed encapsulated TBOS hydrolysis rate within this experiment (3.13µmol/day) was below hydrolysis rates that have been estimated for similar concentrations of TBOS suspended directly in media, (5.91 µmol/day) (Table 25). However, the observed hydrolysis rate calculated from the long-term data in co-encapsulated cell reactors after O_2 was depleted was higher than values determined for abiotic encapsulated TBOS at similar bead mass loadings and solution concentrations, 3.13 and 0.69 µmol/day, respectively (Table 25).

This may be due to several factors including; enzymatic breakdown of the alginate encapsulation matrix causing TBOS to be released to solution, the presences of cells within the encapsulation matrix altering or increasing the diffusion of water into and out of beads allowing for greater access at hydrolysis sites, or simply to differences in alginate bead creation methods between the two experiments. Nonetheless, it is still possible that low mass loadings within beads, ~5%, can provide substrates for several years even at the elevated hydrolysis rates observed within this experiment (Table 25).

C.4 Confirmation of cellular utilization of SRS products

Just after the addition of oxygen to alginate encapsulated cell and co-encapsulated cell remediation (EC and CECR) reactors at ~100 days it was observed that O_2 within CECR reactors was quickly utilized, whereas, O_2 masses within EC reactors remained similar to the levels that were added (Figure 36). The utilization of O_2 within CECR reactors corresponded directly to a consumption of 1-butanol within these reactors.

Stoichiometric analysis was used to estimate the theoretical amount of O_2 that would be required to oxidize the measured mass of 1-butanol consumed within CECR reactors just after addition of O_2 at 100 days. These calculations were based on the oxidation of butanol to CO_2 and water (Equation 3), and were compared to measured change in O_2. The estimated theoretical values were within 10% of the measured values, providing further evidence of microbial oxidation of the released 1-butanol (Table 26).

$$C_4H_{10}O + 6O_2 \xrightarrow{\text{Respiration}} 5H_2O + 4CO_2 \quad \text{Eqn 3}$$

Table 26. Stoichiometric calculations based on total 1-butanol that accumulated within solution at ~100days within co-encapsulated cell reactors.

Butanol Consumed (µmol)	Oxygen Demand (µmol)		Percent Difference
	Theoretical	Observed	
115.05	690.3	628.1	9.01%

In contrast to the immediate O_2 consumption observed within CECR reactors, EC reactors did not consume a measureable amount of O_2 after the refresh at ~100days. A theory for this observed slowing in O_2 consumption in alginate encapsulated cell reactors (EC) is that microbes had utilized the readily available percentage of the alginate matrix. A similar slowing in O_2 consumption was observed in alginate encapsulated cell reactors in section 4.3 and it was calculated that this slowing occurred when ~25% of the added alginate was consumed. As a comparison the

same analysis were used to estimate the theoretical amount of alginate that could be oxidized by the measured decrease in O_2 observed within EC reactors in this experiment. These analysis were based on equation 2, which assumed an average chemical formula for alginate [119]. It was estimated that on average ~24.5% of the total mass of alginate added to EC reactors would have been consumed. The similarities between the estimated percent of alginate oxidized prior to slowing in rates of O_2 utilization, between the separate experiments may indicate that only ~25% of the alginate matrix is readily oxidized by cells, or that the alginate used within these studies contains an impurity of ~25% by mass.

C.5 Proof of Concept: Alginate Co-encapsulation Summary and Conclusions

The data presented as part of this experiment provide strong evidence that microbes co-encapsulated with TBOS are able to utilize 1-butanol as it is released. Also, the rate of utilization of 1-butanol by encapsulated microbes was greater than the rate of release of 1-butanol for encapsulated TBOS, as indicated by measured 1-butanol solution concentrations remaining below the detection limit of ~1ppm. However, this experiment suggested that the energy gained from consumption of the alginate matrix and likely released 1-butanol did not stimulate cometabolic activity. The observed difference between this experiment and data presented in section 4.6.6 is suggested to be due to several factors, including inactivation of ATCC 21198 prior to reactor creation, influence of alginate matrix consumption on induction of enzymes by 1-butanol, the growth substrate 1-butanol being a non-inducing growth substrate, and/or contaminant cultures not capable of cometabolism utilizing 1-butanol and alginate rather than ATCC 21198.

In addition to discovering that microbes can utilize released substrates, it was found that the alginate matrix was able to contain encapsulated TBOS for an extended period of time, at least ~80days. The ability to entrap SRSs and keep them in a localized position around cells provides strong evidence in support of the overarching hypothesis presented in the overview of this

appendix, however, the ability for released substrates to induce co-encapsulated cultures and drive cometabolism was not shown.

It was also made apparent that TBOS co-encapsulated with ATCC 21198 may hydrolyze at elevated rates compared with abiotic encapsulated TBOS. These kinetics are not well understood at this point, however, through estimation of 1-butanol production rates and known masses of TBOS present within beads, it is suggested that beads containing TBOS at low mass loadings (~5%) could sustain microbial cultures within these reactors for over a year. The limiting factor is then projected to be oxygen, as biological oxygen demand associated with release of substrates is a concern due to limited oxygen within the subsurface. Ideally, after optimization this technology will maximize the ratio of contaminants transformed to oxygen consumed. This should be possible through SRS selection, control over mass loading within beads, and control over the added quantity of beads.